MODEL POTENTIALS AND MOLECULAR RYDBERG SERIES

MODEL POTENTIALS AND MOLECULAR RYDBERG SERIES

By

FRANK RICHARD GREENING, B.Sc.

A Thesis

Submitted to the School of Graduate Studies

in Partial Fulfilment of the Requirements

for the Degree

Doctor of Philosophy

McMaster University

August 1973

DEDICATION

To my Parents

"And here are trees and I know their gnarled surface, water and I feel its taste. These scents of grass and stars at night, certain evenings when the heart relaxes--how shall I negate this world whose power and strength I feel? Yet all the knowledge on earth will give me nothing to assure me that this world is mine. You describe it to me and you teach me to classify it. You enumerate its laws and in my thirst for knowledge I admit that they are true. You take apart its mechanism and my hope increases. At the final stage you teach me that this wondrous and multicolored universe can be reduced to the electron. All this is good and I wait for you to continue. But you tell me of an invisible planetary system in which electrons gravitate around a nucleus. You explain this world to me with an image. I realize then that you have been reduced to poetry: I shall never know. Have I the time to become indignant? You have already changed theories...."

Albert Camus
The Myth of Sisyphus

DOCTOR OF PHILOSOPHY (1973) McMASTER UNIVERSITY
(Chemistry) Hamilton, Ontario

TITLE: Model Potentials and Molecular Rydberg Series.

AUTHOR: Frank Richard Greening, B.Sc. (King's College, London)

SUPERVISOR: Professor G.W. King

NUMBER OF PAGES: ix, 162

SCOPE AND CONTENTS:

Model potential calculations have been carried out on the $\pi_g \rightarrow ns\sigma_g$, $np\sigma_u$ and $np\pi_u$ Rydberg series of CO_2, CS_2 and CSe_2. The molecular potential was represented by a superposition of atomic model potentials which were calibrated to atomic data. The Rydberg M.O. was expanded about the molecular mid-point in a linear combination of hydrogen functions and many members of a Rydberg series were obtained in a single calculation on a computer. The results of the calculations were used to check previous assignments of Rydberg series in CO_2 and CS_2. The previously unreported vacuum u-v spectrum of CSe_2 was observed in the region from 1200-2000 Å, and analysed using the model calculations.

ACKNOWLEDGEMENTS

I wish to thank Dr. G.W. King for allowing me complete freedom in my research while still providing the advice and encouragement that was often needed. I wish also to thank Dr. D.P. Santry for considerable assistance with the computational aspects of my research.

I wish to thank my research colleagues, Dr. E.J. Finn and Dr. P. Pichat, for experimental assistance and helpful discussions, and I thank all the other members of this research group in the period 1968-73 for their interest in my work: Dr. G. Kidd, Dr. P.R. McLean, D. Grange, R.C. Meatherall, E.R. Farnworth, R. Lemanczyk, A. Van Putten, M. Danyluk and R. Judge.

I am very grateful to Mrs. Jan Coleman for her excellent work in typing this thesis.

This research was made possible through the financial assistance of the Department of Chemistry of McMaster University.

Finally, I thank my wife, Suzanne, who showed me where to look among the garbage and the flowers, and my daughter Hillarie who showed me sweet innocence.

TABLE OF CONTENTS

LIST OF FIGURES

LIST OF TABLES

INTRODUCTION

Molecular absorption spectra in the far ultraviolet (i.e. at wavelengths below 2000 Å) were first obtained by T. Lyman[1] in the years between 1900 and 1914.

The first theoretical understanding of these spectra was provided at about the same time by N. Bohr[2,3], who suggested that optical spectra in atoms and molecules arise from the excitation of a valence electron to an orbit located mostly outside an ionic core. Bohr predicted that molecular absorption spectra should exhibit series of bands with similar behaviour to atomic line spectra and which fit a Rydberg formula.[4]

If ν_n is the frequency of an absorption band in wave-number units, labelled by a running number n, and ν_∞ is the frequency of the series limit, then Rydberg's formula is:

$$\nu_n = \nu_\infty - \frac{R}{(n-\mu)^2} ,$$

where R is called Rydberg's constant and μ is approximately constant within a given series. Because the lines of the hydrogen spectrum fit the simplified Rydberg formula,

$$\nu_n = \nu_\infty - \frac{R}{n^2} ,$$

where n is the principal quantum number, μ is called the quantum defect and represents the effect of the non-hydrogenic part of the ion-core.

Bohr's important work was followed by the identification of numerous Rydberg series in the absorption spectra of diatomic molecules such as H_2, N_2, CO and W.C. Price and co-workers[5] found series in the polyatomic molecules H_2O, H_2S, CO_2, CS_2, CH_3I, C_6H_6 etc.

At the time of writing, Rydberg series have been identified in over 100 different molecules (see Reference 5 for a list to 1970) but a theoretical description of the electronic structure of Rydberg states in polyatomic molecules is far from complete; such a description is useful in understanding molecular excited states in general and is essential to the analysis and classification of Rydberg series in polyatomic molecules.

In this thesis a theoretical model is developed for the calculation of Rydberg terms in linear triatomic molecules and is applied to the analysis of Rydberg series in CO_2, CS_2 and CSe_2.

CHAPTER 1

Model Potentials and the Calculation of Atomic Rydberg Series

1.1 The Factorisation of Schrödinger's Equation for Excited States

M. Born and R.J. Oppenheimer[6] have shown that a good approximation which greatly simplifies the mathematical description of molecular states is the separation of electronic and nuclear motions in the full molecular Schrödinger equation. This equation is:

$$H(r_N,R,\theta,\phi)\,\Psi_{Mol}(r_N,R,\theta,\phi) = E_{Mol}\,\Psi_{Mol}(r_N,R,\theta,\phi) \qquad 1.1$$

where H is the Hamiltonian operator,

E is the total molecular energy,

r_N represents the $3N$ electronic co-ordinates

and R,θ,ϕ represent the molecular co-ordinates of internuclear separation and orientation.

The Born-Oppenheimer approximation leads to the factorisation of Ψ_{Mol} into the product of an electronic function $\Psi_{elec}(r_N,R)$, a vibrational function $\chi_{vib}(R)$, and a rotational function $\theta_{rot}(\theta,\phi)$, i.e.:

$$\Psi_{Mol}(r_N,R,\theta,\phi) = \chi_{vib}(R)\;\theta_{rot}(\theta,\phi)\;\Psi_{elec}(r_N,R) \qquad 1.2$$

Schrödinger's equation 1.1 can now be written in terms of an electronic wavefunction describing the motion of the electrons in the field of fixed nuclei:

$$H^{elec}(r_N,R)\psi_{elec}(r_N,R) = E\ \psi_{elec}(r_N,R) \qquad 1.3$$

where E is the electronic energy.

The electronic Schrödinger equation 1.3 is usually solved by using the orbital approximation, in which the N electrons are assigned N one-electron functions $\psi_1, \psi_2, \ldots \psi_N$ called orbitals.

$$\psi_{elec}(r_1,r_2, \ldots r_N,R) = \psi_1(r_1,R)\psi_2(r_2,R) \ldots \psi_N(r_N,R) \qquad 1.4$$

A simplified form of the orbital approximation is particularly appropriate for the description of molecular states in which one electron is located mostly outside an ionic core.

The Born-Oppenheimer electronic Schrödinger equation for a molecule having Q nuclei with position co-ordinates R_a (a=1,2...Q) and nuclear charges $Z_a, Z_b, \ldots$ may be written,

$$\left\{-\frac{1}{2}\sum_{k=1}^{N}\nabla_k^2 - \sum_{k}^{N}\sum_{a}^{Q}\frac{Za}{r_{ka}} + \sum_{i<k}^{N}\frac{1}{r_{ik}} + \sum_{a<b}^{Q}\frac{ZaZb}{Rab}\right\}\psi_{elec} = E\ \psi_{elec} \qquad 1.5$$

If one electron is positioned well outside the remaining (core) electrons then one of the r's, say r_1, is large compared to the others. In this case equation 1.5 may be written in the form,

$$\left\{-\frac{1}{2}\nabla_1^2 - \sum_{a}^{Q}\frac{Za}{r_{1a}} + \sum_{k=2}^{N}\frac{1}{r_{1k}} - \frac{1}{2}\sum_{k=2}^{N}\nabla_k^2 - \sum_{k=2}^{N}\sum_{a}^{Q}\frac{Za}{r_{ka}} + \sum_{i=z<k}^{N}\frac{1}{r_{ik}} + \sum_{a<b}^{Q}\frac{ZaZb}{R_{ab}}\right\}\psi_{elec} = E\ \psi_{elec} \qquad 1.6$$

Since r_{1k} is large compared to all other r_{ik}'s, r_{1k} will be approximately the same for all k and,

$$\sum_{k=2}^{N} \frac{1}{r_{ik}} \simeq \frac{N-1}{r_1} \qquad 1.7$$

so that,

$$\{-\frac{1}{2}\nabla_1^2 - \sum_{a}^{Q}\frac{Za}{r_{1a}} + \frac{N-1}{r_1} + [-\frac{1}{2}\sum_{k=2}^{N}\nabla_k^2 - \sum_{k=2}^{N}\sum_{a}^{Q}\frac{Za}{r_{ka}} + \sum_{i=z<k}^{N}\frac{1}{r_{ik}} - \sum_{a<b}^{Q}\frac{ZaZb}{R_{ab}}]\}\psi_{elec} = E\,\psi_{elec} \qquad 1.8$$

Upon separating the variables in equation 1.8 two equations are obtained, one describing the motion of the excited electron in the field of the molecular-ion represented by ψ_{ex} and the other defining the state of the molecular ion ψ_{ion}. i.e.

$$\psi_{elec}(r_N,R) = \psi_{ex}(r_1,R)\;\psi_{ion}(r_{N-1},R) \qquad 1.9$$

and

$$\{-\frac{1}{2}\nabla_1^2 - \sum_{a}^{Q}\frac{Za}{r_{1a}} + \frac{N-1}{r_1}\}\psi_{ex}(r_1,R) = \epsilon_{ex}\,\psi_{ex}(r_1,R) \qquad 1.10a$$

$$\{-\frac{1}{2}\sum_{k=2}^{N}\nabla_k^2 - \sum_{k=2}^{N}\sum_{a}^{Q}\frac{Za}{r_{ka}} + \sum_{i=2<k}^{N}\frac{1}{r_{ik}} - \sum_{a<b}^{Q}\frac{ZaZb}{R_{ab}}\}\psi_{ion}(r_{N-1},R)$$

$$= \epsilon_{ion}\,\psi_{ion}(r_{N-1},R) \qquad 1.10b$$

The exactness's of the product resolution described by equations 1.10a and 1.10b depends on the validity of the

approximation given by equation 1.7. J.C. Slater[7] has shown that the error involved in equation 1.7 is

$$\frac{N-1}{r_1} - \sum_{k=2}^{N} \frac{1}{r_{ik}} \sim \frac{R_{ion}}{r_1^2}$$

where R_{ion} is the effective radius of the ion.

This means that equation 1.10a is a good approximation for excited electrons which have a high probability of being found at large distances from the ion core and ψ_{ex} is an exact representation of the wavefunction of the excited electron in the limit of $r_1 \to \infty$. From equation 1.8 it can be seen that

$$\sum_{a}^{Q} \frac{Za}{r_{1a}} \to \frac{Z}{r_1} \quad \text{as } r_1 \to \infty$$

where Z is the sum of the nuclear charges and the asymptotic limit of equation 1.10a is

$$\left\{-\frac{1}{2}\nabla_1^2 - \frac{(Z-N+1)}{r_1}\right\} \psi_{ex}(r_1) = \kappa_{ex}\, \psi_{ex}(r_1) \qquad 1.11$$

which is the equation of motion of an electron in a coulomb field due to a point charge Z-N+1. Hence an excited electron moves in a hydrogen-like potential at large r.

This conclusion may also be reached from classical considerations of the coupling of angular momenta. At small r the orbital angular momentum $\vec{l}$ is strongly coupled to the nuclear axis and the squared orbital angular momentum projection $(\hbar\lambda)^2$ is a constant of the motion. At large r on the other hand the electron experiences the isotropic coulombic attraction

of an independently vibrating and rotating ion core, $\vec{l}$ is decoupled from the nuclear axis and λ is no longer defined.

1:2 The Atomic Effective Potential

In section 1.1 it was shown that the separation of the electronic wavefunction ψ_{elec} into a product, $\psi_{ex}(r_1,R)\psi_{ion}(r_{N-1},R)$, is valid only when the excited electron is classically at large distances from the ion-core. At small distances the electron repulsion term $\sum_{i<k} \frac{1}{r_{ik}}$ introduces electron correlation and ψ_{elec} cannot be separated. The separation can be maintained if it is possible to construct an effective potential which is a function of the co-ordinates of the excited electron only and represents the average potential experienced by the electron at any position in the ion field. Such an effective potential shall be denoted by U(r) throughout this thesis. For atoms U(r) constitutes a central field containing no angle dependent terms and the electronic wavefunction is separable in spherical polar co-ordinates.

$$\psi_{ex}(r) = \psi(r,\theta,\phi) = R(r)\, Y_l^M(\theta,\phi) \qquad 1.12$$

The radial part of Schrödinger's equation for an electron moving in a central field is:

$$\frac{d^2R(r)}{dr^2} + \frac{2}{r}\frac{dR(r)}{dr} + \left[2E-2U(r) - \frac{l(l+1)}{r^2}\right]R(r) = 0 \qquad 1.13$$

Putting

$$P(r) = r\,R(r) \qquad 1.14$$

in 1.13 gives

$$\frac{d^2P(r)}{dr^2} + [2E - 2U(r) - \frac{\ell(\ell+1)}{r^2}]P(r) = 0 \qquad 1.15$$

D.R. Hartree[8] developed a numerical procedure for the determination of U(r) known as the method of self-consistent fields, but a much simpler semi-empirical approach first used by W. Heisenberg[9] is to construct a "model potential" involving adjustable parameters which reproduce the observed eigenvalue spectrum. In constructing such a model potential it is useful to divide U(r) into two regions, one for small r and the other for large r, where diverse physical environments prevail. The exact form of U(r) is known only in the asymptotic limit of large or small r. Thus for an N-electron atom with nuclear charge Z_N,

$$U(r)_{r\to\infty} = -\frac{(Z_N-N+1)}{r} = -\frac{Z}{r}$$

and $$U(r)_{r\to 0} = -\frac{Z_N}{r} + C \qquad 1.16$$

where Z is the net charge on the ion-core and C is the constant potential arising from the core electrons.

U(r) Outside the Ion-Core

A Rydberg electron situated classically well outside an atomic ion-core experiences an essentially coulombic field except for polarisation corrections. These corrections arise because the Rydberg electron exerts an essentially homogeneous field $-\frac{Z}{r^2}$ on the core and induces a dipole moment $-\frac{\alpha_d Z}{r^2}$ where

α_d is the dipole polarisability of the core. The potential energy due to the polarisation of the atom core is $-\frac{\alpha_d Z^2}{2r^4}$ and at large r this ↓o much more rapidly than the coulomb term and is usually neglected.

U(r) Inside the Ion-Core

The form of the Rydberg wavefunction is determined by the Pauli principle which requires that the wavefunction be orthogonal to all occupied core wavefunctions. This means that the nodes of the Rydberg wavefunction must be located at approximately the same radial distance as the antinodes of a core function with the same ℓ. If a Rydberg orbital has no real core precursors[10] there are no orthogonality constraints on the form of the wavefunction inside the core. Such a Rydberg orbital is non-penetrating in the sense that the radial wavefunction is very small at small r and the boundary condition of these functions is practically the same as for hydrogen. Consequently the term values of non-penetrating Rydberg orbitals are close to the corresponding term values in hydrogen except for small polarisation corrections.

Penetrating Rydberg orbitals may be orthogonalized to the core wavefunctions by the method proposed by C. Herring[11], who showed that the oscillations of the wavefunction produced by the orthogonality constraints in the core region could be reproduced by subtracting a suitable linear combination of core orbitals from a smooth function. In this case the Rydberg

function takes the form:

$$\psi_{Ryd} = \chi_{Ryd} - \sum_{c=1}^{N} a_c \phi_c \qquad 1.17$$

where χ_{Ryd} is a non-orthogonal function and ϕ_c are the N core eigenfunctions. The coefficients a_c are chosen to make ψ_{Ryd} orthogonal to the core orbitals ϕ_c i.e.

$$\langle \psi_{Ryd} | \phi_{core} \rangle = 0 \qquad 1.18$$

J.C. Phillips and L. Kleinman[12] have shown that a function satisfying certain orthogonality constraints can be represented by an unconstrained function satisfying a modified Hamiltonian. The eigenvalue equation for a Rydberg electron is

$$H \psi_{Ryd} = E_{Ryd} \psi_{Ryd} \qquad 1.19$$

where ψ_{Ryd} is orthogonal to all core functions ϕ_{core}. These core functions obey the eigenvalue equation,

$$H \phi_{core} = E_{core} \phi_{core} \qquad 1.20$$

A function χ_{Ryd} which is non-orthogonal to the core orbitals will have the same eigenvalues as ψ_{Ryd} when operated on by a modified Hamiltonian,

$$(H + V_R) \chi_{Ryd} = E_{Ryd} \chi_{Ryd} \qquad 1.21$$

where V_R represents a "pseudopotential" which takes account of the non-orthogonality of χ_{Ryd}. From equations 1.19, 1.20, and 1.21 it is readily seen that

$$V_R \chi_{Ryd} = \sum_{c=1}^{N_c} \langle \phi_{core} | \chi_{Ryd} \rangle [E_{Ryd} - E_{core}] \phi_{core} \qquad 1.22$$

Because the core energies lie lower than the Rydberg energies, V_R behaves like a repulsive potential which largely cancels the coulomb potential inside the core. Hence the effective potential $U(r) = -\frac{Z}{r} + V_R$ is probably small at small r except very close to the origin.

The pseudopotential formalism is inconvenient in practical applications because the pseudowavefunction χ_{Ryd} is limited to the form of equation 1.17 which requires a knowledge of the core orbitals. Instead of remaining within the confines of pseudopotential theory many investigators have preferred to use simple model potentials from which model wavefunctions can be readily determined, and which require no knowledge of the core orbitals. The only restriction placed on the form of the model wavefunction is that it correctly reproduce the eigenvalue spectrum.

Many model potentials have been proposed in the literature, some of which have been suggested by pseudopotential theory. For example M.H. Cohen and V. Heine[13] have suggested a simple cut off-coulomb potential,

$$U(r) = -\frac{Z}{r} \; ; \; r > r_o$$
$$U(r) = 0 \; ; \; r < r_o \qquad 1.23$$

in which r_o is a variable parameter. I.V. Abarenkov and V. Heine[14] proposed a more flexible two parameter potential,

$$U(r) = -\frac{Z}{r} \; ; \; r>r_o$$

$$U(r) = A \; ; \; r<r_o \qquad 1.24$$

in which A is a small constant. This particular model has proved to be successful in treating atomic and molecular Rydberg series and will be used in this thesis.

1.3 Solutions of the One-electron Schrödinger Equation for a Coulomb Field

Although many different atomic model potentials have been proposed they are all such that for $r>r_o$, a quantity of the order of the dimensions of the ion, the Rydberg wavefunction is one of the solutions of the equation:

$$\frac{d^2P_{n^*\ell}(r)}{dr^2} + \left[\frac{2Z}{r} - \frac{\ell(\ell+1)}{r^2} + 2E\right]P_{n^*\ell}(r) = 0 \qquad 1.25$$

This equation constitutes a second order linear homogeneous differential equation and is an example of the Sturm-Liouville boundary value problem. The discrete spectrum of eigenvalues fit a Rydberg type formula,

$$2E = -\frac{Z^2}{n^{*2}} \qquad 1.26$$

and it was pointed out by A. S. Eddington[15] and Y. Sugiura[16] that if the following substitutions are made in equation 1.25

$$y = \frac{2Zr}{n^*} \; ; \; m = i + \frac{1}{2} \; ; \; P_{n^*,\ell}(r) = W_{n^*,m}\left(\frac{2Zr}{n^*}\right) \qquad 1.27$$

the equation of the confluent hypergeometric functions is obtained:

$$\frac{d^2W_{n^*,m}}{dy^2} + [\frac{n^*}{y} - \frac{1}{4} + \frac{\frac{1}{4} - m^2}{y^2}]W_{n^*,m} = 0 \qquad 1.28$$

These functions are discussed in detail in monographs by L. J. Slater[17] and H. Buchholz[18].

D.R. Hartree[19] showed in an early paper on the Schrödinger radial equation that the general solution $W_{n^*,m}(\frac{2Zr}{n^*})$ of equation 1.27 can be written in terms of a variable $\sigma = 2Zr$ in the form:

$$AW_{n^*,k}(\frac{2Zr}{n^*}) = G_\ell(\sigma)\cos\pi n^* + H_\ell(\sigma)\sin\pi n^* \qquad 1.29$$

where $G_\ell(\sigma)$ is the solution regular at the origin,

$$G_\ell(\sigma) = \sigma^{\ell+1}[a_\sigma + a_1\sigma + a_2\sigma^2 + \ldots] \qquad 1.30$$

and $H_\ell(\sigma)$ is the linearly independent solution irregular at the origin,

$$H_\ell(\sigma) = \sigma^{-\ell}[b_0 + b_1\sigma + b_2\sigma^2 + \ldots] + \alpha G_\ell(\sigma)\log\sigma \qquad 1.31$$

Both $G_\ell(\sigma)$ and $H_\ell(\sigma)$ can be represented by a power series in E, and n^* by,

$$n^* = n + \alpha + \beta E + \gamma E^2 + \ldots \qquad 1.32$$

This expansion which was first proposed by R.T. Birge[20] contains the Rydberg and Ritz formulae if the series is terminated at the appropriate term.

An important special case of equation 1.25, known as the zero energy Schrödinger radial equation has been studied by G.H. Wannier.[21] This equation is:

$$\frac{d^2P_{n^*,\ell}(r)}{dr^2} + \left[\frac{2Z}{r} - \frac{\ell(\ell+1)}{r^2}\right] P_{n^*,\ell}(r) = 0 \quad 1.33$$

By making the substitutions,

$$v = \sqrt{8Zr} \text{ and } P_{n^*,\ell} = \frac{1}{2} vf(r) \quad 1.34$$

Bessel's equation of index $(2\ell+1)$ is obtained:

$$\frac{d^2f}{dv^2} + \frac{1}{v}\frac{df}{dv} + \left[1 - \frac{(2\ell+1)^2}{v^2}\right] f = 0 \quad 1.35$$

The general solution of this equation is called a cylinder function $C_{2\ell+1}(v)$ which is an arbitrary linear combination of Bessel functions of the first and second kinds, $J_{2\ell+1}(v)$ and $Y_{2\ell+1}(v)$, i.e.

$$f(r) = C_{2\ell+1}(v) = AJ_{2\ell+1}(v) + BY_{2\ell+1}(v) \quad 1.36$$

Wannier showed that providing $4n^* >> \sqrt{8Zr}$,

$$P_{n^*\ell}(r) = \sqrt{8Zr}\left\{J_{2\ell+1}(\sqrt{8Zr})\cos\pi n^* + \frac{(n^*-\ell-1)!}{(n^*+\ell)!} n^{*2\ell+1} Y_{2\ell+1}(\sqrt{8Zr})\sin\pi n^*\right\} \quad 1.37$$

Replacing n^* by $n-\mu_\infty$ where μ_∞ is the quantum defect at zero energy and assuming the factor

$$\frac{(n^*-\ell-1)!n^{*2\ell+1}}{(n^*+\ell)!} = 1$$

equation 1.37 reduces to:

$$P_{n^*,\ell}(r) \underset{E\to 0}{=} \sqrt{8Zr}\,\{\cos\pi\mu_\infty J_{2\ell+1}(\sqrt{8Zr}) - \sin\pi\mu_\infty Y_{2\ell+1}(\sqrt{8Zr})\} \qquad 1.38$$

Information on the physical meaning of the quantum defect can be obtained by considering the asymptotic behaviour of this equation. The asymptotic expansion of Bessel functions $J_n(x)$, $Y_n(x)$ is, for x very large and n small,

$$J_n(x) \sim \left(\frac{2}{\pi x}\right)^{1/2} \left[\cos\left(x - \tfrac{1}{2}n\pi - \tfrac{1}{4}\pi\right)\right]$$

$$Y_n(x) \sim \left(\frac{2}{\pi x}\right)^{1/2} \left[\sin\left(x - \tfrac{1}{2}n\pi - \tfrac{1}{4}\pi\right)\right] \qquad 1.39$$

With the substitution

$$x - \tfrac{1}{2}n\pi - \tfrac{1}{4}\pi = \sqrt{8Zr} - \frac{2\ell+1}{2}\pi - \tfrac{1}{4}\pi = \omega \qquad 1.40$$

the asymptotic form of 1.38 is:

$$R^{\text{Atom}}_{\infty\ell}(r) = \frac{P_{n^*\ell}(r)}{r} \underset{r\to\infty}{\sim} \sqrt{\frac{2}{\pi\sqrt{8Zr}}}\,\frac{\sqrt{8Zr}}{r}\,\{\cos\pi\mu_\infty\cos\omega - \sin\pi\mu_\infty\sin\omega\}$$

or

$$R^{\text{Atom}}_{\infty\ell}(r) \underset{r\to\infty}{\sim} \frac{(8Z)^{1/4}}{r^{3/4}}\sqrt{\frac{2}{\pi}}\cos(\omega + \pi\mu_\infty) \qquad 1.41$$

Bethe and Salpeter[22] have shown that the zero energy asymptotic form of the hydrogen functions $R_{n\ell}(r)$, for which the field is coulombic all the way to the origin, is

$$R^{Hyd}_{\infty \ell}(r) \underset{r\to\infty}{\sim} \frac{const}{\sqrt{\pi}\, r^{3/4}} \cos\omega \qquad 1.42$$

Comparison of equations 1.41 and 1.42 shows that $\pi\mu_\infty$ is the phase difference, δ, between the asymptotic solution of the radial equation for a potential which is coulombic all the way to the origin and the solution for a potential which departs from the coulomb form at small r, i.e.

$$\pi\mu_\infty = \delta \qquad 1.43$$

This result has also been proved by M.J. Seaton[23] from a consideration of the zero energy form of continuum wavefunctions. Because the quantum defect is a slowly varying function of energy the relationship $\pi\mu_\infty = \delta$ proved at zero energy will be a good approximation at small negative energies of the order of atomic Rydberg term energies. This suggests that the quantum defect may be obtained from a comparison of the relative phase of oscillation outside the ion-core of the actual wavefunction with energy E_n to a hydrogenic wavefunction with the same energy.

1.4 The Variation Principle and the Determination of Atomic Model Potentials

The problem of finding convenient general solutions of the one-electron radial Schrödinger equation for a coulomb field has received much attention from theorists since the pioneering work of Hartree and Wannier[19,21]. Tabulations of particular solutions are now available[24] consisting of numerical

values of the regular and irregular coulomb functions evaluated by numerical integration techniques at given radial distances, r, and energies E. Solutions in this form are useful for matching boundary conditions inside and outside an ion core but do not provide convenient analytic functions which are appropriate for the calculation of entire Rydberg series.

Approximate eigenvalues and eigenfunctions of a differential equation may be obtained by setting up the corresponding variational problem. The one-electron Schrödinger equation to be solved may be written in the form:

$$H P_i(r) = E_i P_i(r) \qquad 1.44$$

where H is the Hamiltonian Operator,

$$H \equiv \{ -\frac{1}{2}\frac{d^2}{dr^2} + U(r) + \frac{\ell(\ell+1)}{2r^2} \} \qquad 1.45$$

The variational method requires the selection of a set of n linearly independent admissible functions ψ_i which constitute minimising sequences for the functional,

$$Q = \frac{(HP,P)}{(P,P)} \qquad 1.46$$

If the ψ_i constitute a complete set then

$$P = \lim_{n\to\infty} \sum_{i=1}^{n} C_i \psi_i \qquad 1.47$$

and the same solution of 1.44 will be obtained irrespective of the particular functions chosen.

In practical applications of the variational method the size of the set of admissible functions is limited to a

finite number of terms and it is important to require that the series converges rapidly to the exact wavefunction. The convergence of a particular set is most rapid when the basis functions ψ_i are themselves approximate eigenfunctions of H.

In the previous section it was shown that the solutions of 1.44 are phase-shifted hydrogenic solutions and it is therefore probable that the discrete hydrogen radial functions $P_{n\ell}(r)$ constitute a convenient orthonomal set with which to expand the one electron atomic wavefunction $P_i(r)$. If this is the case $P_i(r)$ will be given by,

$$P_i(r) = \sum_{n=1}^{N} c_{ni} P_{n\ell}(r) \qquad 1.48.$$

where the c_{ni} are expansion coefficients to be determined. The hydrogen functions $P_{n\ell}(r)$ are given explicitly by the equation:

$$P_{n\ell}(r) = \frac{(n-\ell-1)!Z}{n^2[(n+\ell)!]^3}\left(\frac{2Zr}{n}\right)^{\ell+1} e^{-Zr/n} \Big\lfloor_{n+\ell}^{2\ell+1}\left(\frac{2Zr}{n}\right) \qquad 1.49$$

and are the eigenfunctions of the radial Schrödinger equation:

$$H_o P_{n\ell}(r) = E_{n\ell} P_{n\ell}(r) \qquad 1.50$$

where

$$H_o \equiv \left\{-\frac{1}{2}\frac{d^2}{dr^2} - \frac{Z}{r} + \frac{\ell(\ell+1)}{2r^2}\right\} \qquad 1.51.$$

Equation 1.50 has eigenvalues given by,

$$E_{n\ell} = \int_0^\infty P_{n\ell}(r)\, H_o P_{n\ell}(r)\, dr = \frac{-Z^2}{2n^2}. \qquad 1.52$$

The energy eigenvalues of equation 1.44 are given by,

$$E_i = \sum_n \sum_{n'} c_{ni}\, c_{n'i}\, H_{nn'} \qquad 1.53$$

where $H_{nn'}$ is the matrix element:

$$H_{nn'} = \int_0^\infty P_{n\ell}(r) H\, P_{n'\ell}(r)dr \qquad 1.54$$

If U(r) takes the form (c.f. Equation 1.24)

$$U(r) = \begin{cases} -\frac{Z}{r}\ ;\ r \geq r_o \\ \\ -V_M;\ r \leq r_o \end{cases} \qquad 1.55$$

substitution of 1.45 into 1.53 yields,

$$E_i = \sum_n \sum_{n'} c_{ni}\, c_{n'i} \left[\int_0^{r_o} P_{n\ell}(r) \left\{-\frac{1}{2}\frac{d^2}{dr^2} - V_M + \frac{\ell(\ell+1)}{2r^2}\right\} P_{n'\ell}(r)dr \right.$$

$$\left. + \int_{r_o}^\infty P_{n\ell}(r) \left\{-\frac{1}{2}\frac{d^2}{dr^2} - \frac{Z}{r} + \frac{\ell(\ell+1)}{2r^2}\right\} P_{n'\ell}(r)dr\right] \qquad 1.56$$

From which,

$$E_i = \sum_n \sum_{n'} c_{ni}\, c_{n'i} \left[\int_0^{r_o} P_{n\ell}(r) \left\{\frac{Z}{r} - V_M\right\} P_{n'\ell}(r)dr \right.$$

$$\left. + \int_0^\infty P_{n\ell}(r) \left\{-\frac{1}{2}\frac{d^2}{dr^2} - \frac{Z}{r} + \frac{\ell(\ell+1)}{2r^2}\right\} P_{n'\ell}(r)dr\right] \qquad 1.57$$

The second integral in 1.57 contains the hydrogenic operator H_o (c.f. equation 1.51) so that,

$$E_i = \sum_n \sum_{n'} c_{ni}\, c_{n'i} \left[\int_0^{r_o} P_{n\ell}(r) \left\{\frac{Z}{r} - V_M\right\} P_{n'\ell}(r)dr + \delta_{nn'} E_n\right] \qquad 1.58$$

The expansion coefficients c_{ni} are obtained by following the usual variational procedure of minimising E_i as a function of all the c_{ni}. This leads to a set of N linear simultaneous equations for the c_{ni} which may be written in matrix notation:

$$H c_i = c_i E_i \qquad 1.59$$

where c_i is a column vector,

$$c_i = \{c_{1i}, c_{2i}, \ldots, c_{ni}, \ldots, c_{Ni}\}$$

H may be diagonalized by a similarity transformation when the roots E_i of H are identical with the diagonal elements.

A programme was written in Fortran IV language for use on the McMaster University C.D.C. 6400 computer. A library matrix diagonalization subroutine was employed for the determination of the eigenvalues and eigenvectors. Once the model potential parameters r_o and V_M (Equation 1.58) were selected model Rydberg series were formed by arranging the calculated eigenvalues in order of decreasing energy. The lowest energy eigenvalue was assumed to correspond to the first member of a Rydberg series (i.e. the term with smallest n*), and the number of higher series members calculated depended on the number of functions used in the expansion of the atomic wave-function. Using 10 s-functions (n=1, 2, ... 10) or 9 p-functions (n=2,3, ... 10) it was found that one Rydberg series could be calculated in ~4 sec C.P. time on the C.D.C. 6400 computer.

Results and Discussion

Two forms of the core model potential were investigated in this thesis. These were:

$$V_M = A \quad ; \quad r \leq r_o$$

and

$$V_M = -\frac{Z_c}{r} \quad ; \quad r \leq r_o$$

where A and Z_c are constants.

The form with V_M=A has been used in model potential calculations by A.U. Hazi and S.A. Rice[25] and T. Betts and V. McKoy[26]. These authors determined an A value by setting equal at r_o the logarithmic derivatives of the wavefunction inside and outside r_o. The calculations of these authors are not entirely satisfactory however because an arbitrary value of r_o was selected before an A value was determined by the curve matching procedure; a two parameter potential was thus limited to variation in one parameter. An optimum value of r_o was not determined and the question of the uniqueness of such a potential not discussed. These questions have been discussed in this work since the effect of varying both parameters A and r_o, was investigated.

The above mentioned authors calculated Rydberg series in diatomic molecules using molecular model potentials constructed from superpositions of atomic model potentials. This method has been extended here to the calculation of Rydberg series in linear triatomic molecules and in particular to CO_2, CS_2 and CSe_2; for this purpose the atomic model potentials for the

atoms C, O, S and Se were required. Calculations were carried out for these atoms and the series obtained were compared to known Rydberg series taken from C.E. Moore's Tables of Atomic Energy Levels.[27]

The work of Hazi and Rice and Betts and McKoy[25,26] emphasizes that the model potential does not necessarily resemble the real potential in the core region but serves simply to parametrise the boundary conditions so that a model wavefunction with the same radial derivative as the actual wavefunction at r_o is obtained. For this reason it is not possible to equate the model radius r_o to any physical quantity such as the ionic radius, r_{ion}. Nevertheless some correlation between r_o and r_{ion} may be expected and values of r_{ion} should enable approximate upper and lower bounds to be placed on acceptable values of r_o. Thus, for example, S.C.F. calculations[28] on O^+ show that the radial charge distribution is essentially zero for $r>4$ a.u. and ~90% of the charge distribution is located at $r<2$ a.u. For this reason r_o was restricted to values in the range 2-4 a.u. and an A value was determined which minimised ω for each r_o where,

$$\omega^2 = \sum_i [E_i^{Calc}(A,r_o) - E_i^{Expt.}]^2$$

Calculated series are given for oxygen in Table 1.I . A number of interesting features of the results for oxygen will be discussed although many of the arguments can be generalized to the other atoms studied.

Table 1.I

Observed and Calculated Term Values of the Oxygen ns (^3S_o) Rydberg Series

		3s	4s	5s	6s	7s	8s	9s
Experimental Term Values (a.u.)		.15055	.06202	.03383	.02129	.01462	.01066	.00802
Calculated Term Values (a.u.)								
A	r_o							
-.020	2.5	.15075	.06192	.03365	.02113	.01450	.01057	.00804
-.160	3.0	.15170	.06264	.03396	.02128	.01458	.01061	.00807
-.210	3.5	.15126	.06297	.03411	.02135	.01461	.01063	.00808
-.225	4.0	.15084	.06315	.03419	.02139	.01463	.01064	.00808
Z_c	r_o							
-.290	3.0	.15015	.06445	.03481	.02168	.01478	.01072	.00813
-.425	3.5	.15036	.06277	.03406	.02133	.01461	.01063	.00808

Table I.1 shows that there exists a range of values of A and r_o over which good agreement can be obtained (i.e. to within 3% of the experimental term values). The A and r_o parameters which give the best fit to the oxygen ns(^3S_o) Rydberg series are plotted in Fig. 1.I.

The arbitrariness of the model potential is accompanied by a corresponding arbitrariness in the expansion coefficients c_{ni}. The non-coulombic core serves to mix hydrogen radial functions of the same ℓ but different n and the quantity c_{ni}^2 determines the amount of each hydrogen function, $P_{n\ell}(r)$, in the i^{th} Rydberg A.O. with eigenvalue E_i. The calculation shows that $|c_{ni}|$ is largest for the hydrogen function with n=i+1 and $|c_{n=i+1,i}|$ increases with increasing i. The amount by which $c^2_{n=i+1,i}$ differs from unity measures the degree of "n-spoiling" and this varies with the best fitting parameters as shown in the Table 1.II

Table 1.II

r_o (a.u.)	c_{21}^2 (E_i=0.15055)	c_{87}^2 (E_i=0.00802)
2.5	0.814	0.964
3.0	0.781	0.956
3.5	0.767	0.953
4.0	0.762	0.949

Table II shows that the amount of n spoiling decreases with increasing n, but is a function of the model potential.

Figure 1.I

Curve of Best-fitting parameters for oxygen $ns(^3S_o)$ Rydberg series

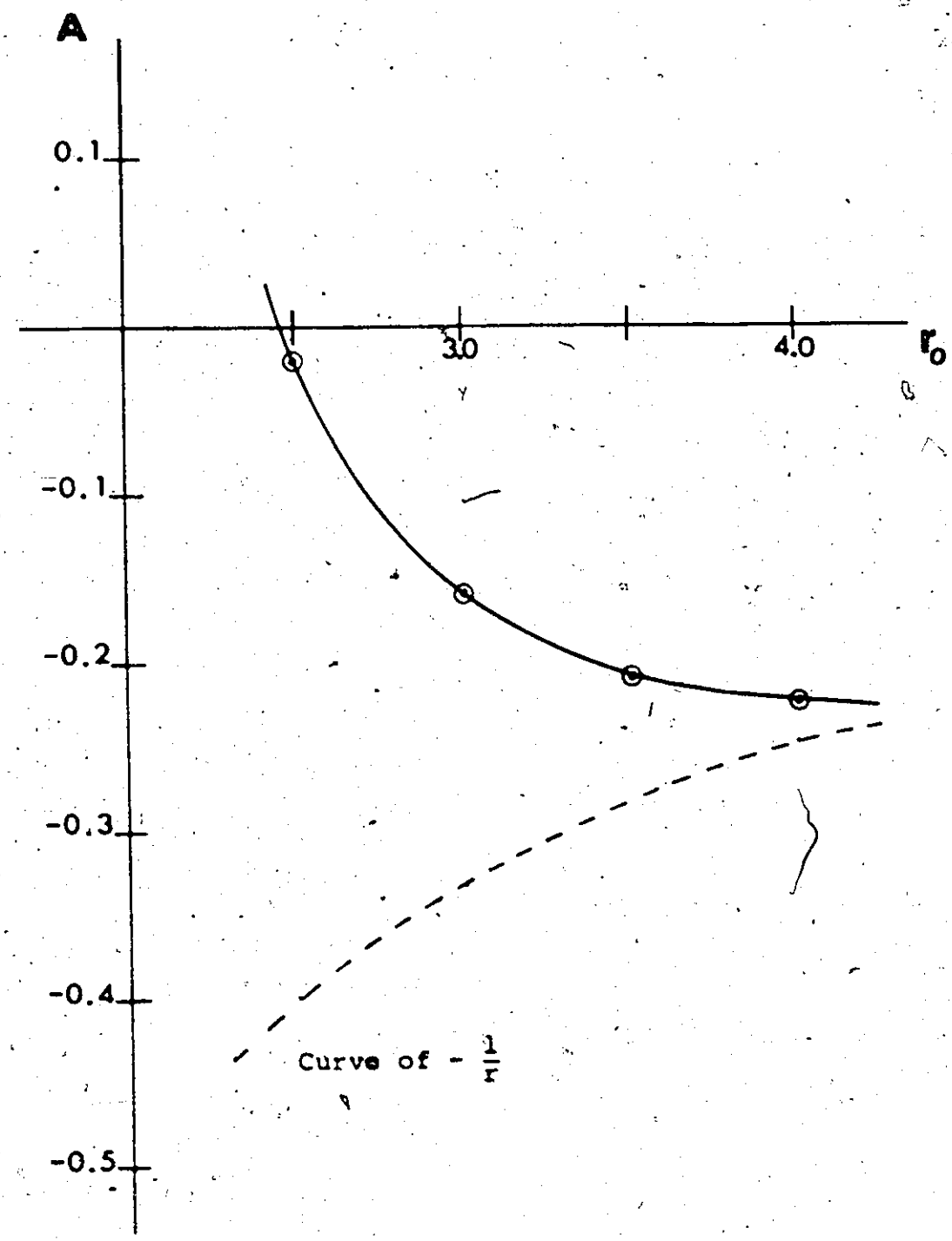

The amount of n spoiling is smaller when r_o is smaller but is never more than 25% even for the largest r_o used. Consequently the first s Rydberg orbital of an oxygen atom has considerable hydrogen 2s character. It should be emphasized however that this conclusion is not incompatible with the usual 3s designation of the lowest s-Rydberg level of oxygen. The designation 3s is made because the lowest possible Rydberg AO of oxygen must have $n_c - \ell$ innermost loops, where n_c is the number of occupied core precursors, plus one phase shifted hydrogenic outer loop giving a total of three loops. A model wavefunction does not reproduce the nodes or loops of the real one-electron wavefunction inside the core because, in the determination of the model wavefunction, the orthogonality constraints applying to the real one-electron wavefunction are replaced by a model (psuedo) potential which removes the oscillations of the real function inside the core; the model wavefunction is an accurate representation only of the largest loop of the real wavefunction which is situated outside the ion core. Our calculation shows that this outermost loop is somewhere between 75 and 82% hydrogen 2s like with smaller amounts of hydrogen 1s, 3s, 4s ... etc mixed in.

The 7% uncertainty in the exact form of the outermost loop arises from the corresponding uncertainty in the optimum choice of the parameters A and r_o. An ambiguity in the model potential parameters appropriate to a model wavefunction is to be expected when two quantities (A and r_o) are varied to obtain

agreement with one quantity, an energy eigenvalue. If unique model potential parameters are to be obtained a second quantity characteristic of the model wavefunction and dependent on the parameters must be found.

As we have seen variation of A and r_o changes not only the eigenvalue, E_i, but also the eigenvectors, (the c_{ni}), of a model wavefunction. Changing the eigenvectors changes the relative amount of a particular hydrogen function in a model wavefunction and consequently changes r_{Max}, the position of the radial maximum of the function. Unique values of model potential parameters could be determined if A and r_o were optimised not only to E_i but also to r_{max}.

It may appear that r_{max} is not a readily accessible quantity but the discussion on pp 14-16 shows that the quantum defect provides a connection between the energy of a Rydberg term and the phase-shift of a hydrogen function with the same energy. This suggests a convenient procedure for the determination of r_{max} for any Rydberg A.O. which will be applied here to the case of an oxygen 3s term:

A hydrogen 3s function is,

$$R^{Hy}_{3s}(r) = N\, e^{-1/3r}(1-0.66667r + 0.074074\, r^2)$$

and

$$E_{3s} = -\frac{1}{2\times 3^2} = -0.05556 \text{ a.u.}$$

An oxygen 3s term has energy -0.15055 a.u. and a hydrogenic function $R_{3s}'(r)$ with the same energy is,

$$R_{3s}'(r) = Ne^{-1/3(Zr)}(1-0.66667(Zr) + 0.074074(Zr)^2)$$

where

$$E_{3s}' = -0.15055 = -\frac{Z^2}{2x3^2}$$

so that

$$Z = 1.646$$

Hence

$$R_{3s}'(r) = N\, e^{-0.5487}(1-0.0975r + 0.2007r^2)$$

The function $[R_{3s}'(r)]^2 r^2$ has been plotted in Fig. 1.II together with an hydrogen 3s function $[R_{3s}(r)]^2 r^2$. The curves show that $[R_{3s}(r)]^2 r^2$ has the radial maximum of it's outermost loop situated at r~13.0 a.u., while $[R_{3s}'(r)]^2 r^2$ has this loop pulled in to r~8.0 a.u. The arguments presented on pp 14-16 indicate that the real one-electron oxygen 3s wavefunction behaves at large r like $R_{3s}'(r)$ but with an inward phase shift of τu_{3s} or 3.7 a.u. (See Equation 1.43). Thus the oxygen 3s wavefunction should have a radial maximum situated at r_{max}=8.0-3.7 or 4.3 a.u.

Before showing how knowledge of r_{max} enables a unique choice of A and r_o to be made it will be shown that our estimated value of r_{max} for an oxygen 3s wavefunction is in good agreement with values of r_{max} obtained by two alternative methods:

1. H. Hosoya[29] has calculated Rydberg orbitals for the atoms Li(I)-F(I) using linear combinations of Slater orbitals with exponents determined by energy and virial optimisation. Hosoya's Rydberg orbitals take the general form,

Fig. 1.II

Hydrogen 3s Function $R_{3s}(r)$ Compared with a Hydrogenic Function $R'_{3s}(r)$ Having the Same Energy as an Oxygen 3s Orbital

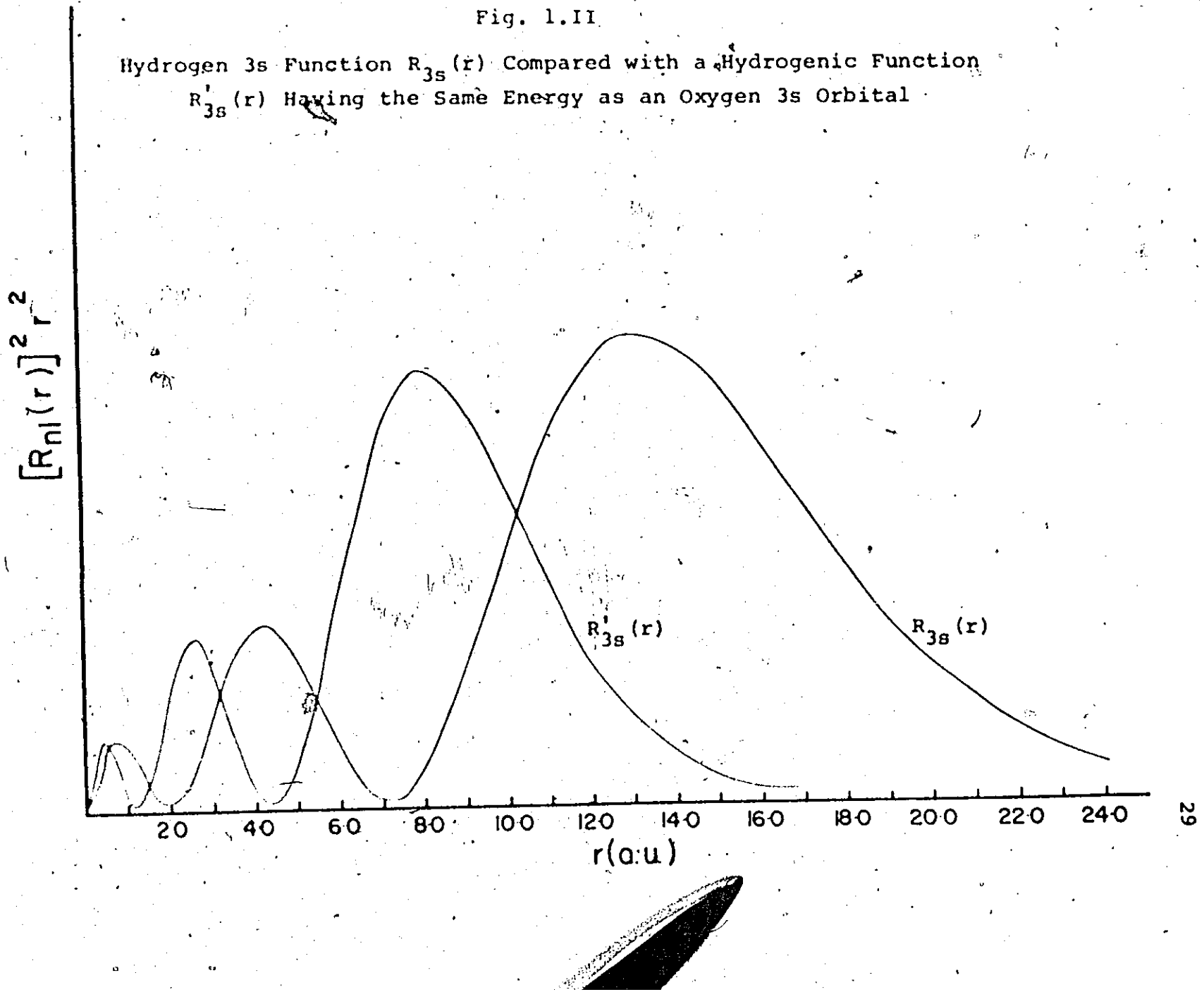

$$R_{n\ell}(r) = \sum_{\alpha=1}^{n-\ell} c_{n\ell\alpha} S(\ell+\alpha, \mu_\alpha)$$

where $S(n,\mu)$ is a Slater atomic orbital;

$$S(n,\mu) = (2\mu)^{n+1/2}[(2n)!]^{-1/2} r^{n-1} e^{-\mu r}$$

For an oxygen 3s function Hosoya gives,

$$R_{3s}(r) = 0.038125\, S(1,7.7) - 0.045052\, S(2,2.45) + 1.004047\, S(3,0.645) - 0.119828\, S(3,3.73)$$

This function (see Fig. 1.III) has $r_{max} = 4.65$ a.u.

2. The procedure of Abarankov and Heine[14] can be used in which the oxygen 3s wavefunction is plotted using tables of coulomb wavefunctions[24] and the observed oxygen 3s term energy. The radial maximum of this function is 4.25 a.u. (See Fig. 1.III)

The use of values of r_{max} in obtaining unique values of A and r_o can be seen from Fig. 1.111 where oxygen 3s model wavefunctions, for two sets of parameters taken from table 1.I, are plotted together with Hosoya's oxygen 3s function and the coulomb wavefunction discussed in (2) above.

The curves show that the model wavefunction, which will be denoted $\psi_{nl}(A,r_o)$, is smooth inside the ion core as expected from the discussion on p. 26. $\psi_{3s}(A,4.0)$ has an r_{max}=3.85 a.u. while $\psi_{3s}(A,2.5)$ has r_{max}=4.15 a.u. Our estimated value of r_{max} was 4.3 a.u. which shows that $\psi_{3s}(A,2.5)$ is a better approximation to the real oxygen 3s wavefunction outside the core than $\psi_{3s}(A,4.0)$

Fig. 1.III

Comparison of Model Wavefunctions with Other Wavefunctions

		r_{max} (a.u.)
1.	Hosoya's Wavefunction,[29]	4.65
2.	Coulomb Wavefunction,[24]	4.25
3.	Model Wavefunctions, $\psi(A,2.5)$	4.15
4.	$\psi(A,4.0)$	3.85

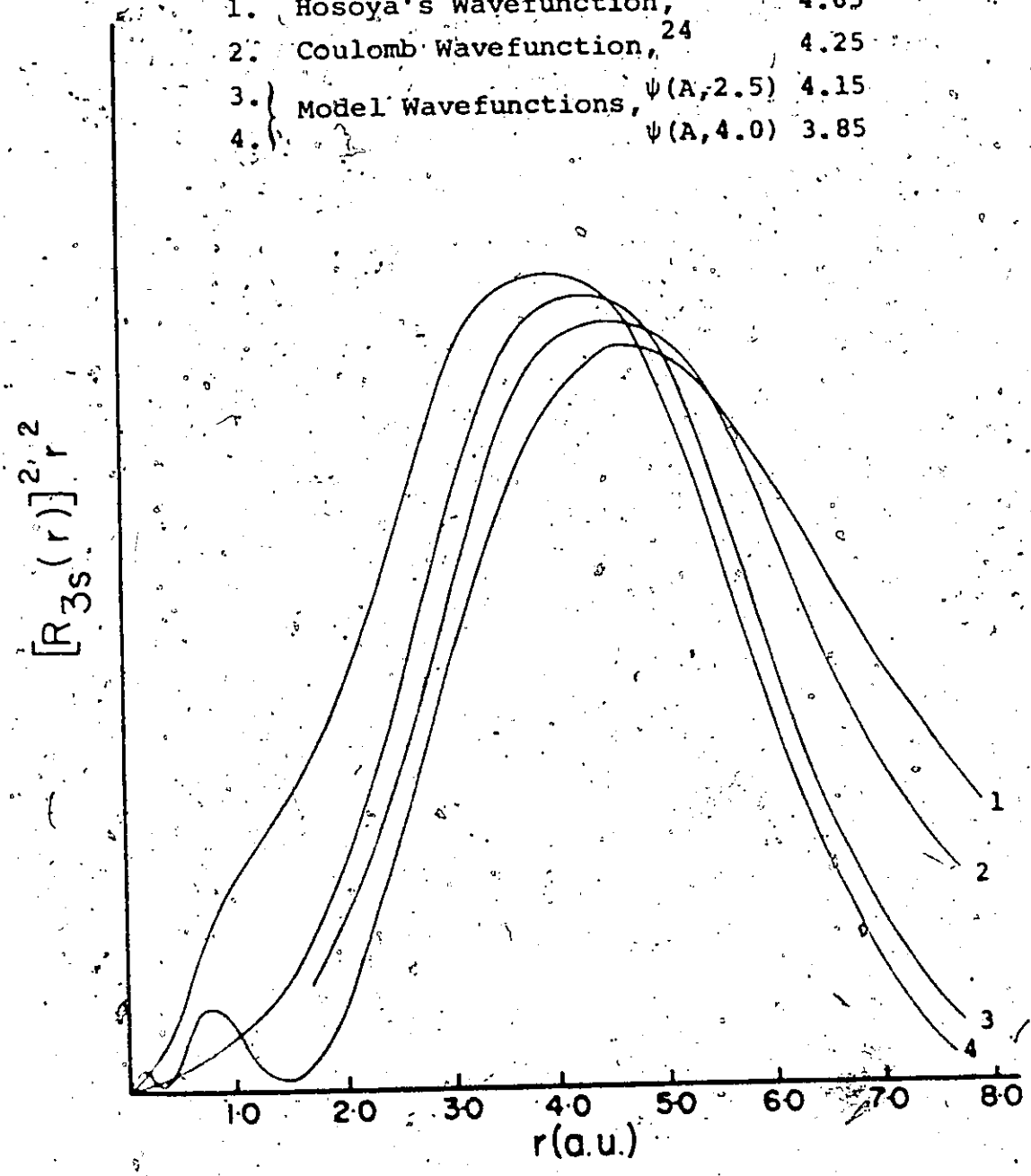

Unfortunately r_{max} is not a very sensitive function of r_o but the procedure outlined here indicates a useful method for estimating optimum values of r_o with more certainty than any method of which the author is aware.

CHAPTER 2

Atomic Model Potentials and the Calculation of Molecular Rydberg Series

2.1 Introduction

In Chapter 1 it was shown that simple atomic model potentials can be used to reproduce accurately Rydberg term series in atomic spectra. We shall now investigate how these atomic model potentials may be used to calculate molecular Rydberg series. In going from the atomic to the molecular case we are naturally interested in what happens to atoms when they combine to form a molecule. This is an extremely complex question to which no simple answer can be given, but a useful start can be made on the problem by considering the two limiting cases of the united-atom and the separated atoms. In the former case the behaviour of the energies of the atomic orbitals is investigated when a "united-atom" nucleus, composed of all the nuclei in the molecule, is split to give slightly separated atoms, while in the latter case the effect of bringing together infinitely separated atoms to form a molecule is studied. Both of these approaches are useful in molecular calculations because the effects on atomic energy levels of slightly separating a united atom or bringing together infinitely separated atoms will be small and can be included as a perturbation to a Hamiltonian which contains purely atomic terms. In special cases the perturbation may be small

even at the equilibrium nuclear spearation; the united-atom limit of small polyatomic hydrides such as CH_2, H_2O, CH_4 etc. is especially important in this respect.

In this chapter we shall use both the united-atom and separated atom concepts to investigate ways of using atomic model potentials for the calculation of molecular Rydberg series.

2.2 The United-Atom Approach

The positions of all the N nuclei in a molecule can be expressed in spherical polar coordinates R_i, θ_i, ϕ_i about an origin located at the centre of nuclear charge. If it is assumed that the electronic energy, E, of the molecule is finite at all R_i, E is an analytic function of the R_i and can be expanded in a convergent power series about $R_i=0$ in powers of R_i:

$$E = E_o + \sum_i E_i R_i + \sum_{i \leq j} E_{ij} R_i R_j + \ldots \qquad 2.1$$

The leading term, E_o, in equation 2.1 is referred to as the energy of the "united-atom" (i.e. the atom having atomic number $Z = \sum_{i=1}^{N} Z_i$), and the higher terms represent the effects of slightly separating the nuclei.

C. E. Wulfman[30] has shown that the first non-zero terms of this expansion are quadratic in the nuclear separations and that there is a zero-order quadratic perturbation of united-atom one-electron states with the same energy and azimuthal quantum number ℓ. W. A. Bingel[31] has given expressions

for the quadratic expansion coefficients in terms of the total electronic charge density of the united-atom and the charge density at the united-atom nucleus. However, these expressions require at least approximate united-atom core wavefunctions and are not suitable for use in model potential calculations.

Quadratic expansion coefficients have been evaluated without knowledge of united-atom core wavefunctions by H. Hosoya[32] for the special case of non-penetrating Rydberg orbitals. In this case the molecular-ion core can be treated as a cluster of point charges with a specified geometry and the Rydberg orbital can be well approximated by a hydrogen orbital.

In order to include penetrating Rydberg orbitals in a calculation of this type the effect of the united-atom core must be taken into account. Our atomic model potential calculations demonstrate how this may be done for atoms and we shall now suggest a method by which these atomic calculations may be extended to a united-atom treatment of the Rydberg series of triatomic molecules.

Let us assume the united-atom appropriate to a linear triatomic molecule has Rydberg term series with energies E_i which can be represented by the eigenvalues of a model Hamiltonian,

$$H^o \psi_i = E_i^o \psi_i \qquad 2.2$$

where $H^o = T^o + V^o$ with $$V^o = \begin{cases} A & ; \ r \leq r_o^o \\ -\frac{1}{r} & ; \ r \geq r_o^o \end{cases} \qquad 2.3$$

The ψ_i are model Rydberg orbitals composed of linear combinations of hydrogen functions:

$$\psi_i = \Sigma \, c_{ni} \, R_{n\ell}(r) \, Y_\ell^M(\theta,\phi) \qquad 2.4$$

The effect of splitting the united-atom to form a linear triatomic molecule, ABC, may be approximated by considering spheroidal deformations of the united-atom core with model radius r_o. The core will then be an ellipsoid governed by the equation:

$$r(\theta) = r^o[1 + \alpha(\tfrac{3}{2}\cos^2\theta - \tfrac{1}{2})] \qquad 2.5$$

where θ is defined in Fig. 2.I and is such that,

$$r(o) = \underline{a} \quad ; \quad r(\tfrac{\pi}{2}) = b \qquad 2.6$$

$\underline{a}$ and b being the semi-major axes of the ellipse.

α is related to the eccentricity ϵ by:

$$\epsilon = \frac{a-b}{r_o^o} \quad ; \quad \alpha = \frac{2}{3}\epsilon \qquad 2.7$$

(i) Outside the core

We shall treat the deviation of the potential from a central field as a perturbation. Outside the ion core this will be:

$$\Delta V_{out} = [-\frac{Z_A}{r_A} - \frac{Z_B}{r_B} - \frac{Z_C}{r_C} + \frac{1}{r_C}] \qquad 2.8$$

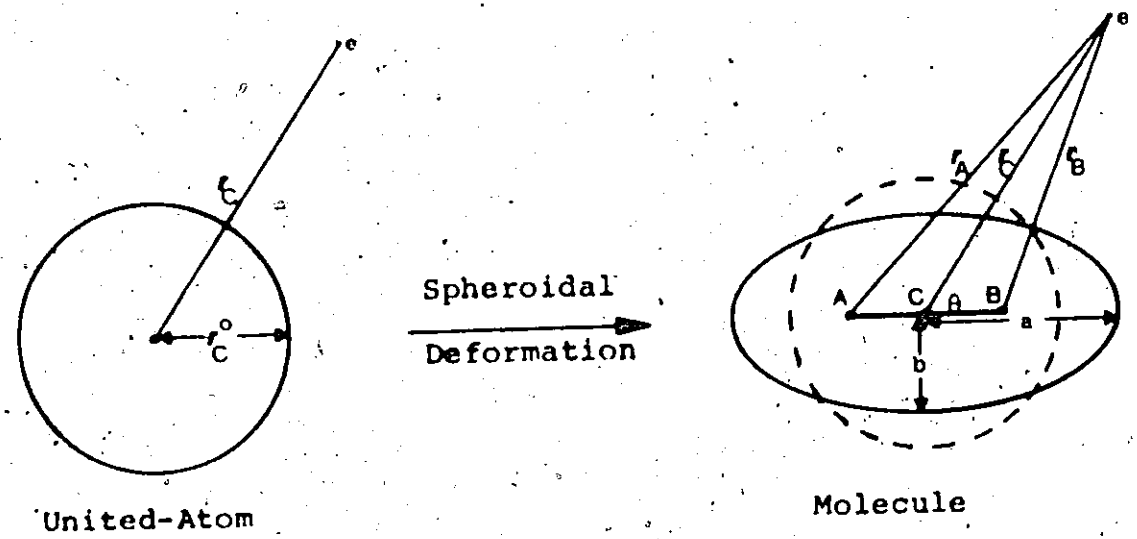

Fig. 2.I

Co-ordinates for the United-Atom Calculation

For the special case of a symmetrical molecule with $Z_A = Z_B = Z$,

$$\Delta V_{out} = 2Z\left[\frac{1}{r_C} - \frac{1}{r_A}\right] \qquad 2.9$$

The first-order energy charge is:

$$\Delta E_i = \int \psi_i \, \Delta V \, \psi_i \, d_\tau \qquad 2.10$$

so from equation 2.4

$$[\Delta E_i]_{out} = 2Z \sum_{n} \sum_{n'} c_{ni} \, c_{n'i} \left[\left\{\int_{r(\theta)}^{\infty} R_{n\ell}(r_C)\frac{1}{r_C} R_{n'\ell}(r_C) r_C^2 dr_C - \int_{r(\theta)}^{\infty} R_{n\ell}(r_C)\frac{1}{r_A} R_{n\ell}(r_C) r_C^2 dr_C\right\} \times \int_{\theta,\phi} \{V_{\ell,m}(\theta,\phi)\}^2 \sin\theta d\theta d\phi\right] \qquad 2.11$$

$R_{ni}(r)$ is a slowly varying function of r in the range $r(\theta)$ to r_C^o. We shall assume the limit $r(\theta)$ can be replaced by r_C^o without serious error.

The only integral in equation 2.11 not already evaluated in the atomic calculations (pp 17 -20) is:

$$I_A = \int_{r_C^o} \int_{\theta,\phi} R_{ni}(r_C) \frac{1}{r_A} R_{n\ell}(r_C) r_C^2 \{Y_{i,m}(\theta,\phi)^2 \sin\theta\} dr \, d\theta d\phi \qquad 2.12$$

We shall consider the case of p-functions for which,

$$I_A = N N' \sum_{s=0}^{n-2} \sum_{t=0}^{n'-2} B_{ns} B_{n't} \left(\frac{2}{n}\right)^{s+1} \left(\frac{2}{n'}\right)^{t+1} Q_{st} \qquad 2.13$$

where

$$N = \sqrt{\frac{4(n-2)!}{n^4[(n+1)!]^3}} \qquad 2.14$$

and the B_{ns} are expansion coefficients for the Laguerre polynomials occurring in $R_{n\ell}(r)$[33].

Q_{st} is the integral left to be evaluated:

$$Q_{st} = \int_{r_C}^{\infty} \int_{\theta,\phi} r_C^{s+1} e^{-r_C/n} \frac{1}{r_A} r_C^{t+1} e^{-r_C/n} \begin{Bmatrix} \cos^2\theta \\ \sin^2\theta\cos^2\phi \end{Bmatrix} d\tau \qquad 2.15$$

with $\alpha_n = \frac{1}{n}$ and $\beta_n = \frac{1}{n}$,

$$Q_{st} = (-1)^{s+t} \frac{\partial^{s+t}}{\partial\alpha_n{}^s \partial\beta_n{}^t} Q_{00} \qquad 2.16$$

If Q_{00} is known Q_{st} can be determined using this equation.

Q_{00} was evaluated by a transformation to elliptical coordinates as shown in Fig. 2.II. Elliptical coordinates are defined by the equations:

$$\mu = \frac{r_C + r_A}{R} \; ; \quad \nu = \frac{r_C - r_A}{R} \; ; \quad \phi = \phi \qquad 2.17$$

$$1 \leq \mu \leq \infty \qquad -1 \leq \nu \leq 1 \qquad 0 \leq \phi \leq 2\pi$$

$$d\tau = \frac{R^3}{8}(\mu^2 - \nu^2)\,d\mu\,d\nu\,d\phi \qquad 2.18$$

After evaluation:

$$[Q_{00}]_{p\sigma} = \frac{\pi R^4}{8} \left\{\frac{1}{15}[10\,C_3(a,u) + 16\,C_1(a,u)]\right\} \qquad 2.19a$$

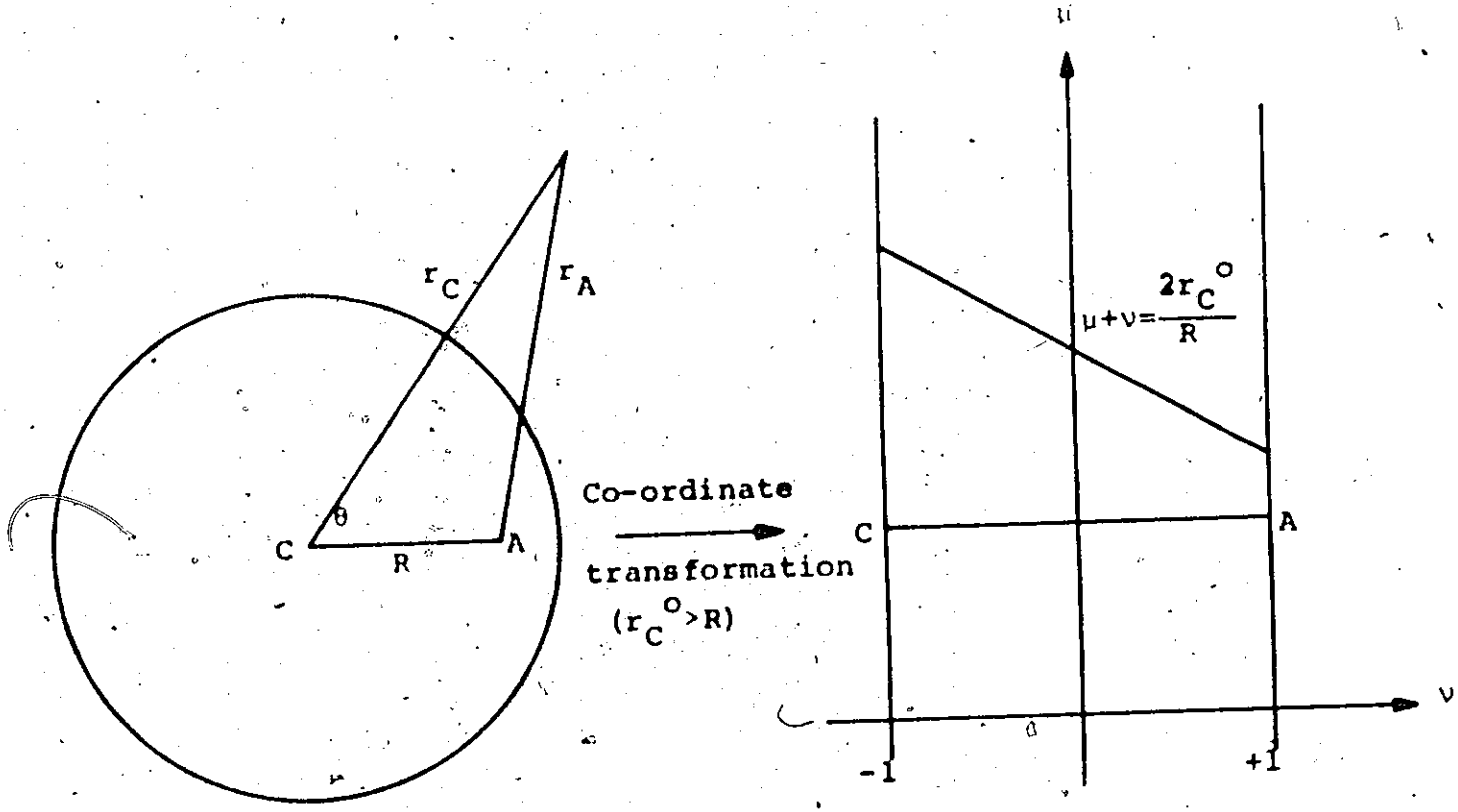

Fig. 2.II

Co-ordinate Transformation for United-Atom Calculation

and,

$$[Q_{oo}]_{p\pi} = \frac{\pi R^4}{8} \cdot \{\frac{1}{15}[10\ C_3(a,u) - 8\ C_1(a,u)]\} \qquad 2.19b$$

where

$$C_n(a,u) = \int_{\mu}^{\infty} x^n\ e^{-ax}\ dx = e^{-au} \sum_{k=0}^{n} \frac{n!}{k!} \frac{u^k}{a^{n-k+1}} \qquad 2.20$$

$$\text{with } a = \frac{R}{2}\ [\frac{1}{n} + \frac{1}{n'}] \qquad 2.21$$

$$\mu + \nu = \frac{2r_o^c}{R} = u$$

A computer programme was written using equations 2.12-2.21 for the evaluation of I_A. I_A values were checked by numerical integration using a 72-point Gaussian quadrature programme.

(ii) Inside the core

If the difference between the potentials of the deformed and undeformed core is ΔV_{in} we have,

$$[\Delta E_i]_{in} = \sum_n \sum_{n'} c_{ni}\ c_{n'i} \int_{r_c^o}^{r_c(\theta)} \int_{\theta,\phi} R_{nl}(r_c)\Delta V_{in} R_{n'l}(r_c)\{Y_{i,m}(\theta,\phi)\}^2$$

$$r_c^2 \sin\theta dr d\theta d\phi \qquad 2.22$$

$[\Delta E_i]_{in}$ may be evaluated by following the closely related theory of deformed nuclei given by H. Kopfermann.[34] $R_{nl}(r)$ is a slowly varying function of r and can be taken outside the integral over r:

$$[\Delta E_i]_{in} = A \sum_n \sum_{n'} c_{ni} c_{n'i} R_{nl}(r_c^o) R_{n'l}(r_c^o) \int_{r_c^o}^{r_c(\theta)} \int_{\theta,\phi} r_c^2 dr\{Y_{i,m}(\theta,\phi)\}^2$$

$$\sin\theta d\theta d\phi \qquad 2.23$$

where A is the united-atom core potential.

From equations 2.5 and 2.7, neglecting terms in ε^2 and ε^3 (i.e. for small deformation):

$$[\Delta E_i]_{in} = \frac{A\varepsilon (r_c^o)^3}{3} \sum_n \sum_{n'} c_{ni} c_{n'i} R_{n\ell}(r_c^o) R_{n'\ell}(r_c^o) I_{\ell m} \qquad 2.24$$

where

$$I_{\ell m} = \int_{\theta,\phi} 2\left(\frac{3}{2}\cos^2\theta - \frac{1}{2}\right)\{Y_{\ell,m}(\theta,\phi)\}^2 \sin\theta d\theta d\phi \qquad 2.25$$

The integral $I_{\ell m}$ is related to the quadrupole moment of the deformed core and is well known in the theory of angular momentum[35]. Explicitly,

$$I_{\ell m} = \frac{\ell(\ell+1) - 3m^2}{(2\ell-1)(2\ell+3)} \qquad 2.26$$

Hence for $p\sigma$ and $p\pi$ orbitals,

$$I_{p\sigma} = \frac{2}{5} \quad ; \quad I_{p\pi} = -\frac{1}{5} \qquad 2.27$$

The formulae derived in the previous pages were used to construct computer programmes for the evaluation of $[\Delta E_i]_{in}$ and $[\Delta E_i]_{out}$. The calculation was applied to particular molecules with the assumption of maximum charge separation ($Z_A = A_B = \frac{1}{2}$, $Z_C = 0$) and ε, the eccentricity of the ellipsoid, was left as an unknown quantity to be determined by comparison with experimental data.

As we have mentioned previously (p.34) the united-atom approach is especially useful for the description of hydrides

of the type XH_n. Unfortunately np-Rydberg series in linear XH_2 molecules (e.g. CH_2) are not well established, but np series are well known for bent XH_2 molecules in general, and for H_2O in particular.

A p orbital centred on the X atom of a bent XH_2 molecule will transform like either an a_1, b_1 or b_2 representation of the C_{2v} point group. The pa_1 and pb_2 orbitals may be formed from suitable combinations of the $p\sigma$ and $p\pi$ orbitals appropriate to linear XH_2, but the pb_1 orbital is identical with the $p\pi$ orbital of linear XH_2. Consequently the formulae we have derived for $np\pi$ orbitals in linear XH_2 can be applied to npb_1 orbitals in bent XH_2.

Calculations were carried out on the npb_1 Rydberg series of H_2O using the united-atom Ne described by a model potential with A = -0.38 and r^o = 2.5 a.u. Calculated series were compared with experimental series tabulated by T.F. Lin and A.B.F. Duncan.[36] The optimum ε value for the core (see equation 2.24) was found to be 0.12. ΔE values are given in Table 2.I with $\Delta E_{tot} = \Delta E_{out} + \Delta E_{in}$.

Table 2.I

	Calculated			Observed
n	ΔE_{out} (a.u)	ΔE_{in} (a.u.)	ΔE_{tot} (a.u.)	ΔE_{tot} (a.u.)
3	.00701	.00447	.01148	.01209
4	.00198	.00172	.00370	.00364
5	.00092	.00090	.00182	.00178

Discussion

The quantum defect for a molecular Rydberg series, μ_{Mol}, can be divided into two parts:

$$\mu_{Mol} = \mu_{pen} + \mu_{c.s.}$$

μ_{pen} is an atomic-like term arising from the spherical, but non-coulombic, contributions to the potential inside the core while $\mu_{c.s.}$, where c.s. stands for core-splitting, is a strictly molecular term representing the effects of the non-spherical part of the potential field inside and outside the core.

In the model potential calculations presented here μ_{pen} can be determined from the model potential of the united-atom and we have also shown how the molecular term $\mu_{c.s.}$ can be estimated.

In view of the approximate nature of our united-atom model the conclusions to be drawn from this calculation are probably only of a rough quantitative nature. Nevertheless the model does give useful information on the origin of the symmetry splittings in XH_2 molecules and thereby the relative contributions to $\mu_{c.s.}$ from inside and outside the ion core. Thus while it is well established that the radial maximum of a molecular Rydberg wavefunction is located well outside the ion core, our calculation shows that about one-half of the energy level splittings due to the non-spherical part of the potential comes from Rydberg electron density inside the ion core. Similar conclusions have been reached for p series in H_2 by G. Herzberg and C. Jungen[37].

Evidently this surprising result comes about because the deviation of the potential from a central field is much larger inside the ion core than well outside, and apparently this is more important than the fact that the probability of finding the Rydberg electron inside the core is very small.

2.3 The Separated Atom Approach

(i) General Discussion

The results of Section 2.1 show that model potential calculations of molecular Rydberg series can be successful only if an accurate representation of the ion-core potential is used. A united-atom model is restricted in practical applications to hydride molecules and we shall therefore consider the more useful separated atom approach in greater detail. We shall show how a model potential applicable to any molecule can be constructed from combinations of separated atom model potentials and discuss the use of these models in calculating Rydberg series in linear triatomic molecules.

In order to bring out the important features of separated atom model potential calculations we shall first develop the theory for a diatomic molecule AB, and then show how it may be extended to polyatomic molecules.

Consider a Rydberg electron moving in the field of a spherical core A with residual charge Z_A, and suppose the observed eigenenergies $E_A(nl)$ of the Rydberg states can be reproduced by a model potential $V_A(r_A)$. The formation of a molecule can be imagined by bringing up a second atom B with Rydberg energies $E_B(nl)$ described by a model potential $V_B(r_B)$.

The combined system is governed by the one-electron Schrödinger equation:

$$\{-\frac{1}{2}\nabla^2 + V_A(r_A) + V_B(r_B) + V_{AB}(R) - E_k(R)\}\psi_k = 0 \qquad 2.28$$

where ψ_k is the wavefunction of the Rydberg electron with energy E_k. $V_{AB}(R)$ represents the effects of bonding interactions between the two cores separated by a distance R. This interaction takes the form:

$$V_{Bonding} = \sum_{i=A}\sum_{j=B}\{\frac{1}{r_{ij}} - \frac{Z_A}{r_{Aj}} - \frac{Z_B}{r_{Bi}} + \text{Core-Core Polarisation Terms}\} \qquad 2.29$$

where $\sum_{i=A}$ represents a summation over all the electrons associated with atom A etc.

Diatomic molecules such as Li_2 and Na_2 have large equilibrium nuclear separations and it is valid to assume that the core electrons do not contribute to the binding of the molecule[38,39]. In this case $V_{AB} \sim 0$ except for small polarisation terms ($\sim\frac{1}{R^4}$). The (weak) binding in these molecules is due to the Rydberg electron moving in the potential field of the two atomic ion cores. For most diatomic molecules, however, the binding arises from an overlapping of the two cores when R_{equilb} is less than the sum of the core radii of the constituent atoms and $V_{AB} \not\sim 0$.

In view of the complex form of V_{AB} a number of molecular model potential calculations have been carried out in which V_{AB}

is ignored completely[25,26,40]. Certainly the neglect of V_{AB} is a valid first approximation because the interatomic interactions which V_{AB} represent are much smaller than the intra-atomic interaction terms V_A and V_B. The effects of ignorning $V_{AB}(R)$ will be discussed later in this chapter.

(ii) Model Potentials for Polyatomic Molecules

The discussion of the previous pages suggests that, for any polyatomic molecule, the potential in which a Rydberg electron moves can be constructed from a sum of atomic contributions:

$$V_{Mol} = \sum_{i}^{Atoms} V_i(r_i) \qquad 2.30$$

In this thesis the V_i are represented by the atomic model potentials discussed in Chapter 1. Each atom i has a core region bounded by a sphere of radius r_i^o centred at the i^{th} nucleus. Inside the core the potential is a constant, A_i, and outside the core the potential is coulombic and depends on the partial charge δZ_i to be associated with the atom i.

Thus:

$$V_i = \frac{Z_i}{r_i} \quad ; \quad r_i \geq r_i^o$$

$$V_i = A_i \quad ; \quad r_i \leq r_i^o \qquad 2.31$$

If the molecular core has a net charge Z_C then,

$$Z_C = \sum_{i}^{Atoms} \delta Z_i \qquad 2.32$$

This molecular model was proposed by A.U. Hazi and S.A. Rice[25] and used for the calculation of Rydberg series in diatomic molecules by these authors and also by T. Betts and W. McKoy[26]. However, as we pointed out previously (p.21), both of these authors used arbitrary values of r^o and the uniqueness of their calculated Rydberg series is questionable. In Chapter 1 it was shown that the ambiguity in the optimum values of the model parameters A and r^o can be eliminated by comparing the model wavefunctions to phase-shifted hydrogen functions to ensure the correct asyptotic behaviour of the model wavefunction.

(iii) The Model Potential for CO_2

In order to calculate Rydberg series for CO_2 optimum atomic model potentials for carbon and oxygen were obtained and it was found that the r^o values for these atoms fall in the range 2.0-2.5 a.u.. The final selection of exact r^o values for carbon and oxygen was based on the observation that the C-O bond length of 2.22 a.u. found in the ground state of CO_2^+ [54] lies in the range of optimum r^o values for these atoms. In addition it was found that allowing the model radius of one atom to pass through the nucleus of the adjacent atom (i.e. setting r^o equal to the bond length) greatly simplified the evaluation of certain integrals important to the calculation of CO_2 Rydberg series. For this reason the r^o's used in calculations on CO_2 were chosen as follows:

$$r_c^o = r_o^o = r_{CO_2} \text{ (C-O)} = 2.22 \text{ a.u.}$$

where r_c^o is the r^o for carbon,

r_o^o is the r^o for oxygen.

Calculated charge distributions for CO_2[41] indicate that the selection of the same model radius for carbon and oxygen is probably a good approximation.

(iv) The Model Potentials for CS_2 and CSe_2

R.F.W. Bader et. al.[41] studied the charge distributions of CO_2, CS_2 and OCS and in particular the changes occurring in the charge population about the carbon atom as the bonding environment is changed. Their conclusions indicate that r_c^o, the model radius for carbon, should remain essentially unchanged in going along the series CO_2, CS_2, CSe_2. Hence, in constructing V_{Mol} for CS_2 and CSe_2, we set r_c^o equal to the same value as r_c^o in CO_2 and, in keeping with the V_{Mol} chosen for CO_2, r_s^o and r_{Se}^o were set equal to r_{CS_2} + (C-S) and r_{CSe_2} + (C-Se) respectively.

A schematic cross-sectional representation of the model potentials used for CO_2 and CS_2 is given in Fig. 2.III.

Table 2.II

Atomic Model Potential Parameters used in the Calculation of CO_2, CS_2 and CSe_2 Rydberg Terms

	C	O	S	Se
r^o (a.u.)	2.196	2.196	2.938	3.233
A_s	1.10	0.11	0.08	0.01
A_p	-0.14	-0.04	-0.01	-0.02

Fig. 2.III

Model Potentials for CO_2 and CS_2

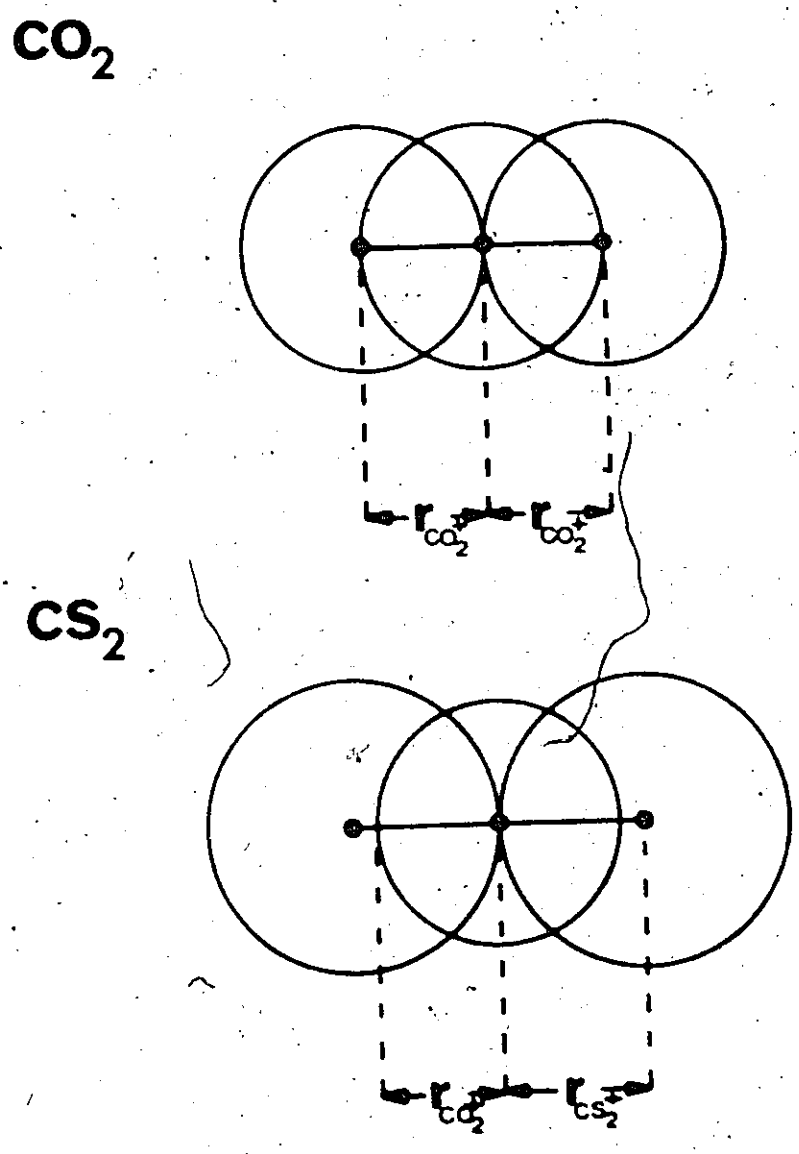

2.4 Expansion of the Molecular Rydberg Wavefunction

In order to calculate molecular Rydberg series we must look for a suitable expansion of the Rydberg wavefunction to use in conjunction with the molecular model potentials described in section 2.3

Consider the case of a Rydberg electron moving in the field of a linear symmetric YX_2^+ ion core. If there is a maximum separation of the net charge on the ion, the Rydberg electron moves in a field which is indistinguishable from that of the diatomic ion X_2^+ outside the core.

R.S. Mulliken[10,42] has pointed out that the MO's of H_2^+ serve as useful prototypes for the Rydberg MO's of homonuclear diatomic molecules because these MO's behave asymptotically like phase-shifted H_2^+ MO's. We therefore expect a knowledge of H_2^+ wavefunctions to be useful in understanding the nature of Rydberg MO's in the same way that hydrogen functions are used as a starting point in the study of atomic Rydberg orbitals.

The wavefunctions of H_2^+ have been studied in detail by D.R. Bates et. al.[43]. The one-electron Schrödinger equation for H_2^+ is separable in confocal-elliptical coordinates:

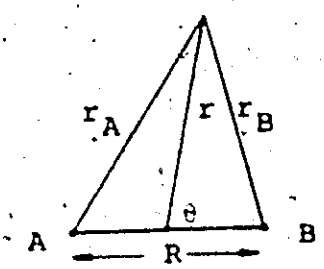

Figure 2.IV
H_2^+ co-ordinates

$$\mu = (r_A - r_B)\frac{R}{2} \quad ; \quad \lambda = (r_A + r_B)\frac{R}{2} \qquad 2.33$$

$$H\Psi(r_A,r_B,R) = E(R)\ \Psi(r_A,r_B,R) \qquad 2.34$$

$$\Psi(r_A,r_B,R) \xrightarrow[\text{Elliptical co-ords}]{\text{Transform to}} \Psi(\lambda,\mu,\phi) = \Lambda(\lambda)\ M(\mu)\Phi(\phi) \qquad 2.35$$

Separation of the variables λ, μ and ϕ leads to three equations:

$$\Phi(\phi) = \{\begin{matrix}\cos\\ \sin\end{matrix}\}(m\phi) \qquad 2.36$$

$$\frac{d}{d\mu}\{(1-\mu^2)\frac{d\mu}{d\mu}\} + \{-A + p^2\mu^2 - \frac{m^2}{1-\mu^2}\}\mu = 0 \qquad 2.37$$

$$\frac{d}{d\lambda}\{(\lambda^2-1)\frac{d\Lambda}{d\lambda}\} + \{A + 2R\lambda - p^2\lambda^2 - \frac{m^2}{\lambda^2-1}\}\Lambda = 0 \qquad 2.38$$

where p, A' and m are separation constants with,

$$p^2 = -\frac{1}{4}R^2 E \quad \text{and} \quad A' = A - p^2 \qquad 2.39$$

It can be shown[44] that the operators H, A' and L_z form a complete set of commuting observables for H_2^+ and therefore provide a classification of the stationary states of the system.

In the limit of $R \to 0$,

$$\Lambda(\lambda) \to R_{ni}(r)$$
$$M(\mu) \to P_i^{|m|}(\cos\phi) \qquad 2.40$$

and

where the $R_{n\ell}(r)$ are hydrogen radial functions and the $P_\ell^{|m|}(\cos\phi)$ are ~~associated~~ Legendre functions and are part of the hydrogen angular functions.

Because H_2^+ functions are asymptotically separable in spherical polar co-ordinates, the behaviour of H_2^+ wavefunctions near the united-atom limit is similar to their behaviour at very large r. At small R,

$$-A' = \ell(\ell+1) \qquad 2.41$$

and consequently H_2^+ Mo's are hydrogenic in their outermost parts with well defined ℓ values.

At smaller r the non-spherical part of the potential introduces a quadrupolar field which couples states of different ℓ and only the ϕ dependent factor of the wavefunction remains the same as in hydrogen. Nevertheless calculations show[45] that even for the lowest excited H_2^+ orbitals the ℓ-purity is quite high and the wavefunctions are still at least approximate eigenfunctions of ℓ. It is for this reason that H_2^+ Mo's are usually classified according to their united-atom designation.

The ℓ-purity of H_2^+ wavefunctions can be estimated using the eigenfunctions $M(\mu)$ which are usually expanded in terms of the associated Legendre polynomials;

$$M(\mu) = \sum_s{}' \; f_s(\ell,m,p)\; P^m_{m+s}(\mu) \qquad 2.42$$

and $\lim_{R\to 0} \mu = \cos\theta$

The summation in 2.42 is over even values of s if (ℓ+m) is even and over odd values of s if (ℓ+m) is odd. D.R. Bates[43] has tabulated values of the coefficients $f_s(\ell,m,p)$ for many states of H_2^+ as a function of the internuclear separation R. We have used these coefficients as an approximate measure of the ℓ-purity of states for CO_2. With a maximum charge separation on the CO_2^+ point ion core the Rydberg electron at large r moves in the field of a H_2^+ -like system with R=4.4 a.u. and charge $Z=\frac{1}{2}$ on each nucleus. The coefficients f_s' (f_s normalised to 100) for this system are given in table 2.III.

Table 2.III shows that at least 90% of the angular part of the wavefunction is composed of terms with an ℓ value appropriate to the ℓ value of a united-atom designation, and this percentage increases with increasing n. Furthermore, if more terms are required to secure a good approximation to the wavefunction only a few will be needed because the ℓ series are rapidly convergent.

Table 2.III

ℓ-purity of H_2^+ Wavefunctions at R=4.4 a.u., $Z=\frac{1}{2}$

United-Atom Designation	f_0'	f_1'	f_2'	f_3'	f_4'	f_5'
$2s\sigma_g$	91.2	0.0	8.7	0.0	~0.1	0.1
$3s\sigma_g$	95.4	0.0	4.5	0.0	~0.04	0.0
$2p\sigma_u$	0.0	93.8	0.0	6.1	0.0	~0.1
$3p\sigma_u$	0.0	97.6	0.0	2.3	0.0	~0.02

From the tabulated values of f_s' it may be estimated that there will be less than 10% s-d mixing in the lower $ns\sigma_g$ orbitals of CO_2 and less than 7% p-f mixing in the lower $np\sigma_u$ orbitals. However while this means that the maximum error in any CO_2 wavefunction calculated without ℓ-spoiling is probably ~10%, the corresponding error in the calculated term energy is certainly much smaller than this. This is because of a well known property of variationally determined wavefunctions[46]. If ϕ is an approximation to an exact one-electron wavefunction ϕ_n with error $\Delta\phi$, the corresponding error in the energy ΔE is $O(\Delta\phi)^2$. In other words a variational wavefunction good to 10% may give an energy good to 1%.

2.5 The Calculation of Rydberg series in Linear Triatomic Molecules Using a Separated Atom Model

(i) Procedure

The discussion of section 2.4 indicates that the Rydberg orbitals of linear triatomic molecules are very similar to united-atom functions outside the ion-core. Model wavefunctions are not intended to reproduce the precise form of one-electron functions inside an ion core; all that is required is that the combined system of model wavefunction and model potential give the correct relative contributions to the quantum defect from inside and outside the ion core. Since our molecular model potential is constructed from the separated atoms it may be expected that separated atom wavefunctions, $\psi_{S.A}$, must be used.

for the inner parts of the Rydberg wavefunction where,

$$\psi_{S.A.} = \chi_A + \chi_B + \chi_C + \ldots$$

and χ_A, χ_B, χ_C... are functions located at the nucleus of the atoms A, B, C ... etc. However, it appears that united atom functions can also be used inside the molecular ion core. Thus Tien Chi Chen[47] has shown that even in the case of the ground state of H_2^+ ~90% of the $1s\sigma_g$ energy is due to contributions of spherical functions located at the molecular mid-point. Hence, in this section, single centre expansions of linear triatomic Rydberg orbitals will be used. The effects of expanding Rydberg wavefunctions in CO_2 about two centres in the molecule will be discussed in Section 2.6.

Consider the case of a linear molecule a-b-c... . The Schrödinger equation for an electron in a Rydberg orbital ϕ_k is:

$$[-\frac{1}{2}\nabla^2 + \sum_{i}^{\text{Atoms}} V_i(r_i)]\,\phi_k(r_q) = E_k\phi_k(r_q) \qquad 2.43$$

where the Rydberg orbital is centred on the nucleus of atom q. As previously ϕ_k will be represented by a linear combination of hydrogen functions ϕ_{ni} centred on q.

$$\phi_k(r_q) = \sum_{n=1}^{N} c_{nk}\,\phi_{ni}(r_q) \qquad 2.44$$

Equations 2.43 and 2.44 lead to matrix elements $H_{nn'}$ given by,

$$H_{nn'} = \int \phi_{ni}(r_q)[-\frac{1}{2}\nabla^2 + V_q(r_q) + \sum_{i\neq q}^{\text{Atoms}} V_i(r_i)]\phi_{n'i}(r_q)\,d\tau_q \qquad 2.45$$

or,

$$H_{nn'} = \int \phi_{n\ell}(r_q)\left[H + V_q(r_q) + \frac{1}{r_q} + \sum_{i\neq q}^{\text{Atoms}} V_i(r_i)\right]\phi_{n',\ell}(r_q)\,d\tau_q \qquad 2.46$$

where H_o is the hydrogenic Hamiltonian Operator.

Hence,

$$H_{nn'} = \delta_{nn'} E_n + \int \phi_{n\ell}(r_q)\left[V_q(r_q) + \frac{1}{r_q} + \sum_{i\neq q}^{\text{Atoms}} V_i(r_i)\right]\phi_{n',\ell}(r_q)\,d\tau_q \qquad 2.47$$

The E_n are hydrogen eigenenergies in a.u.,

$$E_n = -\frac{1}{2n^2} \qquad 2.48$$

Equation 2.47 shall be written in the form:

$$H_{nn'} = \delta_{nn'} E_n + I_{nn'}(r_q) + I_{nn'}(r_i) \qquad 2.49$$

where

$$I_{nn'}(r_q) = \int_o^{r_q^o} \phi_{n\ell}(r_q)\left\{A_q + \frac{1}{r_q}\right\}\phi_{n',\ell}(r_q)\,d\tau_q + (1-Z_q) \int_{r_q^o}^{\infty} \phi_{n\ell}(r_q)\left\{\frac{1}{r_q}\right\}\phi_{n',\ell}(r_q)\,d\tau_q \qquad 2.50$$

and A_q and r_q^o are the model potential parameters for the atom q. $I_{nn'}(r_i)$ represents integrals of the general form:

$$I_{nn'} = \int \phi_{n\ell}(r_A)\, V_B\, \phi_{n',\ell}(r_A)\,d\tau_A \qquad 2.51$$

The evaluation of the integrals in equation 2.51 can be achieved by a transformation to elliptical co-ordinates and

closely follows the procedure outlined on pp 38-41. For the sake of completeness in this section we shall give a brief outline of the method for the case of s-functions. For this case,

$$I_{nn'} = \frac{NN'}{4\pi} \sum_{s=0}^{n-1} \sum_{t=0}^{n'-1} B_{ns} B_{n't} \left(\frac{2}{n}\right)^s \left(\frac{2}{n'}\right)^t \cdot I_{st} \qquad 2.52$$

where

$$I_{st} = \int_0^\infty r_A^s \, e^{-r_A/n} \, V(r_B) \, r_A^t \, e^{-r_A/n'} dr_A = (-1)^{s+t} \frac{\partial^{s+t} I_\infty}{\partial \alpha_n^s \partial \beta_{n'}^t} \qquad 2.53$$

with,

$$\alpha_n = \frac{1}{n} \quad ; \quad \beta_{n'} = \frac{1}{n'} \qquad 2.54$$

Hence

$$I_{00} = \int_0^\infty e^{-\alpha r_A} \, V(r_B) \, e^{-\beta r_A} dr_A \qquad 2.55$$

This integral may be evaluated by a transformation to elliptical co-ordinates, assuming $R \geq r^o \geq \frac{R}{2}$.

$$V(r_B) = A \quad ; \quad r_B \leq r^o$$

$$V(r_B) = -\frac{Z}{r_B} \quad ; \quad r_B \geq r^o \qquad 2.56$$

then,

$$I_{00} = \frac{AR^3}{4} \int_{\nu=-x}^{\nu=+1} \left[\int_{\mu=1}^{\mu=\nu+1+x} e^{-\alpha(\mu+\nu)} (\mu^2-\nu^2) d\mu \right] d\nu$$

$$-\frac{Z\pi R^2}{2}\int_{\nu=-x}^{\nu=+1}\left[\int_{\mu=\nu+1+x}^{\mu=\infty} e^{-a(\mu+\nu)}(\mu+\nu)\,d\mu\right]d\nu - \frac{Z\pi R^2}{2}\int_{\nu=-1}^{\nu=-x}\left[\int_{\mu=1}^{\mu=\infty} e^{-a(\mu+\nu)}(\mu+\nu)\,d\mu\right]d\nu$$

2.57

where $\frac{2r^o}{R} = 1+x = u$ and $a = (\alpha_{n_1} + \beta_{n'})\frac{R}{2}$ 2.58

from which,

$$I_\infty = \frac{2\pi R^3 A}{8}[C_2(a,u)A_o(2a)+2C_1(a,u)A_1(2a)+A_2(a)-A_1(a)+\frac{(1+x)^2}{4}C_1(a,u)-\frac{C_3(a,u)}{4}$$

$$+A_2(a)E_o(a)-A_o(a)E_2(a)-C_2(a,u)E_o(2a)-2C_1(a,u)E_1(2a)]$$

$$-\frac{Z\pi R^2}{2}[\frac{1}{2}\{C_2(a,u)-(1+x)C_1(a,u)\}-C_1(a,u)A_o(2a)-2C_o(a,u)A_1(2a)$$

$$-B_o(a)A_1(a)-A_o(a)B_1(a)-2A_1(a)A_o(a)+A_2(a)-A_1(a)$$

$$+E_o(a)A_1(a)+E_1(a)A_o(a)-C_1(a,u)E_o(2a)-2C_o(a,u)E_1(2a)]$$

2.59

where

$$C_n(a,u) = \int_u^\infty r^n e^{-ar}dr = e^{-au}\sum_{k=0}^{n}\frac{n!}{k!}\frac{u^k}{a^{n-k+1}}$$

$$A_n(a) = \int_1^\infty r^n e^{-ar}dr = C_n(a,1)$$

$$B_n(a) = \int_{-1}^{+1} r^n e^{-ar}dr = (-1)^{n+1}A_n(-a) - A_n(a)$$

$$E_n(a) = \int_{-x}^{o} r^n e^{-ar}dr = \frac{n!}{a^{n+1}}\{e^{ax}\sum_{k=0}^{n}\frac{(-ax)^{n-k}}{(n-k)!} - 1\}$$

2.60

A computer programme was written using these formulae for the calculation of s and p Rydberg series in linear triatomic molecules. Several of the integrals evaluated using equation 2.59 were checked using a 72-point Gaussian Quadrature programme.

(ii) Results and Discussion

In this discussion the computational aspects of the method outlined above will be emphasised and we shall postpone a detailed consideration of the relation of calculated Rydberg series to experimental data, e.g. vacuum u-v and electron impact spectra, to a later chapter.

The computer programme was written so that it could be applied to linear triatomic molecules in general, but it was used in particular for CO_2, CS_2, CSe_2, OCS and OCSe. Model s and p Rydberg series for these molecules were calculated to reproduce observed series converging to the lowest ionisation potential of the particular molecule.

In making these calculations a number of important factors had to be considered:

(a) The choice of expansion centre and the degree of ℓ-spoiling for the Rydberg M.O.

(b) The effect of changing the point-ion charge distribution of the core.

These factors will be discussed for the two cases of symmetrical YX_2 and unsymmetrical XYZ molecules.

Symmetrical YX_2 molecules

(a) For symmetrical YX_2 molecules it is necessary to expand

the Rydberg M.O. about the central atom Y to maintain the inversion symmetry inherent in the ground state nuclear conformation of these molecules and their ions. With a one-centre expansion about the atom Y there are no matrix elements of the potential energy operator connecting s and p functions. The discussion on pp 51-55 suggests that there will be ~10% s-d mixing in the lowest $ns\sigma_g$ terms of CO_2 and ~7% p-f mixing in the lowest $np\sigma_u$ terms. These percentages will decrease in going to higher terms. Inclusion of these mixings in the calculation will cause small perturbations of levels calculated without including ℓ-spoiling. Unfortunately d or f functions have not been included in the calculations presented in this thesis, although they could be incorporated in existing programmes. Since d and f functions are essentially non-penetrating the integrals involved could be evaluated by ignoring contributions from inside the ion-core.

(b) It was shown previously (p 44) that the quantum defect of a molecular Rydberg series, μ_{Mol}, can be divided into two parts $\mu_{pen} + \mu_{c.s.}$. $\mu_{c.s.}$ represents the contribution to the quantum defect arising from the non-spherical part of the potential and can be further subdivided into contributions from inside and outside the ion core;

$$\mu_{c.s.} = \mu^{in}_{c.s.} + \mu^{out}_{c.s.}$$

In the calculation $\mu^{in}_{c.s.}$ is determined by the core

atomic model potential while $\mu_{c.s.}^{out}$ depends on the partial charge δZ_i assigned to the atom i. (see p47). For Rydberg series converging to the lowest ionisation potential of a molecule,

$$\sum_{i}^{Atoms} \delta Z_i = 1,$$

but the individual δZ_i must be determined from an effective point charge distribution assumed for the ion-core. For YX_2 molecules two extreme cases have been considered: Charge distribution A corresponding to a maximum separation of charge and distribution B corresponding to maximum delocalisation of charge

$+\frac{1}{2}$	0	$+\frac{1}{2}$	$+\frac{1}{3}$	$+\frac{1}{3}$	$+\frac{1}{3}$
X	- Y	- X	X	- Y	- X
A			B		

The distributions appropriate to CO_2, CS_2 and CSe_2 should lie somewhere between these two extremes. $ns\sigma_g$, $np\sigma_u$ and $np\pi_u$ Rydberg series were calculated for these molecules using 10s and 9p functions with charge distributions A and B. The results for CO_2 are given as an example in table 2.IV.

Table 2.IV shows that calculated term values are insensitive to changes in the charge distribution of the ion-core. $ns\sigma_g$ terms show the greatest dependence with a variation

Table 2.IV

Calculated Rydberg terms for CO_2

n	CO_2 $ns\sigma_g$		CO_2 $np\sigma_u$		CO_2 $np\pi_u$	
	A (a.u.)	B (a.u.)	A (a.u.)	B (a.u.)	A (a.u.)	B (a.u.)
2	.11565	.11915	.09418	.09673	.09616	.09781
3	.05112	.05238	.04289	.04399	.04525	.04548
4	.02895	.02958	.02481	.02533	.02619	.02622
5	.01864	.01902	.01623	.01651	.01704	.01704
6	.01300	.01326	.01147	.01163	.01196	.01195
7	.00958	.00977	.00855	.00863	.00884	.00883

of ~4% of the lowest term value in going from distribution A to B; $np\pi_u$ terms show the least dependence.

This behaviour is very similar to that found for non-penetrating Rydberg M.O.'s. For these orbitals,

$$\mu_{Mol} = \mu_{pen} + \mu^{in}_{c.s.} + \mu^{out}_{c.s.} \simeq \mu^{out}_{c.s.}$$

The calculations of H. Hosoya[32] show that for linear triatomics the dependence of the term value on the ion-core charge distribution is only a few percent of the term value and, for orbitals with the same n and ℓ quantum numbers, smaller for π components than for σ components.

Non-symmetrical linear XYZ molecules

Linear XYZ molecules do not have the inversion symmetry of their symmetrical YX_2 counterparts and it is no longer necessary to carry out the expansion of the Rydberg wavefunction about the central atom Y. Indeed, one is at liberty to select any of the three atoms X, Y or Z as the expansion centre for the wavefunction, and the effect of expanding about these different centres has been investigated.

Because of the lower symmetry in these molecules it is necessary to include s-p mixing since integrals of the type,

$$\int \phi_{s\sigma}(r_y)\ V_{Z \text{ or } X}\ \phi_{p\sigma}(r_y)d\tau_y$$

are non-vanishing in contrast to their behaviour in symmetrical YX_2 molecules. Calculations on OCS show that s-p mixing is

much larger than the expected s-d mixing in the lower s terms of CO_2; inclusion of s-p mixing causes a mutual repulsion of the sσ and pσ levels and can change term energies calculated without s-p mixing by as much as 15%. For this reason s-p mixing was included in all calculations of sσ and pσ Rydberg series of linear XYZ molecules.

The effect of changing the expansion centre in OCS on calculated nsσ terms is shown in table 2.V. The nsσ series were calculated with charge distribution A. The table shows that changing the expansion centre in OCS affects the calculated nsσ term energies by ~3%. This figure represents the quality of one-centre expansions for XYZ molecules unless there are grounds for favouring an expansion about a particular atom in the molecule.

Table 2.V

Calculated nsσ Rydberg terms for OCS

n	Expansion Centre x_{OCS} (a.u.)	Expansion Centre x_{OCS} (a.u.)
2	.09374	.09671
3	.04392	.04583
4	.02547	.02652
5	.01662	.01724
6	.01170	.01209
7	.00868	.00893

For the case of XYZ molecules in which one atom, say atom X, has a much lower first ionisation potential than any of the other atoms in the molecule the expansion should be about the atom X. Examples of XYZ molecules of this type are SeCO and ICN where X is Se and I respectively. The energy levels of the atom X are so much lower than those of the atoms Y or Z, that the Rydberg Mo's of the XYZ molecule must be built up largely of X atom A.O's. Thus XYZ molecules of this kind have "localized" Rydberg Mo's centred on the atom X and a one-centre expansion about X should be a good approach to the calculation of the Rydberg series in these molecules.

E. Finn[48] has studied the Rydberg series of OCSe and used the model potential approach presented in this thesis, with an expansion of the Mo's about the Se atom. nsσ, npσ and npπ series were calculated for this molecule and the agreement found with observed series in the vacuum u-v spectrum of OCSe demonstrates the usefulness of one-centre calculations for this type of molecule.

2.6 Two-centre expansions of CO_2 Rydberg wavefunctions

(i) Introduction

While the main body of work in this thesis employs one-centre expansions of molecular wavefunctions it is very instructive to attempt a many-centre expansion of wavefunctions if only to demonstrate its inappropriateness for the treatment

of Rydberg orbitals in triatomic molecules. Because of the large amount of work involved in extending one-centre calculations to many centres we have considered only s-functions on two centres; nevertheless the results clearly demonstrate the behaviour of separated atom wavefunctions in going along a Rydberg series and bring out the very important differences between $\sigma_g$ns and $\sigma_u$ns orbitals.

(ii) Linear-dependence and two-centre expansions

The main weakness of the single-centre expansion technique is that it fails to take into account the singularities at the nuclei while often introducing a non-physical singularity at the arbitrarily chosen expansion centre. This deficiency may be overcome in principle by resorting to a multicentre expansion in which sets of functions are located at all of the nuclear positions. However, this approach must be used with great caution because approximate linear dependenceis may arise which can cause serious problems in numerical computations. The two-centre calculations reported in this thesis employed linear combinations of hydrogen functions located at two nuclei in the molecule. The problem of near linear dependence was met with from the very beginning and its manifestations will now be discussed.

To ensure that linear dependence does not arise in a chosen basis set it is sufficient to orthonormalise all the functions of the set because non-degenerate orthogonal functions

are necessarily linearly independent. A non-orthogonal basis set $\{\chi_n\}$ may be converted to an orthonormal set $\{\phi_n\}$ by means of a matrix transformation A:

$$\phi_\mu = \sum_\nu \chi_\nu A_{\mu\nu} \qquad 2.61$$

with

$$\int \chi_\mu \chi_\nu d\tau = S_{\mu\nu} \quad ; \quad \int \phi_\mu \phi_\nu d\tau = \delta_{\mu\nu} \qquad 2.62$$

The non-orthogonality of the set $\{\chi_n\}$ is manifest in the non-zero overlap integrals $S_{\mu\nu}$.

P.O. Löwdin[49] has shown that the general solution of the orthonormality problem has the form

$$\phi = \chi S^{-\frac{1}{2}} \qquad 2.63$$

where $S^{-\frac{1}{2}}$ is the reciprocal square root of the overlap matrix. $S^{-\frac{1}{2}}$ may be determined by finding the unitary transformation, U, which diagonalises S. If U is the matrix formed from the eigenvectors of S then,

$$SU = U[\lambda_i \delta_{ij}] \qquad 2.64$$

where the λ_i are the eigenvalues of the matrix S and

$$S^{-\frac{1}{2}}_{ik} = \sum_j U_{ij} \lambda_j^{-\frac{1}{2}} U_{kj} \qquad 2.65$$

The importance of the overlap matrix in showing the presence of linear dependence or near linear dependence in

a basis set $\{\chi_n\}$ is now apparent. Thus pre-multiplying equation 2.64 by U^+ gives

$$U^+ S U = \text{diag}\ (\lambda_1, \lambda_2 \ldots) \qquad 2.61$$

because $U^+ U = 1$

A relation,

$$U^+ S U = 0 \qquad 2.67$$

necessarily implies

$$\chi U = 0 \qquad 2.68$$

i.e. a linear dependency. Similarly the minimum value of $U^+ S U$ is a measure of the linear dependence of the set $\{\chi_n\}$.

To investigate the possibility of linear dependence in a two-centre calculation of the Rydberg series in CO_2 the overlap matrix must be determined. The non-orthogonal basis set $\{\chi_n\}$ was composed of sub-sets χ_{An}, χ_{Bn} of hydrogen functions separated by a distance R, and overlap integrals were evaluated using the transformation to elliptical co-ordinates given on p.40. Computer programmes were written for the evaluation of overlaps at any internuclear separation, R, for the following cases:

$S(ns, n's)$ $\quad n', n = 1, 2, \ldots 10$

$S(np\sigma, n'p\sigma)$
$S(np^-, n'p^-)$ $\quad n', n = 2, 3, \ldots 10$

Because equilibrium R values in most molecules are in the range 2-4 a.u.'s computed overlaps, when $n=n'$, are given in table 2.VI at R=2.0 and R=4.0 a.u.'s.

Table 2.VI shows that in going to higher n the overlap rapidly obtains a value close to 1.0 at the same time the limit of exact linear dependence is being approached.

Table 2.VI

Overlap Integrals for Hydrogen Functions at R=2.0 and R=4.0 a.u.

	S(ns,ns)		S(npσ,npσ)		S(npπ,npπ)	
n	R=2.0	R=4.0	R=2.0	R=4.0	R=2.0	R=4.0
1	0.5865	0.1893				
2	0.8829	0.7308	-0.7358	-0.2256	0.9074	0.6947
3	0.9426	0.8424	-0.8819	-0.6484	0.9587	0.8627
4	0.9658	0.8971	-0.9324	-0.7893	0.9765	0.9198
5	0.9773	0.9277	-0.9561	-0.8578	0.9849	0.9470
6	0.9838	0.9466	-0.9672	-0.8971	0.9894	0.9623
7	0.9879	0.9589	-0.9771	-0.9220	0.9922	0.9718
8	0.9906	0.9675	-0.9824	-0.9338	0.9940	0.9780
9	0.9925	0.9736	-0.9860	-0.9506	0.9952	0.9824
10	0.9939	0.9781	-	-	-	-

Table 2.VII

Smallest Eigenvalues for 8 Hydrogen s-functions at R=2.0 and R=4.0 a.u.

	λ_n							
R	1	2	3	4	5	6	7	8
4.0	0.99030	0.32362	0.12325	0.05640	0.02733	0.012749	0.00502	0.00117
2.0	0.53477	0.08992	0.03201	0.01433	0.00690	0.00320	0.00126	0.00029

To determine values of,

$$\lambda_{min} = \min(U^{+} SU),$$

the overlap matrix for 10 s-functions on each centre was obtained and diagonalized using the computer library subroutine EA01B. This subroutine employs the Householder method[50] in which the matrix is reduced to a tri-diagonal form by means of similarity transformations. Unfortunately unacceptable eigenvalues were obtained as the result of the accumulation of rounding errors. This comes about because the overlap matrix, S, has large off-diagonal elements and converges to a form with vanishing eigenvalues; a matrix of this type is ill-conditioned for the iterative process needed for diagonalization. Here we observe a manifestation of near linear dependence which sets a limit on the maximum dimension of S and consequently on the size of the basis set used in the two centre calculations.

EA01B successfully diagonalized the overlap matrix for 8 Hydrogen s-functions on each centre at R=2.0 and R=4.0 a.u. and gave the eight smallest eigenvalues λ_n shown in table 2.VII. However, with this 16-function basis set (8 on each centre) rounding errors were still troublesome in the evaluation of certain two-centre integrals, even when double precision arithmetic was employed; these manifestations of near linear dependence were eliminated from the programme when the basis set was restricted to a maximum of 14 functions (7 on each centre). This indicates that, for this type of two-centre calculation, λ_n should be >0.001 if computational problems

due to near linear dependence are to be avoided.

The overlap matrix, S, is not only important in checking for linear dependence in a non-orthogonal basis-set but can also be used to determine the roots of the determinantal equation arising from variational solutions of Schrödinger's equation,

$$H\Psi_i = E_i\Psi_i. \qquad 2.69$$

The M.o's Ψ_i are formed from linear combinations of the non-orthogonal set $\{\chi_n\}$,

$$\Psi_i = \sum_{\mu=1}^{N} \chi_\mu c_{\mu i} \qquad 2.70$$

or in matrix notation,

$$\Psi = \chi c$$

The expansion coefficients, $c_{\mu i}$, are obtained by the application of variational theory leading to the secular equations,

$$Hc = E\,Sc \qquad 2.71$$

Computing the roots of the determinantal equation,

$$|H - SE| = 0, \qquad 2.72$$

involves much more effort than the case in which S is the unit matrix, but the former can be reduced to the latter if the matrix H is replaced by,

$$H' = S^{-\frac{1}{2}} H S^{-\frac{1}{2}}, \qquad 2.73$$

and the substitution,

$$C' = S^{\frac{1}{2}} C \qquad 2.74$$

is made in 2.70

Equation 2.71 now becomes,

$$H'C' = C' E \qquad 2.75$$

This transformation is equivalent to expressing the original operator H as a matrix with the new orthogonal basis $\{\phi_n\}$, since from equations 2.70 and 2.74,

$$\Psi = \chi C = \chi S^{-\frac{1}{2}} C' = \phi C' \qquad 2.76$$

A computer programme was written to calculate s Rydberg series in linear YX_2 molecules using an expansion of hydrogen functions about the two X atoms. It was necessary to evaluate three centre integrals of the type:

$$V_{nn'} = \int \chi_n(r_A) V_C \chi_{n'}(r_B) d\tau = \langle a|V_C|b\rangle \qquad 2.77$$

Although these can be evaluated exactly it was more convenient to use the well known Mulliken approximation in these initial studies:

$$\langle a|V_C|b\rangle = \frac{1}{2} S_{ab} \{\langle a|V_C|a\rangle + \langle b|V_C|b\rangle\} \qquad 2.78$$

(iii). Results and Discussion

With 7 s-functions located on each of the two oxygen atoms in CO_2 two Rydberg series should be obtained from the calculation corresponding to in-phase and out-of-phase overlap

of the functions. These series may be given the usual separated atom designations, $\sigma_g ns$ and $\sigma_u ns$. R.S. Mulliken[10] has shown that the forms $\sigma_g ns$ and $\sigma_u ns$ correlate at small R with the united-atom Mo's $ns\sigma_g$ and $(n+1)p\sigma_u$ respectively.

The one-centre (united-atom) and two-centre (separated atoms) calculations presented in this thesis represent different approximations to the same Rydberg Mo's, and should presumably give similar series of Rydberg terms.

Table 2.VIII gives a comparison of calculated one-centre and two-centre σ_g and σ_u term energies for CO_2.

Table 2.VIII

Calculated One and Two-centre Rydberg Terms for CO_2

n	$ns\sigma_g$ (a.u.)	$\sigma_g ns$ (a.u.)	$np\sigma_u$ (a.u.)	$\sigma_u (n-1)s$ (a.u.)
2	0.1157	0.1089	0.0942	-0.0313
3	0.0511	0.0567	0.0429	-0.0913
4	0.0290	0.0351	0.0248	-0.1140
5	0.0186	0.0236	0.0162	-0.1305

Inspection of the table shows that for the σ_g series the two-centre term values are in reasonable agreement with the one-centre terms, but the $\sigma_u ns$ terms bear no resemblance to the one-centre σ_u terms. Indeed the negative sign in front of the calculated $\sigma_u ns$ terms means the states are unbound and lie above the ionisation limit.

In order to see why the one-centre and two-centre calculations approximately agree for σ_g levels but totally disagree for σ_u levels it is necessary to investigate the behaviour of the two-centre functions close to the united-atom limit.

The two-centre Rydberg Mo's are built from linear combinations of hydrogen s-functions χ_μ;

$$\psi_i = \sum_{\mu=1}^{N} \chi_\mu c_{\mu i} \qquad 2.79$$

where the set $\{\chi_\mu\}$ is composed of N/2 functions χ_{An} on centre A and N/2 functions χ_{Bn} on B.

Because,

$$(\chi_{A\nu} + c_{\nu 1}\chi_{A1} + c_{\nu 2}\chi_{A2} + \ldots) \pm (\chi_{B\nu} + c_{\nu 1}\chi_{B1} + c_{\nu 2}\chi_{B2} + \ldots)$$
$$= (\chi_{A\nu} \pm \chi_{B\nu}) + c_{\nu 1}(\chi_{A1} \pm \chi_{B1}) + c_{\nu 2}(\chi_{A2} \pm \chi_{B2}) + \ldots,$$

symmetrized σ Mo's are:

$$\psi_i(\sigma_g) = \sum_{\nu=1}^{N/2} (\chi_{A\nu} + \chi_{B\nu}) c_{\nu i} \qquad 2.80$$

$$\psi_i(\sigma_u) = \sum_{\nu=1}^{N/2} (\chi_{A\nu} - \chi_{B\nu}) c_{\nu i} \qquad 2.81$$

Very close to the united-atom limit $\psi_i(\sigma_g)$ consists of LCAO forms of the type,

$$\psi_g = \frac{1}{\sqrt{2+2S_n}} \{\chi_{An} + \chi_{Bn}\} \qquad 2.82$$

and these will be almost identical to the united-atom functions C_n where C is the mid-point of A and B. Hence the one-centre

and two-centre calculations should give similar results in this case.

$\Psi_i(\sigma_u)$ contains LCAO forms of the type,

$$\Psi_u = \frac{1}{\sqrt{2-2s_n}} \{\chi_{An} - \chi_{Bn}\} \qquad 2.83$$

and close to the united-atom limit $\{\chi_{An} - \chi_{Bn}\}$ becomes zero and the normalising factor $\frac{1}{\sqrt{2-2S_n}}$ becomes infinite. The form Ψ_u in the limit can be obtained by applying the theory of indeterminant forms. With the Z-axis joining A to B,

$$\lim_{z\to 0} \Psi_u = \frac{d\psi u}{dz} \qquad 2.84$$

which is not a united-atom wavefunction. Correlation diagrams show that the correct anti-symmetric combination of two s levels at the united-atom limit must be a p level, and Ψ_u must be given some p character to allow for this. The inclusion of p functions in the basis-set is necessary because of "forced s-p hybridization" - a term used to describe the consequences of the fact than an s-orbital on one centre is non-orthogonal to a p-orbital on another centre. Thus the correct forms for $\sigma_g$ns and $\sigma_u$ns must be:

$$\Psi(\sigma_g ns) = N\{\sum_{n=1} c_n(ns_A+ns_B) + \sum_{m=1} c_m(mp\sigma_A-mp\sigma_B)\} \qquad 2.85$$

$$\Psi(\sigma_u ns) = N\{\sum_{n=1} c_n(n'p\sigma_A+n'p\sigma_B) + \sum_{m=1} c_m(ms_A-ms_B)\} \qquad 2.86$$

Close to the united-atom the $C_m \to 0$, $\Psi(\sigma_g ns)$ becomes equivalent to $\Psi_i(\sigma_g)$ in 2.80, but $\Psi(\sigma_u ns)$ does not become equivalent to $\Psi_i(\sigma_u)$ in 2.81.

The fact that the calculated energies for the two-centre σ_g, MO's using only s-functions, are similar to the one-centre σ_g energies shows that the c_m in 2.85 must indeed be small and

$\Psi(\sigma_g ns)$ is close to a united-atom $ns\sigma_g$ function. On the other hand the calculated energies of two-centre σ_u Mo's derived from s-functions must be seriously in error because $\Psi_i(\sigma_u)$ cannot even approximately represent a united-atom $np\sigma_u$ function. The out-of-phase overlap of s-functions in $\Psi_i(\sigma_u)$ forms very unstable states which become unbound close to the united-atom limit; the inclusion of p-functions in $\Psi(\sigma_u ns)$ stabilizes the M.O. by allowing electron density to move out of regions of unfavourable overlap. (See Fig. 2.V).

Fig. 2.V

The Effect of Including p Functions in Two-centre $\sigma_u$ns MO's

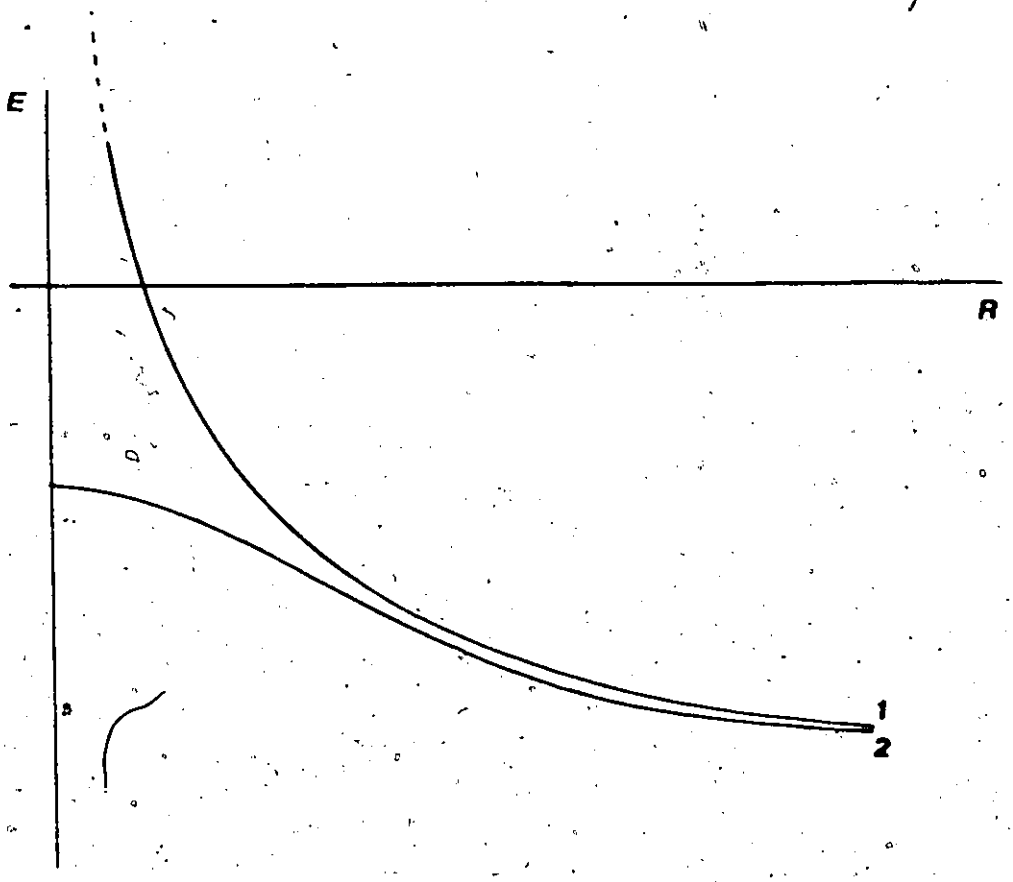

$$\sigma_u ns = N\{ns_A - ns_B\}$$

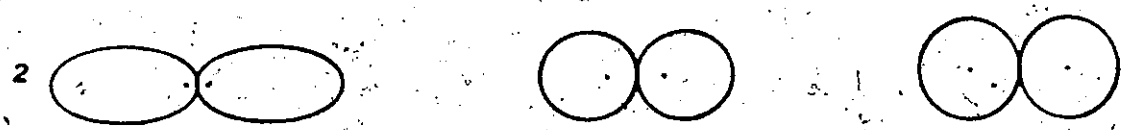

$$\sigma_u ns = N\{\alpha(ns_A - ns_B) + \beta(np\sigma_A + np\sigma_B)\}$$

CHAPTER 3

RYDBERG TRANSITIONS IN CO_2

3.1 Coupling Schemes for the Rydberg States of CO_2

(i) Introduction

The basic problem studied in this thesis is the interpretation of Rydberg series observed in the absorption spectra of certain linear triatomic molecules. Rydberg absorption spectra arise when a molecule in its ground electronic state undergoes a transition to an excited state, and a clear understanding of these transitions requires a knowledge of both the ground and excited states of the molecule.

A molecular state is specified to a first approximation by an electron configuration in which each of the electrons in the molecule is assigned a one-electron function or orbital. These orbitals are eigenfunctions of a first order Hamiltonian H_o^e which ignores electron correlation and contains only one-electron operators.

Ground state MO configurations can be obtained from LCAO-MO-SCF calculations. The first MO calculation on the ground state of CO_2 was carried out by J.F. Mulligan[51] in 1951 and since then the calculations have been repeated, with improvements, by several authors[52,53]. These calculations indicate that the ground state configuration of CO_2 is:

$$(1\sigma_g)^2\ (1\sigma_u)^2\ (2\sigma_g)^2\ (3\sigma_g)^2\ (2\sigma_u)^2\ (4\sigma_g)^2\ (3\sigma_u)^2\ (1\pi_u)^4\ (1\pi_g)^4,$$

although the ordering of some of the inner Mo's depends on

the basis set used in the calculation.

The most important feature of this configuration is the form of the highest occupied $1\pi_g$ M.O. This M.O. is essentially non-bonding and is mainly composed of two oxygen 2p A.O.'s. This conclusion is confirmed by the observation that removal of an electron from CO_2 to form CO_2^+ in its ground state is accompanied by a very small change in the bond length (1.1621 Å → 1.1770 Å)[54].

Rydberg states of CO_2 with excitation energies less than the lowest ionisation potential of the molecule, $I.P._{CO_2}$, are formed by the promotion of a $1\pi_g$ electron to a united-atom orbital designated by the quantum numbers $n\ell\lambda$ with $n \geq 3$ and $n \geq \ell+1$.

The single-centre model potential calculations presented in the first half of this thesis determine the ionisation potential, $I.P._{Ryd}$, of an electron in one of these united-atom Rydberg orbitals, and the approximate form of the orbital. If the lowest ionisation potential of CO_2 is known the excitation energy, ΔE, for the transition,

$$\ldots(1\pi_g)^3\, n\ell\lambda_{g \text{ or } u} \leftarrow \ldots(1\pi_g)^4 \qquad 3.1$$

may be calculated because $\Delta E = I.P._{CO_2} - I.P._{Ryd}$.

The Rydberg transition indicated by 3.1 does not necessarily represent a single transition in the CO_2 absorption spectrum because a configuration is obtained from an approximate Hamiltonian, H_o^e, and does not fully specify the state of the system. A complete specification can be obtained from a

Hamiltonian, H^e, which includes the electron interaction term, $\frac{1}{r_{ij}}$. This term introduces couplings between spin and orbital motions of the electrons.

The effects of using the approximate Hamiltonian H_o^e are apparent for configurations involving open-shells because spin-functions can be added to these orbital configurations in many different ways. In this case several wavefunctions may belong to a single orbital configuration and represent states which are degenerate with respect to H_o^e. This degeneracy is resolved by the complete electrostatic Hamiltonian, H^e, giving states with slightly different energies.

The form of the eigenfunctions of H^e can be obtained from a consideration of the coupling of the various spin and orbital angular momenta in the molecule, and from this the number and symmetry properties of states belonging to the same electron configuration can be determined.

(ii) The $\ldots(\pi_g)^3$ configuration of the ion CO_2^+

The coupling in the $\ldots(\pi_g)^3$ core of CO_2^+ is designated (Λ,S), the molecular analogue of the well known Russell-Saunders or (L,S) coupling applicable to light atoms. In (Λ,S) coupling it is assumed that the spin-spin and orbit-orbit interactions are much larger than spin-orbit interactions.

The individual components, λ_i, of the orbital angular momenta along the molecular axis couple to form a resultant M_L and the energy of orientation depends on $|M_L| = \Lambda$.

The individual spins, s_i, from a resultant S and the component of S along the molecular axis is called Σ. Σ is taken as positive when it has the same sign as M_L and negative when it has the opposite sign.

The multiplet splitting due to the magnetic interaction of Λ and Σ is given to first order by,

$$T = T_o + \tilde{A}\,\Lambda\,\Sigma \qquad 3.2$$

where $\tilde{A}$ is called the spin-orbit coupling constant, and the energy of a multiplet component is specified by the total angular momentum along the molecular axis:

$$\Omega = |\Lambda+\Sigma| = |M| \qquad 3.3$$

For the $\ldots(\pi_g)^3$ configuration of CO_2^+, $\Lambda=1$ and $S=\frac{1}{2}$. Possible determinantal wavefunctions, $\phi(M_L,\Sigma)$ are:

$$\phi(1,\tfrac{1}{2}) = \frac{1}{\sqrt{4!}}\left|\pi_g^+(1)\alpha(1)\,\pi_g^+(2)\beta(2)\,\pi_g^-(3)\alpha(3)\right|$$

$$\phi(1,\tfrac{1}{2}) = \frac{1}{\sqrt{4!}}\left|\pi_g^-(1)\alpha(1)\,\pi_g^-(2)\beta(2)\,\pi_g^+(3)\alpha(3)\right|$$

$$\phi(1,\tfrac{1}{2}) = \frac{1}{\sqrt{4!}}\left|\pi_g^+(1)\alpha(1)\,\pi_g^+(2)\beta(2)\,\pi_g^-(3)\beta(3)\right|$$

$$\phi(1,\tfrac{1}{2}) = \frac{1}{\sqrt{4!}}\left|\pi_g^-(1)\alpha(1)\,\pi_g^-(2)\beta(2)\,\pi_g^+(3)\beta(3)\right|$$

Two states may be constructed from these wavefunctions: (written using an abbreviated notation for the determinants)

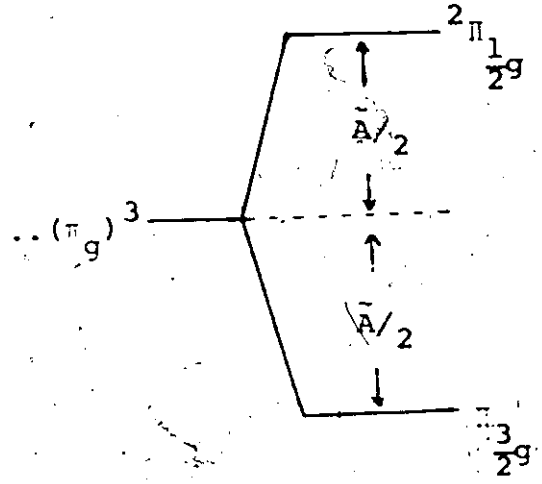

$$\psi = \frac{1}{\sqrt{2}\sqrt{4!}}\{|\alpha\beta\beta| \pm |\alpha\beta\alpha|\}$$

$$\psi = \frac{1}{\sqrt{2}\sqrt{4!}}\{|\alpha\beta\alpha| \pm |\alpha\beta\beta|\}$$

The spin-orbit coupling constant, $\tilde{A}$, for CO_2^+ is 159.5 cm^{-1}[54].

(iii) The $(\pi_g)^3$ σ_u or g configuration of CO_2

In highly excited Rydberg states of CO_2, derived from the $(\pi_g)^3$ σ_u or g configuration, the Rydberg electron is subject to a very small $\frac{1}{r_{ij}}$ interaction and is coupled to the core by the coulomb field of the combined system of nuclei and core electrons. The total angular momentum of the Rydberg electron, ω, is coupled to the molecular axis via the total angular momentum of the core, Ω_c. This situation is referred to as (Ω_c,ω) coupling.

Wavefunctions, $\psi_o(\Omega_c,\omega,\Omega)$ for (Ω_c,ω) coupled states of CO_2 in the $(\pi_g)^3$ σ_u or g configuration are:

$$\psi_o(\tfrac{1}{2},\tfrac{1}{2},1) = \frac{1}{\sqrt{2}\sqrt{4!}}\{|\alpha\beta\overset{++-}{\beta}\alpha| + |\alpha\beta\overset{--+}{\alpha}\beta|\}$$

$$\psi_o(\tfrac{1}{2},\tfrac{1}{2},0^+) = \frac{1}{\sqrt{2}\sqrt{4!}}\{|\alpha\beta\overset{++-}{\beta}\beta| + |\alpha\beta\overset{--+}{\alpha}\alpha|\}$$

$$\psi_o(\tfrac{3}{2},\tfrac{1}{2},1) = \frac{1}{\sqrt{2}\sqrt{4!}}\{|\alpha\beta\overset{++-}{\alpha}\alpha| + |\alpha\beta\overset{--+}{\beta}\alpha|\}$$

$$\psi_o(\tfrac{3}{2},\tfrac{1}{2},2) = \frac{1}{\sqrt{2}\sqrt{4!}}\{|\alpha\beta\overset{++-}{\alpha}\alpha| + |\alpha\beta\overset{--+}{\beta}\beta|\}$$

If the σ electron is in a low lying Rydberg orbital the $\frac{1}{r_{ij}}$ interaction of the Rydberg electron with the core electrons is comparable to the average $\frac{1}{r_{ij}}$ interaction between the core electrons, and the $(\pi_g)^3\ \sigma_{u\ \text{or}\ g}$ configuration will exhibit (Λ,S) coupling.

Wavefunctions $\psi_o(^{2S+1}\Lambda_\Omega)$ for (Λ,S) coupled states of CO_2 in the $(\pi_g)^3\ \sigma_{u\ \text{or}\ g}$ configuration are:

$$\psi_o(^1\Pi_1) = \frac{1}{\sqrt{4}\sqrt{4!}}\left[\left|\overset{++-}{\alpha\beta\beta\alpha}\right| + \left|\overset{--+}{\alpha\beta\alpha\beta}\right| - \left\{\left|\overset{++-}{\alpha\beta\alpha\beta}\right| + \left|\overset{--+}{\alpha\beta\beta\alpha}\right|\right\}\right]$$

$$\psi_o(^3\Pi_{0^\pm}) = \frac{1}{\sqrt{2}\sqrt{4!}}\left[\left|\overset{++-}{\alpha\beta\beta\beta}\right| \pm \left|\overset{--+}{\alpha\beta\alpha\alpha}\right|\right]$$

$$\psi_o(^3\Pi_1) = \frac{1}{\sqrt{4}\sqrt{4!}}\left[\left|\overset{++-}{\alpha\beta\beta\alpha}\right| + \left|\overset{--+}{\alpha\beta\alpha\beta}\right| + \left\{\left|\overset{++-}{\alpha\beta\alpha\beta}\right| + \left|\overset{--+}{\alpha\beta\beta\alpha}\right|\right\}\right]$$

$$\psi_o(^3\Pi_2) = \frac{1}{\sqrt{2}\sqrt{4!}}\left[\left|\overset{++-}{\alpha\beta\alpha\alpha}\right| + \left|\alpha\beta\beta\beta\right|\right]$$

A diagram showing the correlation of states derived from a $(\pi_g)^3\ \sigma_u$ configuration in ideal (Λ,S) and ideal (Ω_C,ω) coupling can be constructed using the following considerations.

(i) The wavefunctions for the Ω=0 and Ω=2 states are the same in (Λ,S) and (Ω_C,ω) coupling. The wavefunctions and energy levels for these states remain unchanged throughout intermediate coupling ranges.

(ii) The two Ω=1 states mix in coupling intermediate between (Λ,S) and (Ω_C,ω). Starting from the (Λ,S) states $^3\Pi$, and $^1\Pi$,

new wavefunctions for intermediate coupling are:

$$\Psi_1(^3\Pi) = N\{\alpha\psi_o(^3\Pi_1) + \beta\psi_o(^1\Pi_1)\}$$

$$\psi_1(^1\Pi) = N\{\gamma\psi_o(^3\Pi_1) + \delta\psi_o(^1\Pi_1)\}$$

Comparison with the (Ω_C,ω) coupled states $\psi_o(\frac{1}{2},\frac{1}{2},1)$ and $\psi_o(\frac{3}{2},\frac{1}{2},1)$ shows that for ideal (Ω_C,ω) coupling $\Psi_1(^3\Pi)$ and $\Psi_1(^1\Pi)$ consist of equal mixtures of $\psi_o(^3\Pi_1)$ and $\psi_o(^1\Pi_1)$. (i.e. $\alpha=\beta=1$ and $\gamma=1$, $\delta=-1$).

The correlation diagram (Fig. 3.I) shows that the type of coupling applicable to the Rydberg states of CO_2 derived from the $(\pi_g)^3\,\sigma_u$ configuration depends on the ratio of the singlet-triplet splitting in the Rydberg state, X, to the spin-orbit coupling in the ion core A.

The correlation diagram is also valid for the $\ldots(\pi_g)^3\,\sigma_u$ configuration of CS_2 and CSe_2 except that case (c) effects[55] must be taken into account because of the larger spin-orbit coupling in these molecules.

In Hund's case (a) the multiplet splittings are given by equation 3.2. The molecular electric field is so strong that $\vec{L}$ precesses rapidly around the figure axis and the vector component of $\vec{L}$ perpendicular to the axis averages to zero. In Hund's case (c) the atomic $\vec{L}$ and $\vec{S}$ couplings are strong compared to the effects of the departure of the molecule from atomic conditions and the magnetic interaction of the perpendicular components of $\vec{L}$ and $\vec{S}$ causes the different multiplet

Fig. 3.1

Correlation of States Between Ideal (Λ,S) and Ideal (Ω_C,ω) Coupling for a $(\pi_g)^3\sigma_u$ Configuration

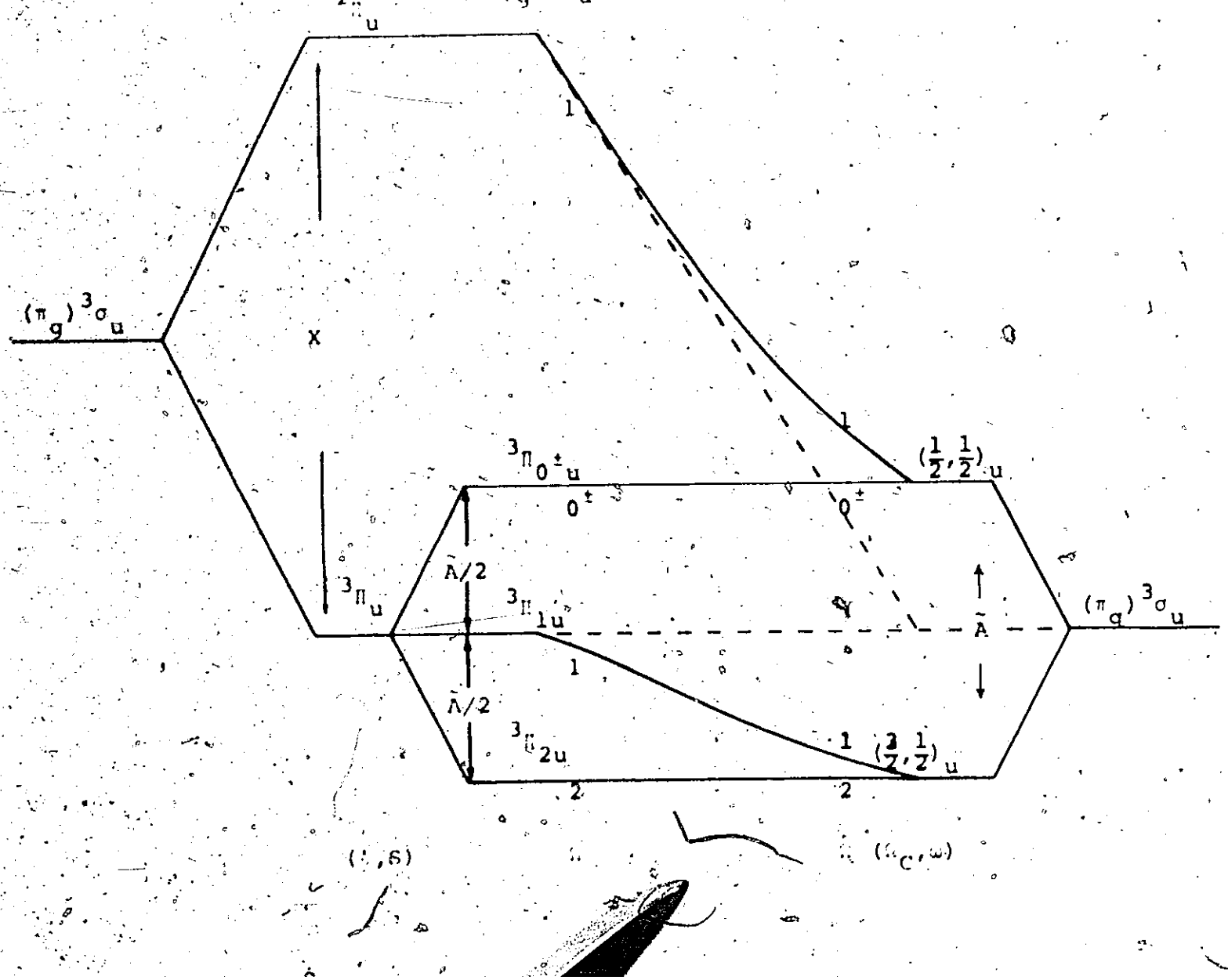

components to depart from the spacings given by equation 3.2. The degeneracies associated with states having $\Lambda=-\Sigma$ if $\Lambda+\Sigma=0$ are removed so that $\Omega=0$ states are split into two components classified 0^+ or 0^- according as the wavefunction is even or odd as regards reflection of orbital and spin co-ordinates together in any plane containing the nuclei.

(iv) The $\ldots(\pi_g)^3\,\pi_u$ configuration of CO_2.

The $(\pi_g)^3\,\pi_u$ configuration of CO_2 in (Ω_C,ω) coupling has $\omega=\frac{1}{2}$ or $\frac{3}{2}$ for the π_u Rydberg electron and $\Omega_C=\frac{1}{2}$ or $\frac{3}{2}$ for the $(\pi_g)^3$ core. The spin-orbit coupling constant $\tilde{a}$ of the π_u electron is very much smaller than the spin-orbit coupling constant $\tilde{A}$ of the core and $\tilde{a}\to 0$ as the Rydberg electron moves to higher orbitals.

The state wavefunctions, $\psi_o(\Omega_C,\omega,\Omega)$ for the $(\pi_g)^3\,\pi_u$ configuration of CO_2 in (Ω_C,ω) coupling are:

$$\psi_o(\tfrac{1}{2},\tfrac{3}{2},2) = \frac{1}{\sqrt{2}\sqrt{4!}}\left[|\overset{++-+}{a\beta\beta a}| + |\overset{--+-}{a\beta a\beta}|\right]$$

$$\psi_o(\tfrac{1}{2},\tfrac{3}{2},1) = \frac{1}{\sqrt{2}\sqrt{4!}}\left[|\overset{++--}{a\beta\beta\beta}| + |\overset{---+}{a\beta aa}|\right]$$

$$\psi_o(\tfrac{1}{2},\tfrac{1}{2},0^-) = \frac{1}{\sqrt{2}\sqrt{4!}}\left[|\overset{++--}{a\beta\beta a}| - |\overset{---+}{a\beta a\beta}|\right]$$

$$\psi_o(\tfrac{1}{2},\tfrac{1}{2},1) = \frac{1}{\sqrt{2}\sqrt{4!}}\left[|\overset{++-+}{a\beta\beta\beta}| + |\overset{---+}{a\beta a\alpha}|\right]$$

$$\psi_o(\tfrac{3}{2},\tfrac{3}{2},0^-) = \frac{1}{\sqrt{2}\sqrt{4!}}\left[|\overset{++--}{a\beta a\beta}| - |\overset{---+}{a\beta\beta a}|\right]$$

$$\psi_o(\tfrac{3}{2},\tfrac{3}{2},3) = \frac{1}{\sqrt{2}\sqrt{4!}}\left[|\overset{++-+}{a\beta aa}| + |\overset{---+}{a\beta\beta\beta}|\right]$$

$$\psi_o(\tfrac{3}{2},\tfrac{1}{2},2) = \frac{1}{\sqrt{2}\sqrt{4!}}\left[\left|\overset{++-+}{\alpha\beta\alpha\beta}\right| + \left|\overset{--+-}{\alpha\beta\beta\alpha}\right|\right]$$

$$\psi_o(\tfrac{3}{2},\tfrac{1}{2},1) = \frac{1}{\sqrt{2}\sqrt{4!}}\left[\left|\overset{++--}{\alpha\beta\alpha\alpha}\right| + \left|\overset{--++}{\alpha\beta\beta\beta}\right|\right]$$

The $(\pi_g)^3\pi_u$ configuration in (Λ,S) coupling has $\Lambda=0$ or 2 and $S=1$ or 0 giving $^{1,3}\Sigma$ and $^{1,3}\Delta$ states. In a strong electric field with $M_L=0$ there is no magnetic field to orient the spin S so that M_S and Σ are not defined for Σ states. However for singlet Σ levels a virtual Ω value of 0^- can be assigned. For triplet Σ levels the zero coupling of S to the internuclear axis is reffered to as Hund's case (b). Tendencies towards Hund's case (c) when the magnetic interactions are large, cause $^3\Sigma^+$ states to split into 0^- and 1 states while $^3\Sigma^-$ states give 0^+ and 1 states.

The state wavefunctions, $\psi_o(^{2s+1}\Lambda_\Omega)$, for the $(\pi_g)^3\pi_u$ configurations of CO_2 in (Λ,S) coupling are:

$$\psi_o(^3\Sigma_3) = \frac{1}{\sqrt{2}\sqrt{4!}}\left[\left|\overset{++-+}{\alpha\beta\alpha\alpha}\right| + \left|\overset{--+-}{\alpha\beta\beta\beta}\right|\right]$$

$$\psi_o(^3\Sigma_2) = \frac{1}{\sqrt{4}\sqrt{4!}}\left[\left|\overset{++-+}{\alpha\beta\beta\alpha}\right| + \left|\overset{--+-}{\alpha\beta\alpha\beta}\right| + \left|\overset{++-+}{\alpha\beta\alpha\beta}\right| + \left|\overset{--+-}{\alpha\beta\beta\alpha}\right|\right]$$

$$\psi_o(^3\Sigma_1) = \frac{1}{\sqrt{2}\sqrt{4!}}\left[\left|\overset{++-+}{\alpha\beta\beta\beta}\right| + \left|\overset{--+-}{\alpha\beta\alpha\alpha}\right|\right]$$

$$\psi_o(^1\Sigma_2) = \frac{1}{\sqrt{2}\sqrt{4!}}\left[\left|\overset{++-+}{\alpha\beta\beta\alpha}\right| + \left|\overset{--+-}{\alpha\beta\alpha\beta}\right| - \left\{\left|\overset{++-+}{\alpha\beta\alpha\beta}\right| + \left|\overset{--+-}{\alpha\beta\beta\alpha}\right|\right\}\right]$$

$$\psi_o(^1\Sigma_0^+) = \frac{1}{\sqrt{4}\sqrt{4!}}\left[\left|\overset{++--}{\alpha\beta\beta\alpha}\right| - \left|\overset{--++}{\alpha\beta\alpha\beta}\right| - \left\{\left|\overset{++--}{\alpha\beta\alpha\beta}\right| - \left|\overset{--++}{\alpha\beta\beta\alpha}\right|\right\}\right]$$

$$\psi_o(^1\Sigma_0^-) = \frac{1}{\sqrt{4}\sqrt{4!}}\left[\left|\overset{++--}{\alpha\beta\beta\alpha}\right| + \left|\overset{--++}{\alpha\beta\alpha\beta}\right| - \left\{\left|\overset{++--}{\alpha\beta\alpha\beta}\right| + \left|\overset{--++}{\alpha\beta\beta\alpha}\right|\right\}\right]$$

$$\psi_o(^3\Sigma_0^+-) = \frac{1}{\sqrt{4}\sqrt{4!}}\left[|\overset{++--}{\alpha\beta\beta\alpha}| + |\overset{--++}{\alpha\beta\alpha\beta}| + \{|\overset{++--}{\alpha\beta\alpha\beta}| + |\overset{--++}{\alpha\beta\beta\alpha}|\}\right]$$

$$\psi_o(^3\Sigma_0^-+) = \frac{1}{\sqrt{4}\sqrt{4!}}\left[|\overset{++--}{\alpha\beta\beta\alpha}| - |\overset{--++}{\alpha\beta\alpha\beta}| + \{|\overset{++--}{\alpha\beta\alpha\beta}| - |\overset{--++}{\alpha\beta\beta\alpha}|\}\right]$$

$$\psi_o(^3\Sigma_1^+) = \frac{1}{\sqrt{2}\sqrt{4!}}\left[|\overset{++\ --}{\alpha\beta\{\alpha\alpha\}}| + |\overset{--\ ++}{\alpha\beta\{\alpha\alpha\}}|\right]$$

$$\psi_o(^3\Sigma_1^-) = \frac{1}{\sqrt{2}\sqrt{4!}}\left[|\overset{++\ --}{\alpha\beta\{\alpha\alpha\}}| - |\overset{--\ ++}{\alpha\beta\{\alpha\alpha\}}|\right]$$

A diagram showing the correlation of states derived from the $(\sigma_g)^3\pi_u$ of CO_2 in (Λ,S) and (Ω_c,ω) coupling can be constructed using the following considerations:

(i) Δ States

There is only one state whose Ω value occurs only once, this is $^3\Delta_3$ in (Λ,S) coupling and $(\frac{3}{2},\frac{3}{2})_3$ in (Ω_c,ω) coupling. The state wavefunctions are the same in either coupling scheme and remain unchanged throughout intermediate coupling ranges.

There are two $\Omega=2$ states corresponding to $^3\Delta_2$ and $^1\Delta_2$ in (Λ,S) coupling and $(\frac{1}{2},\frac{3}{2})_2$ and $(\frac{3}{2},\frac{1}{2})_2$ in (Ω_c,ω) coupling. The (Λ,S) wavefunctions for these states will become increasingly mixed in going over to (Ω_c,ω) coupling.

The $^3\Delta_1$ wavefunction is the same as the (Ω_c,ω) wavefunction for $(\frac{1}{2},\frac{1}{2})_1$. In the intermediate coupling range, however, $^3\Delta_1$ will contain admixtures of other $\Omega=1$ states.

(ii) Σ States

The correlation of (Λ,S) coupled Σ states with (Ω_c,ω)

states having $\Omega=1$ or $0^{\pm}$ cannot be made on the basis of qualitative arguments alone. A. Recknagel[56] has shown that the relative energies of the Σ and Δ states are:

$$^3\Sigma_u^- : E = C + a \qquad ^1\Sigma_u^- : E = C + a$$

$$^3\Delta_u : E = C \qquad ^1\Delta_u : E = C + 2b$$

$$^3\Sigma_u^+ : E = C - a \qquad ^1\Sigma_u^+ : E = C - a + 4c$$

where

$$a = \int\int \pi_g^{\pm}(1)\bar{\pi}_u(2)\ \frac{1}{r_{12}}\ \bar{\pi}_g(1)\pi_u^{\pm}(2)\ d\tau_1\ d\tau_2$$

$$b = \int\int \pi_g^{\pm}(1)\bar{\pi}_u(2)\ \frac{1}{r_{12}}\ \pi_g^{\pm}(2)\bar{\pi}_u(1)\ d\tau_1\ d\tau_2$$

$$c = \int\int \pi_g^{\pm}(1)\pi_u^{\pm}(2)\ \frac{1}{r_{12}}\ \pi_g^{\pm}(2)\pi_u^{\pm}(1)\ d\tau_1\ d\tau_2$$

and

$$a, b, c > 0.$$

It follows that the lowest state of the $(\pi_g)^3\ \pi_u$ configuration of CO_2 is $^3\Sigma^+_{1,0^-\ u}$ in (Λ,S) coupling and because of the non-crossing rule this must correlate with an $(\Omega,-)$ coupled state derived from the $^2\pi_{\frac{3}{2}g}$ core.

Recent unpublished calculations by N. Winter et al.[57] on the lower excited states of CO_2 show that the $^1\Delta_u$ state lies at much higher energy than any of the other $^{1,3}\Delta$ states derived from a $(\pi_g)^3\ \pi_u$ configuration and that the $^{1,3}\Sigma_u^-$ states lie below $^1\Delta_u$.

Fig. 3.II

Correlation of States Between Ideal (Λ,S) and (Ω_C,ω) Coupling for a $(\pi_g)^3\pi_u$ Configuration

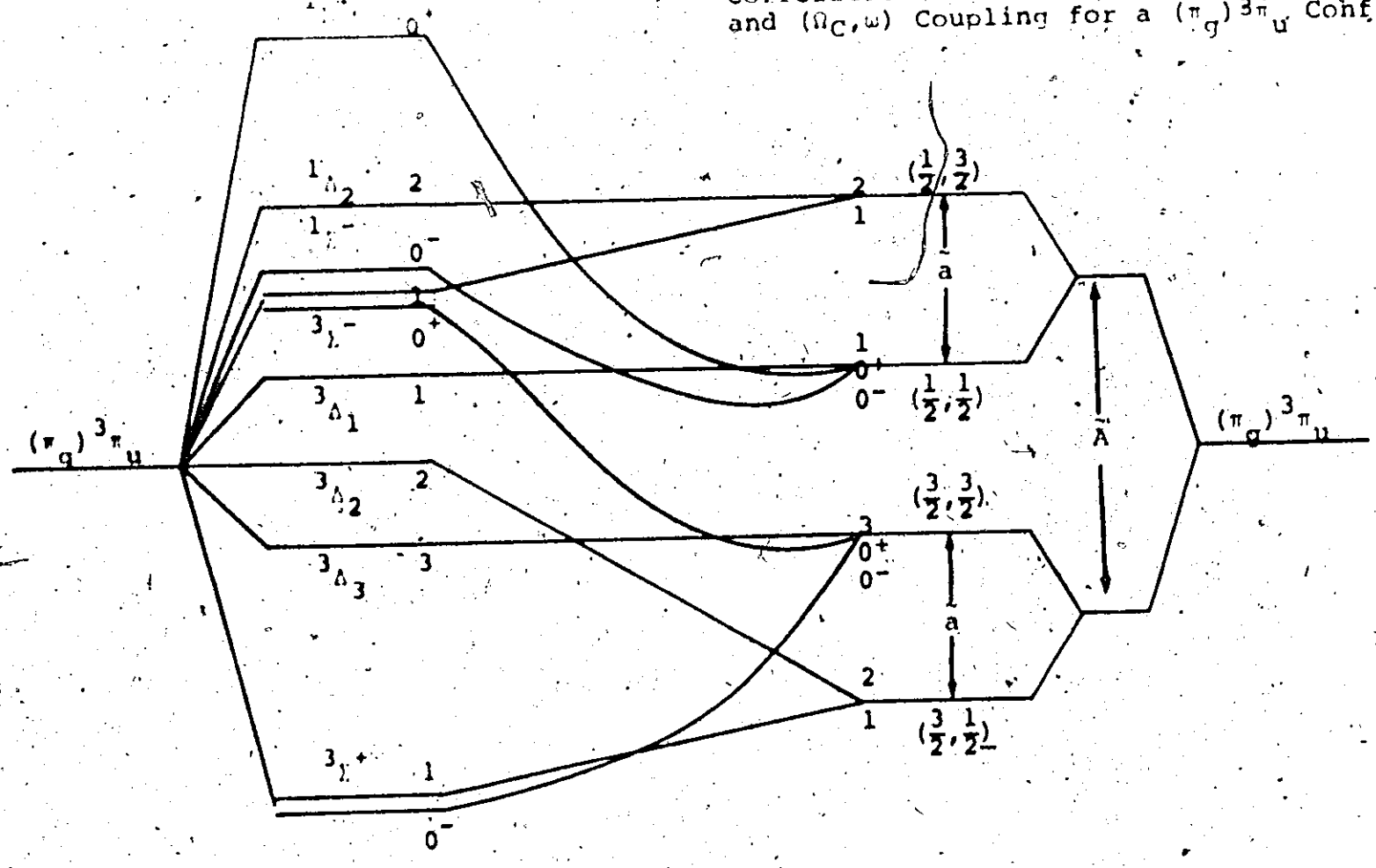

(Λ,S) Ω (Ω_C,ω)

3.2 Selection Rules for Rydberg Transitions in CO_2

(i) General Selection Rules in (Λ,S) and $(\Omega_c,\omega)_c$ coupling schemes.

Electromagnetic radiation constitutes dipole, quadrupole and higher electric and magnetic radiation fields. If an electromagnetic wave encounters a molecule in an electronic state $\psi_{e''}$ the interaction of the electric or magnetic vector of the radiation field with the electric moments of the molecule can lead to absorption of radiation as the molecule undergoes a transition to a state of higher energy $\psi_{e'}$. The probability of a transition between $\psi_{e'}$ and $\psi_{e''}$ depends on the square of the magnitude of the matrix elements of the electric or magnetic multipole moments, P.

$$R_{e'e''} = \int \psi_{e'} P \psi_{e''} d\tau_e \qquad 3.4$$

A transition is said to be allowed if $R_{e'e''}$ is different from zero and forbidden if $R_{e'e''} = 0$. Selection rules are the conditions under which transitions are allowed or forbidden.

Electric dipole transitions are the most important in the u-v or vacuum u-v region of the electromagnetic spectrum. If the dependence of ψ_e on the nuclear co-ordinates is neglected (Born-Oppenheimer approximation) the electric dipole transition probability is determined by:

$$R_{e'e''}(Q_o) = \int \psi_{e'}(q,Q_o) M_e \psi_{e''}(q,Q_o) d\tau_e \qquad 3.5$$

where q stands for all the electronic co-ordinates, and Q for all the nuclear co-ordinates. M_e is the electric dipole

moment vector.

An electronic transition between $\psi_{e'}$ and $\psi_{e''}$ is allowed if the product $\psi_{e'}$, $\psi_{e''}$ belongs to the same symmetry species (Γ) as one of the components of M_e, or equivalently if;

$\Gamma(\psi_{e'}) \otimes \Gamma(\psi_{e''}) \otimes \Gamma(M_e)$ is totally symmetric.

This requirement leads to certain general selection rules for electric dipole transitions in molecules belonging to the $D_{\infty h}$ point group,[54] which is the symmetry group of linear XY_2 molecules.

Table 3.I gives these selection rules for transitions from the $^1\Sigma g^+(0^+)$ ground state of CO_2 to states derived from the excited $(\pi_g)^3\,\sigma_u$ or $(\pi_g)^3\,\pi_u$ configuration in (Λ,S) or (Ω_C,ω) coupling. In addition to these rules there is the general selection rule valid for any coupling scheme:

$$g \leftrightarrow u \; ; \; g \nleftrightarrow g \; ; \; u \nleftrightarrow u.$$

The table shows that the only transition from the ground state of CO_2 to states derived from $\ldots(\pi_g)^3\,\sigma_u$ allowed throughout the range of coupling is:

$$^1\Pi_1 \leftarrow {}^1\Sigma g^+(0^+)$$

In intermediate coupling $^1\Pi_1$ mixes with $^3\Pi_1$ and the transition,

$$^3\Pi_1 \leftarrow {}^1\Sigma g^+(0^+)$$

will be allowed, and borrow intensity from $^1\Pi_1 \leftarrow {}^1\Sigma g^+(0^+)$.

In the limit of ideal (Ω_C,ω) coupling the transitions:

Table 3.I

Selection Rules for Rydberg Transitions in CO_2

Configuration	(Λ,S) States	Selection Rules $\Delta\Lambda=0,\pm1$	$\Delta S=0$	$+\leftrightarrow+$	$\Delta\Omega=0,\pm1$	$0^+\leftrightarrow0^+$	(Ω_C,ω) States
$(\pi_g)^3\sigma_u$	$^1\Pi_1$	a	a	-	a	-	$(1/2,1/2)_1$
	$^3\Pi_{0^+}$	a	f	a	a	a	$(1/2,1/2)_{0^+}$
	$^3\Pi_{0^-}$	a	f	f	a	f	$(1/2,1/2)_{0^-}$
	$^3\Pi_1$	a	f	-	a	-	$(3/2,1/2)_1$
	$^3\Pi_2$	a	f	-	f	-	$(3/2,1/2)_2$
	$^1\Sigma^+_{0^+}$	a	a	a	a	a	$(1/2,1/2)_{0^+}$
	$^1\Delta_2$	f	a	-	f	-	$(1/2,3/2)_2$
	$^1\Sigma^-_{0^-}$	a	a	f	a	f	$(1/2,1/2)_{0^-}$
	$^3\Sigma^-_1$	a	f	-	a	-	$(1/2,3/2)_1$
$(\pi_g)^3\pi_u$	$^3\Sigma^-_{0^+}$	a	f	a	a	a	$(3/2,3/2)_{0^+}$
	$^3\Delta_1$	f	f	-	a	-	$(1/2,1/2)_1$
	$^3\Delta_2$	f	f	-	f	-	$(3/2,1/2)_2$
	$^3\Delta_3$	f	f	-	f	-	$(3/2,3/2)_3$
	$^3\Sigma^+_1$	a	f	-	a	-	$(3/2,1/2)_1$
	$^3\Sigma^-_{0^-}$	a	f	f	a	f	$(3/2,3/2)_{0^-}$

$^1\Pi_1 \leftarrow {}^1\Sigma_g^+(0^+)$ and $^3\Pi_1 \leftarrow {}^1\Sigma_g^+(0^+)$ will have equal intensity.

Transitions to $(\frac{1}{2},\frac{1}{2})_{0^+}$ are apparently allowed in ideal (Ω_C,ω) coupling but the wavefunction for this state is the same as for $^3\Pi_{0^+}$, transitions to which are spin forbidden in (Λ,S) coupling. However it is possible that extraconfigurational mixing with nearby 0^+ states may make transitions to $(\frac{1}{2},\frac{1}{2})_{0^+}$, $(^3\Pi_{0^+})$ weakly allowed.

The only transition from the ground state of CO_2 to states derived from the $(\pi_g)^3\pi_u$ configuration allowed throughout the range of coupling is:

$$^1\Sigma_u^+(0^+) \leftarrow {}^1\Sigma g^+(0^+)$$

However inspection of the state wavefunctions shows that $^1\Sigma_{0^+}^+$ and $^3\Sigma_{0^+}^-$ both consist of $[(\frac{1}{2},\frac{1}{2})_{0^+} \pm (\frac{3}{2},\frac{3}{2})_{0^+}]$ in ideal (Ω_C,ω) coupling so the transition $^3\Sigma_{0^+}^- \leftarrow {}^1\Sigma g^+(0^+)$ will be allowed in intermediate coupling. Transitions from the ground state to $^3\Sigma_1^+$ and $^3\Sigma_1^-$ are also possible close to ideal (Ω_C,ω) coupling.

(ii) Vibronic Interaction

The selection rules based on the equation 3.5

$$R_{e'e''} = \int \psi_{e'}(q,Q_o) M \psi_{e''}(q,Q_o) d\tau_e \neq 0,$$

are valid only if it is possible to separate the electronic motion from the nuclear motion and write the molecular wavefunction as a product of two functions one of which depends on the electronic co-ordinates q for fixed nuclear positions Q and the other which depends on the nuclear co-ordinates Q. ie.

$$\psi_{ev} = \psi_e(q,Q)\ \psi_v(Q) \qquad 3.6$$

While this separation is usually a good first approximation, the coupling of electronic and nuclear motions must be included to higher order.[54] In this case the selection rule 3.5 must be written as:

$$R_{e'v'e''v''} = \int \psi_{ev'} M \psi_{ev''} d\tau_{ev} \neq 0 \qquad 3.7$$

and an electric dipole transition between $\psi_{ev'}$ and $\psi_{ev''}$ is allowed if the product of the vibronic species belongs to the same species as one of the components of the dipole moment M. (The symmetry species of the vibronic wavefunction ψ_{ev} is the direct product of the species of ψ_e and ψ_v even when the product resolution 3.6 does not hold). Because of the change of the selection rule 3.5 to selection rule 3.7 in a higher approximation, certain transitions which are forbidden by 3.5 can become allowed by 3.7 if suitable vibrations are excited. For example a $^1\Pi_g \leftrightarrow {}^1\Sigma_g^+$ transition is forbidden by the rule g ↮ g but if one quanta of a bending (π_u) vibration is singly excited in the ground or excited electronic state, transitions are allowed between certain vibronic states.[54]

3.3 Changes in Geometry in the excited state

It is well established that CO_2 and CO_2^+ are linear in the equilibrium conformation of their ground states[54] and so far in this thesis it has been assumed that CO_2 is also linear in the equilibrium conformation of its Rydberg excited states. However, A.D. Walsh[58] has shown that CO_2 is probably bent in

certain sub-Rydberg excited states and it is possible that CO_2 is also bent in some Rydberg states. The excited states of bent CO_2 cannot be classified under the $D_{\infty h}$ point group but transform like the irreducible representations of the C_{2v} point group, and the selection rules given on p.94 are no longer valid. It is therefore worthwhile investigating if any CO_2 Rydberg states are in fact bent in their equilibrium conformation.

It was shown in Chapter 1 of this thesis that the factorisation of the wavefunction, $\Psi_{Mol} = \Psi_{ion}\,\Psi_{Ryd}$, is a good approximation for Rydberg States. It follows that the energy, E_{CO_2*} of a Rydberg state of CO_2 is equal to the sum of the energy of the ion-core, $E_{CO_2^+}$, and the energy of the Rydberg electron, E_{Ryd}, i.e.

$$E_{CO_2*} = E_{CO_2^+} + E_{Ryd} \qquad 3.8$$

Because CO_2^+ is linear in its equilibrium conformation, bending CO_2^+ will increase the energy of the ion and only if E_{Ryd} decreases on bending can the equilibrium conformation of the Rydberg state be bent.

The equilibrium internuclear angle, θ_e, of a Rydberg state of CO_2 is determined by the condition that E_{CO_2*} is a minimum, and

$$\left(\frac{\partial E}{\partial \theta}\right)_{\theta_e} = 0 \qquad 3.9$$

Therefore, from equation 3.8

$$\left(\frac{\partial E_{CO_2^+}}{\partial \theta}\right)_{\theta_e} = -\left(\frac{\partial E_{Ryd}}{\partial \theta}\right)_{\theta_e} \qquad 3.10$$

The bending force-constant of CO_2^+ is,

$$k_{CO_2^+}(\theta) = \frac{\partial^2 E_{CO_2^+}}{\partial \theta^2} \qquad 3.11$$

so that,

$$\left(\frac{\partial E_{CO_2^+}}{\partial \theta}\right)_{\theta_e} = \int_{\theta=180°}^{\theta=\theta_e} k_{CO_2^+}(\theta)\,d\theta \qquad 3.12$$

Then assuming that E_{Ryd} is a linear function of θ,

$$\left(\frac{\partial E_{Ryd}}{\partial \theta}\right)_{\theta_e} = \left(\frac{\partial E_{Ryd}}{\partial \theta}\right)_{\theta=180°} = -\int_{\theta=180°}^{\theta=\theta_e} k_{CO_2^+}(\theta)\,d\theta \qquad 3.13$$

Equation 3.13 allows θ_e to be determined from the behaviour of E_{Ryd} on bending linear CO_2, provided the bending force constant of CO_2^+ is known as a function of θ.

Values of E_{Ryd} for Rydberg states of linear CO_2 are given to a first approximation by the model potential calculations discussed in Chapter 2 of this thesis. Symmetry rules[54] for the resolution of $D_{\infty h}$ species into those of C_{2v} can be applied to the calculated united-atom Rydberg orbitals to obtain symmetry components of Rydberg orbitals in bent CO_2.

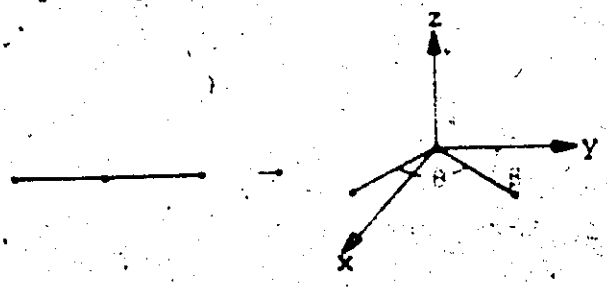

$D_{\infty h}$ C_{2v}

$D_{\infty h}$	C_{2v}
$ns\sigma_g$	nsa_1
$np_y\sigma_u$	np_yb_2
$np_x\pi_u$	np_xb_1
$np_z\pi_u$	np_za_1

The symmetry splittings of united-atom orbitals due to the non-spherical part of the potential can be divided into two contributions:

$$\mu_{c.s.} = \mu^{in}_{c.s.} + \mu^{out}_{c.s.} \quad \text{(see p.61)} \qquad 3.14$$

(i) Outside the ion-core

Because Rydberg Mo's are like phase-shifted hydrogen orbitals outside the ion-core, $\mu^{out}_{c.s.}$ is similar to $\mu^{out}_{c.s.}$ for a hydrogen orbital in a point-charge distribution with the same geometry as the core.

The one-electron perturbation calculations of H. Hosoya[32] can be used to estimate the splitting pattern of hydrogenic orbital components in going from $D_{\infty h}$ to C_{2v} point-charge distributions. The most important feature of these splittings is the behaviour of the $np\pi_u$ orbital on bending the ion-core. The matrix elements involving p_x orbitals are independent of β so $np_x\pi_u \rightarrow np_xb_1$ without changing energy. On the other hand $\langle np_y\sigma_u|V_{pert}|np_y\sigma_u\rangle$ and $\langle np_z\pi_u|V_{pert}|np_z\pi_u\rangle$ are both functions of $(1 + \cos 2\beta)$ while the second-order term $\langle np_y\sigma_u|V_{pert}|np_z\pi_u\rangle$ is a function of $\sin 2\beta$. The components np_z and np_y are mixed as the molecule is bent forming two new orbitals which transform as

a_1 and b_2 under the symmetry operations of the C_{2v} point group.

$$npa_1 = np_y\sigma_u \sin\beta + np_z\pi_u\cos\beta$$

$$npb_2 = np_z\pi_u\sin\beta - np_y\sigma_u\cos\beta$$

When $\beta=45°$, equivalent to a bond-angle $\theta=90°$, npa_1 and npb_2 have the same energy, mid-way between the energies of $np\pi_u$ and $np\sigma_u$ in the linear molecule.

In the bent conformation of CO_2 nsa_1 and npa_1 can mix (2nd order perturbation) and will repell each other. However, because the energy interval $E(ns\sigma_g - np\pi_u)$ is quite large compared to $E(np\sigma_u - np\pi_u)$, this repulsion will be small relative to the lowering of $np\pi_u(a_1)$ on bending.

(ii) Inside the ion-core

Model wavefunctions do not give accurate representations of "true" Rydberg orbitals inside the ion-core because of the nature of the model potential method (See Chapter 2). The form of a Rydberg orbital inside the core is governed by the orthogonality constraints imposed on the Rydberg orbital by it's real core precursors. The M.O. core precursors for the $ns\sigma_g$, $np\sigma_u$ and $np\pi_u$ Rydberg orbitals of CO_2 are given in Table 3.II. (These do not include core Mo's composed of 1s orbitals).

Table 3.II

Rydberg Orbital	M.O. Core Precursors
$ns\sigma_g$	$3\sigma_g$, $4\sigma_g$
$np\sigma_u$	$2\sigma_u$, $3\sigma_u$
$np\pi_u$	$1\pi_u$

Inside the core a Rydberg orbital takes the form of a linear combination of core precursor M.o's. e.g.

$$\phi_{3s\sigma_g}(\text{core}) = c_1\ 3\sigma_g + c_2\ 4\sigma_g.$$

Each core Mo acts like a loop creating function with small coefficients, c_1 and c_2, in the complete Rydberg orbital. Hence the core part of a Rydberg orbital will behave in the same way as it's real core precursors on bending the molecule.

The variation of orbital energies of an XY_2 molecule in going from the linear (θ=180°) to the bent (θ=90°) conformation is usually represented in a Walsh diagram[54,58]. S.P. McGlynn et al.[59] have given a semi-quantitative Walsh diagram for CO_2 which indicates that the behaviour of CO_2 Mo's on bending the molecule is as follows:

$3\sigma_g$, $4\sigma_g$	Stabilized
$2\sigma_u$	Destabilized
$3\sigma_u$	Slightly stabilized
$1\pi_u \begin{cases} a_1 \\ b_1 \end{cases}$	Slightly destabilized
	Unchanged

By analogy with equation 3.14, the total change in orbital energy, ΔE, on bending the molecule is given by,

$$\Delta E = \Delta E^{in} + \Delta E^{out} \qquad 3.15$$

The ΔE are negative when the orbital energy is lowered on bending the molecule. A summary of the signs of ΔE^{in} and ΔE^{out}

with the resultant sign of ΔE is given in table 3.III.

Table 3.III

Orbital	ΔE^{out}	ΔE^{in}	ΔE
$ns\sigma_g$	-	-	-
$np\sigma_u$	+	0	+
$np\pi_u\{a_1$	-	+	-
$np\pi_u\{b_1$	0	0	0

From the total change in orbital energy on bending the molecule to $\theta=90°$ it is possible to estimate that for both $3s\sigma_g(a_1)$ and $3p\pi_u(a_1)$,

$$\frac{\partial E_{Ryd}}{\partial \theta} \sim -4 \times 10^{-4} \text{ a.u./deg}$$

If the bending force constant of CO_2^+, $k_{CO_2^+}$, were known as a function θ, θ_e could be determined from this estimate of $\frac{\partial E_{Ryd}}{\partial \theta}$ using equation 3.13. Unfortunately $k_{CO_2^+}(\theta)$ cannot be obtained reliably from force-constant calculations because the bending frequency, ν_2, of CO_2^+ is not an experimentally known quantity. However, a comparison with $k_{CO_2}(\theta)$ indicates that CO_2 is only slightly bent (i.e. $\theta_e > 170°$) in the $(\pi_g)^3$ $3p\pi_u(a_1)$ and $(\pi_g)^3$ $3sa_1$ configuration of CO_2.

If $(\pi_g)^3$ $3s\sigma_g$ $(^1\Pi_g)$ is slightly bent the forbidden transition,

$$\ldots(\pi_g)^3\ 3s\sigma_g(^1\Pi_g) \rightarrow {}^1\Sigma_g^+$$

is actually,

$$\ldots(a_2)^2\ b_2\ 3sa_1(^1B_2) \rightarrow {}^1\Sigma_g^+$$

which is allowed.

CHAPTER 4

RYDBERG SERIES IN CO_2

4.1 Experimental Studies of the Rydberg Excited States of CO_2

The lower excited states of CO_2 (i.e. states with excitation energies less than the first ionisation potential) have been investigated by optical absorption spectroscopy on several occasions since the pioneering work of T. Lyman[1] in 1908.

A Rydberg series extending from 1120-900 Å and converging to the first ionisation potential of CO_2 at 13.79 ev. was identified in the absorption spectrum by W.C. Price et al. in 1938[60]. Recently several additional series have been found in the region below 1200 Å by Y. Tanaka et al.[61] and their published table of frequencies has been adopted in this thesis. A plot of the absorption coefficient of CO_2 in the region 1670-580 Å has been published by K. Watanabe[62] et al. and gives a useful representation of Tanaka's Rydberg series; this plot is reproduced on p. 122 (Fig. 4.II)

In addition to conventional optical spectroscopy the technique of electron-impact spectroscopy has proved to be useful in the study of molecular excited states; electron impact spectra of CO_2 have been obtained by E.W. Lassettre et al.[63,64,65] at different accelerating voltages and scattering angles. At high accelerating voltages (impact

energy >> excitation potentials) and zero scattering angle, energy loss spectra are very similar to optical absorption spectra. However, at low impact energy and high scattering angles optically forbidden singlet-triplet and electric quadrupole transitions increase in intensity relative to optically allowed transitions. This fact can be used to identify spin and symmetry forbidden transitions.

4.2 Theoretical Studies of the Lower Excited States of CO_2

Introduction

With the best resolution possible on modern spectrographs the vacuum u-v spectrum of CO_2 consists of diffuse bands with no discernible fine structure. Rotational analysis of this type of spectrum is not possible and excited state assignments of absorption bands must be made on the basis of theoretical considerations.

Several ab. initio calculations of the excited states of CO_2 have been published[66,67,68] but none of these has included Rydberg orbitals in the basis set, and consequently a description of only sub-Rydberg states has been obtained. An extended Gaussian basis set containing diffuse Rydberg-like orbitals has been used by N.W. Winter et al.[57] in recent unpublished calculations on the lowest five (singlet and triplet) Rydberg states of CO_2.

In Chapter 2 of this thesis a semi-empirical model potential approach to the calculation of Rydberg series in small polyatomic molecules has been developed and its applications

to CO_2, CS_2 and CSe_2 will be discussed below. First however, a brief comparison of this type of semi-empirical calculation with the ab initio calculations typified by those of Winter et al[57], will be made.

Semi-empirical calculations based on model potentials rather than self-consistent fields are approximations to ab initio calculations with self-consistent field Hamiltonians. However, the elimination of core wavefunctions in model potential calculations gives the approach at least two practical advantages over ab initio methods:

1) The model potential method is numerically simple and requires only a few minutes of computer time for the calculation of a complete Rydberg series. By contrast ab initio calculations require several hours for the determination of one Rydberg state.

2) Model potential calculations are applicable to any small molecule while ab initio calculations are restricted to molecules containing first-row atoms due to practical limitations on the size of the basis set.

Because part of this thesis deals with molecules containing second and third-row atoms, semi-empirical calculations have been used throughout. Nevertheless the ab initio calculations of Winter et al[57] have been useful because they provide assignments of the first members of the $ns\sigma_g$, $np\sigma_u$ and $np\pi_u$ Rydberg series of CO_2, and serve to test the accuracy of the model potential derived for CO_2 in this thesis. The extent to which model potential calculations agree with assignments of low lying

CO_2 Rydberg states based on ab initio calculations, establishes the validity of the model potential and justifies its applications to higher Rydberg states.

Model Potential Calculations and the Rydberg Series of CO_2

Prior to the present work the only excited state configuration assignments for the Rydberg series of CO_2 were made by E. Lindholm[69] on the basis of qualitative arguments on the relative magnitudes of quantum defects. The model potential calculations presented in Chapter 2 of this thesis place Lindholm's qualitative arguments on a quantitative theoretical basis.

Lindholm assumed that Rydberg orbitals are essentially hydrogenic in character with quantum defects, $\mu(n\ell\lambda)$, depending on the degree of core penetration of the orbital. For linear molecules he assumed quantum defects in the order,

$$\mu(ns\sigma) > \mu(np\sigma) > \mu(np\pi) > \mu(nd\sigma) > \mu(nd\pi) > \mu(nd\delta)$$

and analysed Tanaka's[61] Rydberg series of CO_2 on this basis. He assigned Main series (1) to $1\pi_g \rightarrow np\sigma_u$ and Minor series (1) to $1\pi_g \rightarrow np\pi_u$. Minor series (2) was assigned to the forbidden transitions $1\pi_g \rightarrow nd\delta_g$. No series involving $ns\sigma_g$ orbitals were assigned. Lindholm considered Rydberg series in many diatomic and small polyatomic molecules in a similar manner and acknowledged that the order of $\mu(np\sigma)$ and $\mu(np\pi)$ appeared to be reversed in some molecules.

In this thesis it has been shown that the quantum - defect of a molecular Rydberg series can be written as (see p44):

$$\mu_{Mol} = \mu_{pen} + \mu_{c.s.}$$

Lindholm is correct in assuming,

$$\mu_{Mol}(ns\sigma) > \mu_{Mol}(np\sigma, np\pi),$$

because $ns\sigma$ orbitals are more penetrating than $np\sigma$ or $np\pi$, and the difference in quantum defects between orbitals with different ℓ is largely determined by μ_{pen}. However, Lindholm's arguments do not account for the difference in quantum defects between orbitals with the same ℓ but different λ. Thus, for example, $p\sigma$ - $p\pi$ splittings are determined by $\mu_{c.s.}$ which can be subdivided into contributions from inside and outside the ion-core.

$$\mu_{c.s.} = \mu^{in}_{c.s.} + \mu^{out}_{c.s.}$$

The symmetry splittings of a hydrogenic orbital outside an ion-core with the point-charge distribution of a linear triatomic molecule are such that,

$$\mu^{out}_{c.s.}(np\sigma) > \mu^{out}_{c.s.}(np\pi)$$

Values for $\mu^{in}_{c.s.}(np\lambda)$ cannot be determined by qualitative arguments but it is apparent that $\mu^{in}_{c.s.}(np\sigma)$ and $\mu^{in}_{c.s.}(np\pi)$ are numerically different because $np\sigma$ and $np\pi$ orbitals extend over different regions of core space. (See Fig. 4.I).

Fig. 4.I

The Approximate Form of the $3p\sigma_u$ and $3p\pi_u$ CO_2 Rydberg MO's

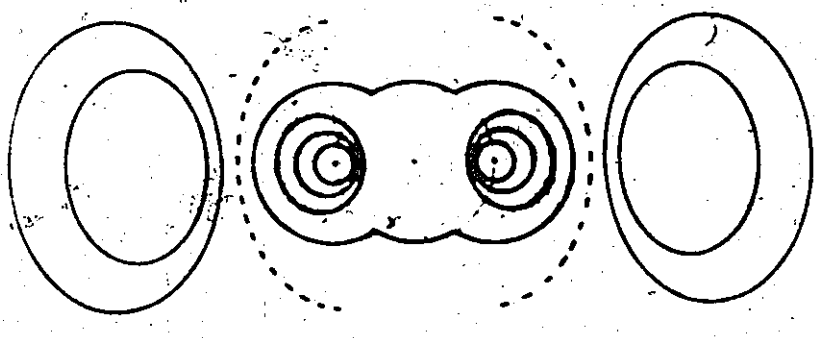

$3p\sigma_u$

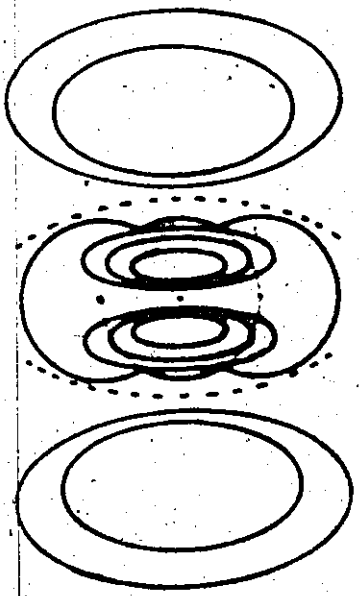

$3p\pi_u$

If $\mu^{in}_{c.s.}(np\sigma) < \mu^{in}_{c.s.}(np\pi)$ it is possible that $p\sigma - p\pi$ splittings can be the reverse of the ordering predicted by Lindholm.

Results

Rydberg series calculated for CO_2 using the model potential method developed in Chapter 2 are given in table 4.I. The relationship of the calculated term values for the first member of each series to Rydberg transitions observed in the CO_2 spectrum will now be considered.

(i) $3s\sigma_g$.

The $3s\sigma_g$ term of CO_2 is calculated to be +0.1175 a.u. corresponding to a quantum defect of 0.95. If $1\pi_g \rightarrow ns\sigma_g$ is weakly allowed in the u-v spectrum of CO_2, the calculation predicts the first member of this series should be observed ~1200 Å. In this region of the CO_2 spectrum there is a weak absorption system extending from 1400-1200 Å with a maximum at 1330 Å and there is a considerable body of evidence favouring the assignment of this transition to $1\pi_g \rightarrow 3s\sigma_g$. This evidence is as follows:

(i) E.N. Lassettre et al[63,64,65] have shown that the envelope shape of the absorption from 1700-1200 Å in the electron impact energy-loss spectrum changes with scattering angle and impact energy and suggest this is evidence for changes from a dipole to quadrupole spectrum. The absorption system is attributed to the quadrupole allowed transition $^1\pi_g \leftarrow {}^1\Sigma^+_g$ which is electric

Table 4.I

Calculated Rydberg Terms for CO_2

(Average of values given in Table 2.IV)

n	$ns\sigma_g$ (a.u.)	$np\sigma_u$ (a.u.)	$np\pi_u$ (a.u.)
2	0.1175	0.0955	0.0970
3	0.0518	0.0434	0.0454
4	0.0293	0.0251	0.0262
5	0.0189	0.0163	0.0170
6	0.0131	0.0116	0.0120
7	0.0097	0.0086	0.0088

dipole allowed if the excited state, $^1\Pi_g$, is slightly bent.

(ii) S.P. McGlynn et al[59] have assigned the 1330 Å transition to $^1\Pi_g \leftarrow {}^1\Sigma_g^+$ with a slightly bent upper state. The Franck-Condon principle for a bent ← linear transition predicts that the strongest absorption bands should involve excitation of the upper state bending vibration, ν_2'. Transitions of this type are subject to very strong rotation-vibration interaction leading to an irregular arrangement of energy levels. McGlynn listed the observed vibrational frequencies of the 1330 Å transition and found that they were "irregular but consisted of a simple progression ~624 cm^{-1}". This is close to the bending frequency of the ground state of CO_2 (667 cm^{-1}).

(iii) The unpublished calculations of N.W. Winter et al[57] on CO_2 excited states give a vertical excitation energy for $^1\Pi_g \leftarrow {}^1\Sigma_g^+$ of 9.23 ev corresponding to a transition in the u-v spectrum ~1350 Å. These calculations show that the $^1\Pi_g$ state has the basic S.C.F. orbital form $\ldots(\pi_g)^3\ 3s\sigma_g$.

If the 1330 Å transition in the CO_2 u-v spectrum is due to $\ldots(\pi_g)^3\ 3s\sigma_g\ (^1\Pi_g) \leftarrow {}^1\Sigma_g^+$, the $3s\sigma_g$ term value is +.1634 a.u. compared to a value of +.1175 a.u. determined by the model potential calculation. Clearly the observed $3s\sigma_g$ level is considerably more stable than the calculated level. The difference,

$$E_{dif} = E_{obs} - E_{calc} = -0.045 \text{ a.u.},$$

between theory and experiment can be accounted for by a number

of factors which have been omitted from the calculation:

(a) Changes in Geometry in the Excited State

In this thesis all Rydberg terms have been calculated for the linear conformation of CO_2 although the discussion on pp 96-102 showed that the excited configuration $(\pi_g)^3\ 3s\sigma_g$ of CO_2 is more stable in a slightly bent conformation. This indicates that the transition $\ldots(\pi_g)^3\ 3s\sigma_g(^1\Pi_g) \leftarrow {}^1\Sigma_g^+$ in CO_2 corresponds to a bent ← linear transition and is fully in accord with the assignments of Lassettre[63,64,65] and McGlynn[59] concerning the 1330 Å transition of CO_2. However the lowering of the Rydberg term energy of bent CO_2 relative to linear. $^1\Pi_g$ is small (probably 0.005 a.u.) and accounts for only a small part of E_{dif}.

(b) The Effects of s-d Mixing

The calculation of the $ns\sigma_g$ terms of CO_2 has been carried out using only s functions and assumes the Rydberg orbital is an exact eigenfunction of ℓ. Actually there is probably ~10% s-d mixing (see p.61) in the $3s\sigma_g$ orbital which will lower a $3s\sigma_g$ level calculated without this mixing. However, because the closest d level which can mix with $3s\sigma_g$ is $3d\sigma_g$ and the energy interval $3s\sigma_g - 3d\sigma_g$ is quite large, it can be estimated that the inclusion of s-d mixing will lower the $3s\sigma_g$ level by no more than 0.007 a.u.

(c) Bonding Effects

The model potential used in the calculation of CO_2 Rydberg terms consists of a superposition of free-atom model

potentials and neglects terms of the type $V_{AB}(R)$ which arise from the interaction of atomic cores (see p.46). $V_{AB}(R)$ allows for the fact that a real molecule does not consist of its constituent free atoms at their equilibrium separations but contains atoms modified by bond formation. In this thesis Rydberg orbitals have been calculated with non-bonding core potentials (i.e. $V_{AB}(R)$ has been omitted). These will be denoted $\phi(n\ell\lambda)$, while Rydberg orbitals calculated with bonding cores ($V_{AB}(R)$ included) will be denoted $\phi'(n\ell\lambda)$.

The difference between $\phi(n\ell\lambda)$ and $\phi'(n\ell\lambda)$ can be estimated qualitatively from the bonding/anti-bonding characteristics of M.O. core precursors. Thus inside the core, $\phi'(ns\sigma_g)$ is bonding, $\phi'(np\sigma_u)$ anti-bonding and $\phi'(np\pi_u)$ weakly bonding relative to its $\phi(n\ell\lambda)$ counterpart. If it is assumed that after allowing for neglect of geometry changes and ℓ-spoiling in the calculation,

$$E_{dif.} = E_{obs} - E_{calc} = E(\phi'_{n\ell\lambda}) - E(\phi_{n\ell\lambda})$$

then for the $3s\sigma_g$ orbital,

$$E(\phi'_{3s\sigma_g}) - E(\phi_{3s\sigma_g}) = -0.03 \text{ a.u.}$$

If the $3s\sigma_g$ Rydberg electron gives a bonding contribution to CO_2^+, the vibrational frequencies $(\nu_n)_{CO_2}$ of the CO_2 excited state $\ldots(^1\pi_g)^3\ 3s\sigma_g,\ ^1\pi_g$, should be higher than the equivalent frequencies, $(\nu_n)_{CO_2^+}$, in CO_2^+. The ground state frequencies $(\nu_n)_{CO_2}$ and $(\nu_n)_{CO_2^+}$ are:[54]

	CO_2 (cm^{-1})	CO_2^+ (cm^{-1})
ν_1	1388	1280
ν_2	667	~400
ν_3	2349	1469

$(\nu_2)_{CO_2^+}$ has been estimated from a comparison of the behaviour of ν_2 for CS_2 and CS_2^+ and force constant calculations on CO_2^+.

According to McGlynn[59], $(\nu_2)_{CO_2^*}$ for $^1\Pi_g((\pi_g)^3\ 3s\sigma_g)$ is ~624 cm^{-1} which is very close to ν_2 for the ground state of CO_2, and much larger than the estimated value of $(\nu_2)_{CO_2^+}$. Thus there is experimental evidence for the prediction that $3s\sigma_g$ is bonding in the CO_2^+ core and the omission of such bonding effects in the model potential calculation probably accounts for the major part of E_{dif}.

(ii) $3p\sigma_u$ and $3p\pi_u$

The model potential calculation for the lowest p Rydberg terms, $T_{n\ell}$, of CO_2 gives:

$$T_{3p\sigma_u} = 0.0955 \text{ a.u.}$$

$$T_{3p\pi_u} = 0.0970 \text{ a.u.}$$

This ordering is the reverse of that proposed by E. Lindholm[69] and suggests that the correct assignment of Tanaka's[61] series is:

Main series (1) : $^1\Sigma_g^+ \rightarrow np\pi_u$ 4.1

Minor series (1) : $^1\Sigma_g^+ \rightarrow np\sigma_u$

If this is the case the calculated $np\sigma_u - np\pi_u$ splittings are too small but this can be accounted for by the neglect of the same factors in the model potential calculation which caused errors in the calculated $3s\sigma_g$ term. These are:

(i) Geometry changes in the excited state

(ii) ℓ-spoiling

(iii) core bonding effects.

The discussion on pp 96-102 shows that... $(\pi_g)^3\ 3p\pi_u$ is probably bent while ... $(\pi_g)^3\ 3p\sigma_u$ is linear, and the observed $3p\pi_u$ term will be lowered by $\sim$0.005 a.u. relative to a $3p\pi_u$ term calculated for a linear conformation. This implies that the observed $p\sigma - p\pi$ splittings are larger than those calculated for linear CO_2.

The effects of ℓ-spoiling on calculated $3p\lambda$ levels are smaller than for $3s\sigma_g$ levels and should not affect the ordering of $p\sigma$ and $p\pi$ levels.

Core bonding effects for $\mathcal{D}$ orbitals are smaller than those for s orbitals because p orbitals are less penetrating than s orbitals. However, the differences that do exist between $\phi(np\lambda)$ and $\phi'(np\lambda)$ (see p.113) are such that observed $p\sigma - p\pi$ splittings are larger for calculated values of $E(\phi'_{np\lambda})$ than for $E(\phi_{np\lambda})$.

Thus changes in the geometry in the excited state and core bonding effects tend to make $\mu(np\sigma) < \mu(np\pi)$ in CO_2. There is, in any case, additional evidence which favours the

ordering of pσ and pπ levels suggested by the model potential calculation and rules out the ordering proposed by Lindholm.[69]

The ab initio calculations of N.W. Winter[57] give the term values:

$$T_{3p\pi_u}(^1\Sigma_u^+) = +\ 0.0996 \text{ a.u.}$$

and $$T_{3p\sigma_u}(^1\Pi_u) = +\ 0.0827 \text{ a.u.}$$

The first terms in Tanaka's series are:

Main series (1) = + 0.1034 a.u.

Minor series (1) = + 0.0883 a.u.

The ab initio calculations therefore favour assignment 4.1.

Experimental confirmation of this assignment comes from the observed vibrational structure of the absorption bands at 1129 Å and 1088 Å in the CO_2 spectrum corresponding to the first members of Tanaka's[61] Main series (1) and Minor series (1) respectively. The transition at 1129 Å is part of a broad and complex system of bands extending from 1115 to 1185 Å. The bands are diffuse and show many intervals between 520 and 670 cm^{-1}. Like the 1330 Å system of CO_2 this is suggestive of a bent upper state and is compatible with the assignment of an excited state configuration $\ldots(^1\pi_g)^3\ 3p\pi_u$ in a slightly bent conformation. In contrast to the transition at 1129 Å, the band at 1088 Å is very sharp and shows little vibrational structure; this is to be expected for a state derived from a

$3p\sigma_u$ Rydberg orbital which is anti-bonding with respect to CO_2^+ and destabilized on bending.

The Higher members of the $1\pi_g \rightarrow n\ell\lambda$ Rydberg series of CO_2

(i) $ns\sigma_g$ and $nd\lambda_g$ series

As n increased along the $1\pi_g \rightarrow n\ell\lambda$ Rydberg series of CO_2 the core bonding effects mentioned in the previous section should diminish because of the diminishing relative amplitude of the innermost loops of the Rydberg orbital $\phi(n\ell\lambda)$. At the same time the ℓ-spoiling of $\phi(n\ell\lambda)$ decreases and the excited state geometry approaches the linear geometry of the ion-core. For these reasons the model potential calculations used in this thesis should give better agreement with observed term values for higher members of Rydberg series than for the first members of the series.

The calculation predicts $1\pi_g \rightarrow 4s\sigma_g$ should be observed $\sim$1004 Å (99560 cm^{-1}) in the CO_2 spectrum, while a quantum defect equal to that observed for the $3s\sigma_g$ term would place the $1\pi_g \rightarrow 4s\sigma_g$ transition $\sim$1036 Å (96560 cm^{-1}). Transitions due to $1\pi_g \rightarrow 3d\lambda_g$ should also be observed in this region of the CO_2 spectrum. If a $3d\delta_g$ orbital is non-penetrating (quantum defect = 0), $1\pi_g \rightarrow 3d\delta_g$ should be observed $\sim$1010 Å and Lindholm[69] has assigned the band observed at 1007 Å in the CO_2 spectrum to this transition. Because $3d\sigma_g$ and $3d\pi_g$ are more penetrating than $3d\delta_g$, $1\pi_g \rightarrow 3d(^{\pi g}_{\sigma g})$ will be to the red

of $1\pi_g \rightarrow 3d\delta_g$ in the CO_2 spectrum and $4s\sigma_g - 3d\sigma_g$ mixing will push $3d\sigma_g$ to the red of $3d\pi_g$.

There are many transitions observed in the CO_2 spectrum between 1000 and 1080 Å, and an assignment of each band is not possible; the following approximate scheme is proposed:

Transition	Observed Bands (Å)
$1\pi_g \rightarrow 3d\sigma_g$	1040-1080
$1\pi_g \rightarrow 3d\pi_g$	1035
$1\pi_g \rightarrow 3d\delta_g$	1007
$1\pi_g \rightarrow 4s\sigma_g$	1000-1040

The calculation predicts $1\pi_g \rightarrow 5s\sigma_g$ should be observed in the CO_2 spectrum ~956 Å (104600 cm^{-1}). On this basis the group of bands observed in this region 955-965 Å are assigned to $1\pi_g \rightarrow 5s\sigma_g$ and $1\pi_g \rightarrow 4d\lambda_g$. However the resolution of published spectra in this region is insufficient to allow the different λ components of the d series to be assigned to particular bands in the spectrum.

(ii) $np\sigma_u$ and $np\pi_u$ series

The selection rules for electric dipole transitions in CO_2 indicate that the strongest Rydberg series converging to the first ionisation potential of CO_2 should be due to transitions of a valence $1\pi_g$ electron to an $np\lambda_u$ orbital.

The Rydberg series identified by W.C. Price et al[60] in

the 1120-900 Å region of the CO_2 spectrum has been resolved by Tanaka et al[61], at wavelengths longer than 930 Å, into four component transitions with similar intensity for each n. Tanaka[61] grouped these four components into three Rydberg series as follows:

Main series (1) - two transitions

Main series (2) - one transition

Minor series (1) - one transition

In Chapter 3 it was shown that of the possible transitions from the CO_2 ground state to the manifold of states derived from the excited configuration $\ldots(\pi_g)^3 np\lambda_u$ only $^1\Sigma_u^+ \leftarrow {}^1\Sigma_g^+$ and $^1\Pi_u \leftarrow {}^1\Sigma_g^+$ are allowed in (Λ,S) coupling, while the additional transitions $^3\Sigma^-_{0+u} \leftarrow {}^1\Sigma_g^+$ and $^3\Pi_{1u} \leftarrow {}^1\Sigma_g^+$ become allowed on going over to (Ω_C,ω) coupling.

The ab initio calculations of N. Winter et al[57] give $E(^1\Pi - {}^3\Pi) \sim 320\ cm^{-1}$ for states derived from the $(\pi_g)^3\ 3p\pi_u$ configuration of CO_2 and the doublet splitting of the ground state of CO_2^+ is $\sim 160\ cm^{-1}$. Consequently the intensity ratio, $I(\frac{1}{3})$, should be $\sim 2:1$ for the first members of the $1\pi_g \rightarrow np\pi_u$ series. For higher members of the series $I(\frac{1}{3}) \rightarrow 1$ as ideal (Ω_C,ω) coupling is approached. Similar behaviour is expected for the $^1\Sigma_u^+$ and $^3\Sigma_u^-$ components of the $1\pi_g \rightarrow np\pi_u$ series. Hence that Tanaka's[61] Main series (1) and (2) and Minor series (1) constitute four component transitions of similar intensity for

each n can be accounted for by assuming these series are due to the transitions:

$$1\pi_g \rightarrow np\sigma_u \begin{cases} {}^1\Pi(1) \\ {}^3\Pi(1) \end{cases}$$

and

$$1\pi_g \rightarrow np\pi_u \begin{cases} {}^1\Sigma_u^+(0^+) \\ {}^3\Sigma_u^-(0^+) \end{cases}$$

and that, for n>3, the excited states are (Ω_C,ω) coupled.

Inspection of the spectrum of CO_2 in the region 1150-900 Å shows many weak transitions in addition to the principal components assigned by Tanaka[61] to Rydberg series. Tanaka groups some of these weaker transitions into "vibration series" but it is also possible that some of these absorption bands are due to transitions to (Ω_C,ω) coupled states with $\Omega=1$ or 0^+ which are weakly allowed through intra and extra configurational state mixing. Detailed excited state symmetry assignments of these bands will require extensive C.I. calculations of the higher Rydberg states of CO_2 which are currently not available.

Excited state configuration assignments of Tanaka's series have been made by E. Lindholm[69] who assigned Main series (1) to:

$$1\pi_g \rightarrow np\sigma_u \qquad (\mu \sim 0.71),$$

and Minor series (1) to

$$1\pi_g \rightarrow np\pi_u \qquad (\mu \sim 0.56),$$

These assignments were made on the basis of qualitative arguments which have been discussed on pp. 106-107 of this thesis. It was shown that Lindholm's assignments are probably correct for series with different ℓ but are unreliable for series with the same ℓ and different λ.

The model potential calculations developed in this thesis and the ab initio calculations of N. Winter show that,

$$\mu(3p\sigma) < \mu(3p\pi)$$

in contrast to Lindholm's assignments. For the higher members of the $1\pi_g \rightarrow np\lambda_u$ series the model potential calculations presented in this thesis constitute the only theoretical studies available and indicate that the ordering,

$$\mu(np\sigma) < \mu(np\pi)$$

is maintained along the series. It is therefore probable that Tanaka's Main series (1) and (2) are due to:

$$1\pi_g \rightarrow np\pi_u$$

and Minor series (1) to

$$1\pi_g \rightarrow np\sigma_u$$

A comparison of calculated terms with Tanaka's series is given in table 4.II. The calculated $np\sigma - np\pi$ splittings are too small but an explanation of this has already been given for the $n=3$ terms and applies to higher terms (see pp. 114 - 117).

Fig. 4.11

CO_2 Spectrum from 1000-1400 Å Showing $1\pi_g \rightarrow n\ell\lambda$ Assignments

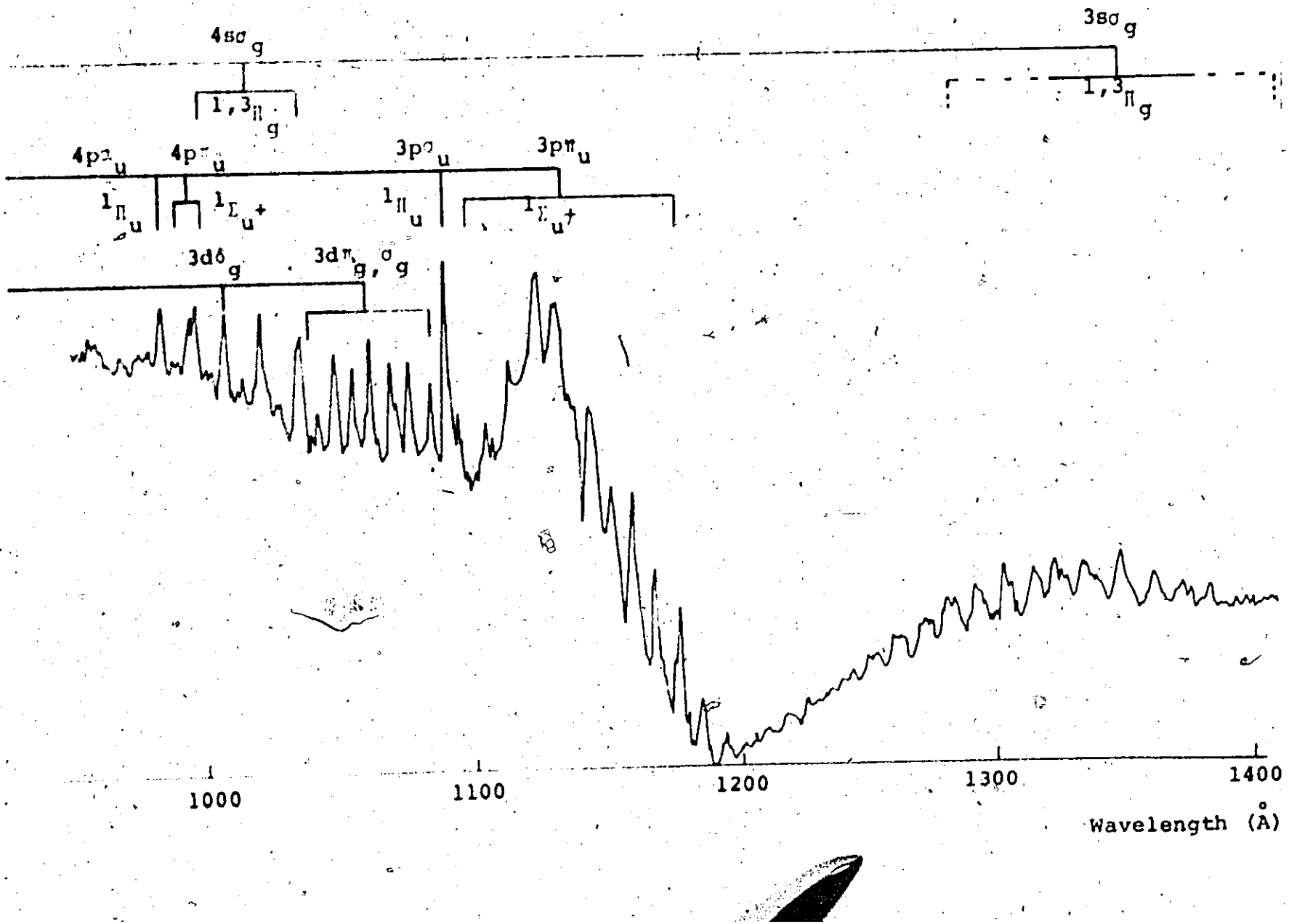

Table 4.II

A Comparison of Some Calculated and Observed Rydberg Series in CO_2

Observed Series (a.u.)			Calculated Series (a.u.)	
Main Series (1)	Main Series (2)	Minor Series (1)	$np\sigma_u$	$np\pi_u$
.1034	.1026	.0883	.0955	.0970
.1008				
.0486	.0461	.0425	.0434	.0454
.0482				
.0282	.0277	.0252	.0251	.0262
.0278				
.0186	.0186	.0168	.0163	.0170
.0183				
.0127	.0125	.0118	.0116	.0120
.0125				
.0095	.0093	.0088	.0086	.0088

CHAPTER 5

RYDBERG SERIES IN CS_2

5.1 Previous Experimental and Theoretical Work

The vacuum u-v spectrum of CS_2 was first investigated by W.C. Price et al.[70] in 1938. Price grouped many of the observed absorption bands in the region from 1400-1200 Å into two Rydberg series converging to limits separated by 436 cm^{-1}, the doublet separation of the ground state, $^2\Pi_g$, of CS_2^+. The CS_2 vacuum u-v spectrum was reinvestigated in 1960 by Y. Tanaka et al.[71] at wavelengths below 1600 Å and Price's Rydberg series were confirmed.

J.B. Hasted et al.[72] have obtained electron energy-loss spectra of CS_2 and grouped most of the observed energy-loss peaks at energies less than 11 e.v.(88, 700 cm^{-1}) into four Rydberg series, two of which correspond to those of Price et al. Hasted proposed Rydberg orbital assignments for these four series and, to date, the only other orbital assignments of Rydberg transitions in CS_2 have been made by S.P. McGlynn[59] et al. who identified and assigned seven Rydberg series.

Both Hasted[72] and McGlynn[59] based their Rydberg orbital assignments on the size of the quantum defect for a particular series and it was shown in Chapter 4 that assignments made in this way, by E. Lindholm[69] for the Rydberg series of CO_2 were erroneous in certain cases. However, quite apart from the absence of any theoretical justification of the assignments

of Hasted and McGlynn the assignments of these two authors are quite different and further work is obviously needed.

In the following pages the Rydberg spectrum of CS_2 in the region from 2000 to 1200 Å will be reanalysed and the assignments made will be compared with those of Hasted and McGlynn.

5.2 Model Potential Calculations of the Rydberg Series of CS_2

The model potential calculations developed in Chapter 2 were used to estimate term values for the $\pi_g \rightarrow ns\sigma_g$, $np\sigma_u$ and $np\pi_u$ Rydberg series in CS_2. The calculated term values are listed in table 5.I . These calculations constitute the only theoretical studies on the Rydberg series of CS_2 available to date, and form the basis of the analysis of the CS_2 spectrum presented in this thesis.

Because CS_2 has 16 valence electrons it is valence isoelectronic to CO_2 and similarities between the electronic spectra of CS_2 and CO_2 should exist. For the same reason there should be a correlation between observed and calculated term values in CO_2 and CS_2. In particular, two important trends which were observed in the model potential calculations on CO_2 (See pp.109) should also be found in the calculations on CS_2.

(i) Calculated $ns\sigma_g$ term values are smaller than the observed $ns\pi_g$ terms especially for the lower members of series.

(ii) Calculated $np\pi_u$ term values are close to observed $np\pi_u$ terms, but calculated $np\sigma - np\pi$ splittings are too small.

General Discussion of Results

A comparison of the calculated $ns\sigma_g$, $np\sigma_u$ and $np\pi_u$ term values for CO_2 (table 4.I) and CS_2 (table 5.I) shows that the calculated CS_2 term values are all smaller than the corresponding CO_2 term values but the difference is never more than 20% between terms. This indicates that the value of the effective quantum number, n*, for the lowest term of a particular series in CS_2 is similar to the value of the lowest term of the equivalent series in CO_2. At the same time the principal quantum number, n, of the Rydberg orbital, $\phi(n\ell\lambda)$, in CO_2 must be increased by unity in CS_2 if $\phi(n\ell\lambda)$ has real core precursors in the separated atoms. Hence for $ns\lambda_g$ and $np\lambda_u$ series in CO_2 and CS_2,

$$n^*_{\ell\lambda}(CO_2) = n - \mu_{\ell\lambda}(CO_2) \qquad \ell \leq 1$$

and

$$n^*_{\ell\lambda}(CS_2) = n + 1 - \mu_{\ell\lambda}(CS_2)$$

Then because,

$$n^*_{\ell\lambda}(CO_2) = n^*_{\ell\lambda}(CS_2),$$

$$\mu_{\ell\lambda}(CS_2) = \mu_{\ell\lambda}(CO_2) + 1 \qquad \ell \leq 1$$

On the other hand, for $nd\lambda_g$ and $nf\lambda_u$ series,

$$\mu_{\ell\lambda}(CS_2) = \mu_{\ell\lambda}(CO_2) \qquad \ell > 1$$

Because the internuclear separations in CS_2 are larger than in CO_2, λ splittings may be larger in CS_2 than in CO_2.

but nevertheless, for terms with the same n, λ splittings will certainly be smaller than ℓ splittings for CS_2 Rydberg terms.

With these facts in mind it may be concluded that the ordering of Rydberg terms in CS_2 is similar to CO_2 and is probably:

$$4s\sigma_g > 4p\pi_u > 4p\sigma_u > 3d\sigma_g = 3d\pi_g > 3d\delta_g$$

$$> 5s\sigma_g > 5p\pi_u > 5p\sigma_u > 4d\sigma_g, \pi_g, \delta_g > 6s\sigma_g > 4f\sigma_u, \pi_u \ldots \text{etc.}$$

This compares with McGlynn's[59] ordering based on his assignment of CS_2 Rydberg transitions:

$$4s_1 > 3d_1 > 4p_1 > 3d_2 > 3d_3 > 4s_2 > 5s_1 > 4p_2 > 5p_1 > 4d_1 \ldots \text{etc,}$$

where the subscripts label different symmetry components of terms with the same ℓ.

McGlynn[59] does not explain why two $\pi_g \rightarrow ns\sigma_g$ and two $\pi_g \rightarrow np\lambda_u$ series should be observed in CS_2 although presumably the two p series are the singlet components of $\pi_g \rightarrow np\sigma_u$ and $np\pi_u$ series. However the existence of two $\pi_g \rightarrow ns\sigma_g$ series can only be rationalised in terms of transitions to singlet and triplet components of the same excited state configuration $\ldots(\pi_g)^3\, ns\sigma_g$. In this case McGlynn's[59] assignment of the $\pi_g \rightarrow ns\sigma_g$ series in CS_2 implies that the singlet-triplet interval for the $(\pi_g)^3\, 4s\sigma_g$ configuration is $\sim$12,286 cm^{-1}. The Rydberg states of CS_2 should be closer to ideal (L_C-

coupling than ideal (Λ,S) coupling and singlet-triplet intervals should be similar to, but greater than, the spin-orbit coupling constant, Ã, for CS_2^+. For CS_2^+ Ã is 436 cm^{-1} so that McGlynn's[59] singlet-triplet interval is clearly unacceptable.

McGlynn's[59] Rydberg assignments are unsatisfactory in other respects. For example, a non-penetrating $3d\lambda_g$ Rydberg electron should have a term value ∿12,200 cm^{-1}. Hence the transition $\pi_g \rightarrow 3d\lambda_g$ (non-penetrating) in CS_2 should be observed at an energy ∿(81,500 - 12,200) or ∿69,300 cm^{-1}, corresponding to a wavelength ∿1443 Å in the CS_2 spectrum. Transitions to a penetrating $3d\lambda_g$ orbital must lie to the red of 1443 Å, but certainly no higher than the $\pi_g \rightarrow 4p\lambda_u$ transition. McGlynn assigns the CS_2 band at 1595.5 Å to a $\pi_g \rightarrow 4p\lambda_u$ transition and the 1612 Å band to $\pi_g \rightarrow 3d\lambda_g$. This assignment is therefore unacceptable and in addition gives $\pi_g \rightarrow nd\lambda_g$ series with very poor fits to Rydberg formulae.

Hasted et al.[72] do not assign any $\pi_g \rightarrow nd\lambda_g$ series in their work on CS_2; the assignments that are made by these authors are in accord with the ordering of terms predicted by the calculations in the present work except that the $np\sigma$ and $np\pi$ terms are reversed. This is similar to the situation in CO_2 where E. Lindholm[69] assigned certain CO_2 series to $\pi_g \rightarrow np\lambda_u$ in such a way that,

$$^1\Sigma_u(np\sigma_u) > {}^1\Delta_u(np\pi_u),$$

but model potential calculations and independent ab initio calculations favoured

$$\mu(np\pi_u) > \mu(np\sigma_u)$$

Neither Lindholm[69] nor Hasted[72] were able to supply any evidence for favouring the ordering of $np\lambda_u$ terms they selected.

In the following pages we shall consider in detail the assignment of individual CS_2 Rydberg transitions and, where possible, supply spectroscopic evidence for assignments based on model potential calculations.

(i) $4s\sigma_g$

The calculated $4s\sigma_g$ term value in CS_2 was 0.1039 a.u. and comparison with CO_2 results indicates that the observed $4s\sigma_g$ term value in CS_2 will be ~25% larger than this. On this basis, the probable location of the $\pi_g \rightarrow 4s\sigma_g$ transition in the CS_2 spectrum is between 1800 and 1900 Å. Two transitions occur in this region (see Fig.5 .I):

(i) The very intense $\tilde{A}$ system which extends from 1850-2300 Å and which has been partially analysed by A.E. Douglas et al.[73] as having a bent, $^1B_2$, upper state.

(ii) A less intense diffuse transition at 1818 Å.

In Price's early paper[70] on the vacuum u-v spectrum of CS_2 it was suggested that the absorption band at 1818 Å was due to "a transition between non-bonding atomic orbitals

(possibly 3p → 4s)". Unfortunately this statement is misleading because it implies that the transition is allowed by the atomic selection rule $\Delta\ell = \pm 1$. It is true that the highest occupied non-bonding π_g Mo in CS_2, from which Price suggests the electron is excited, is composed largely of sulphur 3p orbitals, but in an atomic (united-atom) description the π_g Mo becomes $nd\pi_g$.

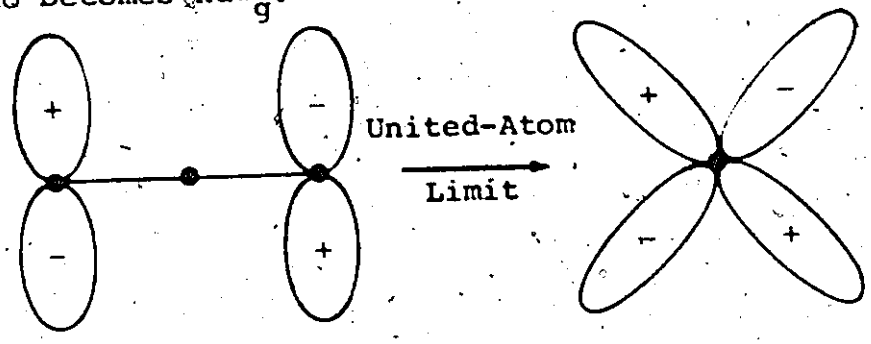

$\pi_g \equiv N\{3p\pi - 3p\pi\}$ $\pi_g \equiv nd\pi_g$

Therefore the transition is 3d → 4s, not 3p → 4s, and is forbidden.

McGlynn et al.[59] assign the 1818 Å transition in CS_2 to $\pi_g \rightarrow 4s\sigma_g$ but there are certain ambiguities in their discussion of the transition. Thus, in the text of McGlynn's paper it is stated that the 1818 Å band is "weak but very wide in agreement with the forbidden nature of the $\pi_g \rightarrow ns\sigma_g$ series". However, the same paper includes tables of esitmated oscillator strengths for CS_2 Rydberg transitions which show that the 1818 Å band is in fact one of the strongest CS_2 absorptions in the region 1900-1200 Å and is certainly more intense than CS_2 bands described elsewhere by McGlynn[59] as being "very strong".

It is clear from this discussion that misleading statements have been made by both Price[70] and McGlynn[59] concerning the 1818 Å transition in CS_2 and a clarification of the assignment of the transition is required.

Because the model potential calculations of the present work locate the $\pi_g \rightarrow 4s\sigma_g$ transition in CS_2 between 1800 and 1900 Å, two assignments of the transitions in this region of the CS_2 spectrum appear to be possible:

(A) The 1818 Å transition is due to,

$$(\pi_g)^3\ 4s\sigma_g\ {}^1\Pi_g \leftarrow (\pi_g)^4\ {}^1\Sigma_g^+,$$

and the intense $\tilde{A}$ system is, as Walsh[58] has proposed,

$$^1B_2 \leftarrow (\pi_g)^4\ {}^1\Sigma_g^+,$$

where the $^1B_2$ state is derived from the sub-Rydberg, $(\pi_g)^3\ \pi_u, {}^1\Sigma_u^+$, state in a bent conformation.

(B) The $\tilde{A}$ system is due to the Rydberg transitions,

$$(a_2)^2\ b_2\ \begin{Bmatrix} 4sa_1 \\ 4pa_1 \end{Bmatrix}\ {}^1B_2 \leftarrow (\pi_g)^4\ {}^1\Sigma_g^+$$

where the $4sa_1$ and $4pa_1$ Mo's are derived from $4s\sigma_g$ and $4p\pi_u$ Mo's in a bent conformation. In this case the 1818 Å transition may arise from the excitation of a bonding π_u electron to a Rydberg orbital i.e.,

$$(\pi_u)^3(\pi_g)^4 4s\sigma_g, {}^1\Pi_u \leftarrow (\pi_u)^4(\pi_g)^4\ {}^1\Sigma_g^+,$$

which is an allowed transition.

Neither assignments (A) or (B) is completely satisfactory but if assignment (B) is correct, the 1818 Å band is the first member of a $\pi_u \rightarrow ns\sigma_g$ series converging to the $^2\Pi_u$ limit of CS_2, identified by M. Ogawa et al.,[74] and the $4s\sigma_g$ term value is exceptionally high. Furthermore a comparison with the CSe_2 spectrum (see Chapter 6) shows that the analogue of the CS_2 1818 Å transition in CSe_2 is very weak and certainly corresponds to a forbidden transition. For this reason we shall follow McGlynn[59] in assuming the 1818 Å band in CS_2 is due to a $\pi_g \rightarrow 4s\sigma_g$ transition and assignment A is correct. The most unsatisfactory aspect of such an assignment is that a $\pi_g \rightarrow 4s\sigma_g$ transition is forbidden by the $g \nleftrightarrow g$ selection rule which is applicable to linear symmetric molecules; alternatively, if the upper state is bent and/or unsymmetrical the transition is allowed but should then show extended vibrational structure. Thus if assignment (A) is correct the high intensity and band profile of the 1818 Å transition are anomalous.

(ii) $4p\sigma_u$ and $4p\pi_u$

The calculated term values for the $4p\sigma_u$ and $4p\pi_u$ levels of CS_2 are 0.0847 and 0.0865 a.u. respectively, although comparison with the CO_2 calculation shows that the observed $np\sigma - np\pi$ splitting in CS_2 is probably larger than the calculated value of ~0.003 a.u.

A very strong transition is observed in the CS_2 spectrum at 1595 Å with a term value of 0.0857 a.u. This transition is accompanied by a much weaker band at 1612 Å (see fig. 5.I). In view of the similarity of the 1595 Å transition to the 1088 Å band in CO_2, which was assigned to $\pi_g \rightarrow 3p\sigma_u$ in this thesis, the following assignments of these CS_2 bands have been made:

1595 Å Band $\quad \pi_g \rightarrow 4p\sigma_u(^1\Pi_u)$

1612 Å Band $\quad \pi_g \rightarrow 4p\sigma_u(^3\Pi_u)$

Transitions to the triplet state are weakly allowed due to tendencies away from (Λ,S) coupling and towards (Ω_c,ω) coupling in CS_2 Rydberg states.

This assignment is in partial agreement with McGlynn[59] and Hasted[72]. Thus both of these authors assign the CS_2 1595 Å band to $\pi_g \rightarrow 4p\lambda_u$; McGlynn[59] does not state whether the Rydberg orbital is $4p\sigma_u$ or $4p\pi_u$ while Hasted[72] proposes $4p\pi_u$. The 1612 Å band apparently does not show up in Hasted's[72] electron energy-loss spectra of CS_2 and we have already demonstrated (p.128) that McGlynn's[59] assignment of the 1612 Å band to $\pi_g \rightarrow 3d\sigma_g$ is unacceptable. We shall now present spectroscopic evidence for the assignment of the 1595, 1612 Å bands to $\pi_g \rightarrow 4p\sigma_u, (^{1,3}\Sigma_u)$, rather than $\pi_g \rightarrow 4p\pi_u$:

(i) In (Ω_c,ω) coupling the interval $E(^1\Pi_u \rightarrow {}^3\Pi_u)$ should be similar to, but larger than, the spin-orbit coupling constant, $\tilde{A}$, for CS_2^+. This is found to be the case because $\tilde{A} = 436\ cm^{-1}$

and $E(^1\Pi_u - {}^3\Pi_u) \approx 675\ cm^{-1}$. This value for $E(^1\Pi_u - {}^3\Pi_u)$ was obtained by E. Finn[48] using high resolution photographs of the CS_2 spectrum taken on a 21 ft. off-plane Eagle mounted vacuum spectrograph.

(ii) The high resolution photographs, mentioned in (i) above, show that the 1595 Å band has three heads corresponding to the P, Q and R branches expected for a $\Pi \leftarrow \Sigma$ transition.

Turning our attention to the $\pi_g \rightarrow 4p\pi_u$ transition in CS_2, we have shown (p. 102) that for the analogous transition in CO_2 the upper state is probably bent. It is therefore likely that the upper state is also bent for $\pi_g \rightarrow 4p\pi_u$ in CS_2 and the absorption due to this transition should show progressions in quanta of the bending vibration, ν_2. The model potential calculations indicate that $\pi_g \rightarrow 4p\pi_u$ should be observed in the CS_2 spectrum between the $\pi_g \rightarrow 4p\sigma_u$ and $\pi_g \rightarrow 4s\sigma_g$ transitions, but the only observed transition in this region is the very weak system ~1720 Å. McGlynn[59] has suggested that this system consists of a progression in two quanta of the bending vibration in which case the upper state may be $(\pi_g)^3\ 4p\pi_u$, $^1\Sigma_u^+$, correlating with $^1B_2$ in a bent conformation.

It is interesting that the assignment proposed here of the $\pi_g \rightarrow 4p\sigma_u$ and $4p\pi_u$ transitions to the 1595 and 1720 Å systems of CS_2 is the reverse of that suggested by Hasted[72], but, as we have already pointed out, the latter author gave no justification for the ordering of p terms he selected.

The Higher Members of the $\pi_g \rightarrow n\ell\lambda$ Rydberg series of CS_2

(i) $ns\sigma_g$ and $nd\lambda_g$ series

The model potential calculation predicts that the transition $\pi_g \rightarrow 5s\sigma_g$ should be observed ~1406 Å (71100 cm^{-1}) in the CS_2 spectrum. On the other hand the quantum defect for the observed $\pi_g \rightarrow 4s\sigma_g$ transition places the $\pi_g \rightarrow 5s\sigma_g$ transition ~1435 Å (69700 cm^{-1}). Transitions to a non-penetrating $3d\delta_g$ level should be observed ~1440 Å while transitions to a penetrating $3d\pi_g$ or $3d\sigma_g$ orbital will be to the red of this.

Inspection of the CS_2 spectrum shows that a strong transition occurs at 1410 Å, the strongest band in the 1420 Å group listed by Tanaka et al.[71] This band is assigned to the transition $\pi_g \rightarrow 5s\sigma_g$ although McGlynn[59] assigns it to $\pi_g \rightarrow 4p\lambda_u$, i.e. the first member of an $np\lambda_u$ series. McGlynn's[59] assignment is not followed because the 1410 Å band has an unacceptable quantum defect for an np term.

The absorption bands ~1500 Å are assigned to members of a $\pi_g \rightarrow 3d\lambda_g$ complex, while the bands ~1440 Å probably belong to a $\pi_g \rightarrow 3d\delta_g$ transition.

On the basis of the quantum defects of CS_2 transitions already assigned to $\pi_g \rightarrow ns\sigma_g$ and $nd\lambda_g$, the $\pi_g \rightarrow 4d\lambda_g$ and $6s\sigma_g$ transitions should lie between 1320 and 1340 Å in the CS_2 spectrum. These transitions are very close to the $\pi_g \rightarrow 6p\lambda_u$ and $\pi_g \rightarrow 4f\lambda_u$ transitions and it is also possible that the

allowed transition $\pi_u \rightarrow 4s\sigma_g$ occurs in this region of the CS_2 spectrum. Because the CS_2 spectrum below 1350 Å is very complex and high resolution spectra of this region were not available we have not made detailed assignments of $ns\sigma_g$ and $nd\lambda_g$ terms below 1400 Å. Instead, we shall consider the CS_2 Rydberg series that have been well established in this region of the spectrum, viz Price's[70] series I and II. These series are assigned to $\pi_g \rightarrow np\lambda_u$ for reasons discussed in the next sub-section.

(ii) $np\sigma_u$ and $np\pi_u$ series

The calculated values for the $5p\lambda_u$ terms of CS_2 predict that the $\pi_g \rightarrow 5p\lambda_u$ transitions should be observed ~1380 Å (72460 cm^{-1}) in the CS_2 spectrum, with the $5p\pi$ level to the red of the $5p\sigma$ level. There is a complex absorption system in this region of the spectrum referred to by Tanaka et al. as the 1385 Å group. Two bands at 1369 Å and 1378 Å constitute members of Price's[70] Rydberg series I and II. The 1385 Å group is assigned to transitions belonging to a $\pi_g \rightarrow 5p\lambda_u$ complex in which the $5p\pi_u$ components are much weaker than the $5p\sigma_u$ components in analogy to the $\pi_g \rightarrow 4p\lambda_u$ transitions in CS_2.

Price's[70] series I and II are listed in table 5.II together with calculated $np\sigma_u$ and $np\pi_u$ term values. Because the $\pi_g \rightarrow np\pi_u$ series appears to be very weak in CS_2 the series I and II are assigned to the singlet and triplet components of the Π_u states derived from the excited state configuration $(\pi_g)^3 np\sigma_u$.

Hasted et al.[72] have suggested that Price's[70] series I and II constitute "vibrationally excited and unexcited versions of the same series"; this is possible but does not account for the fact that the strongest Rydberg series converging to the lowest I.P. in CO_2, CS_2 and CSe_2 all consist of two components split by an interval which approaches the spin-orbit splitting in the respective ion. In CS_2 this splitting is similar to ν_2 but comparison with CO_2 and CSe_2 shows that Price's[70] series I and II in CS_2 are as assigned in this thesis i.e. singlet and triplet components of the same series occuring with similar intensity in (Ω_c,ω) coupling.

The only intense CS_2 absorption above 1325 Å that has not been assigned in this thesis is located at 1342 Å. The term value of this transition is very close to a non-penetrating $4f\lambda_u$ term and the transition is therefore assigned to the first member of the $\pi_g \rightarrow nf\lambda_u$ series in CS_2.

A summary of the CS_2 Rydberg assignments made in this thesis compared with those made previously by McGlynn[59] and Hasted[72] is given in table 5.III. A diagram showing the complete CS_2 assignments of the present work is given in Fig. 5.I.

Fig. 5.I

CS_2 Spectrum from 1300-1900 Å Showing $\pi_g \rightarrow n\ell\lambda$ Assignments

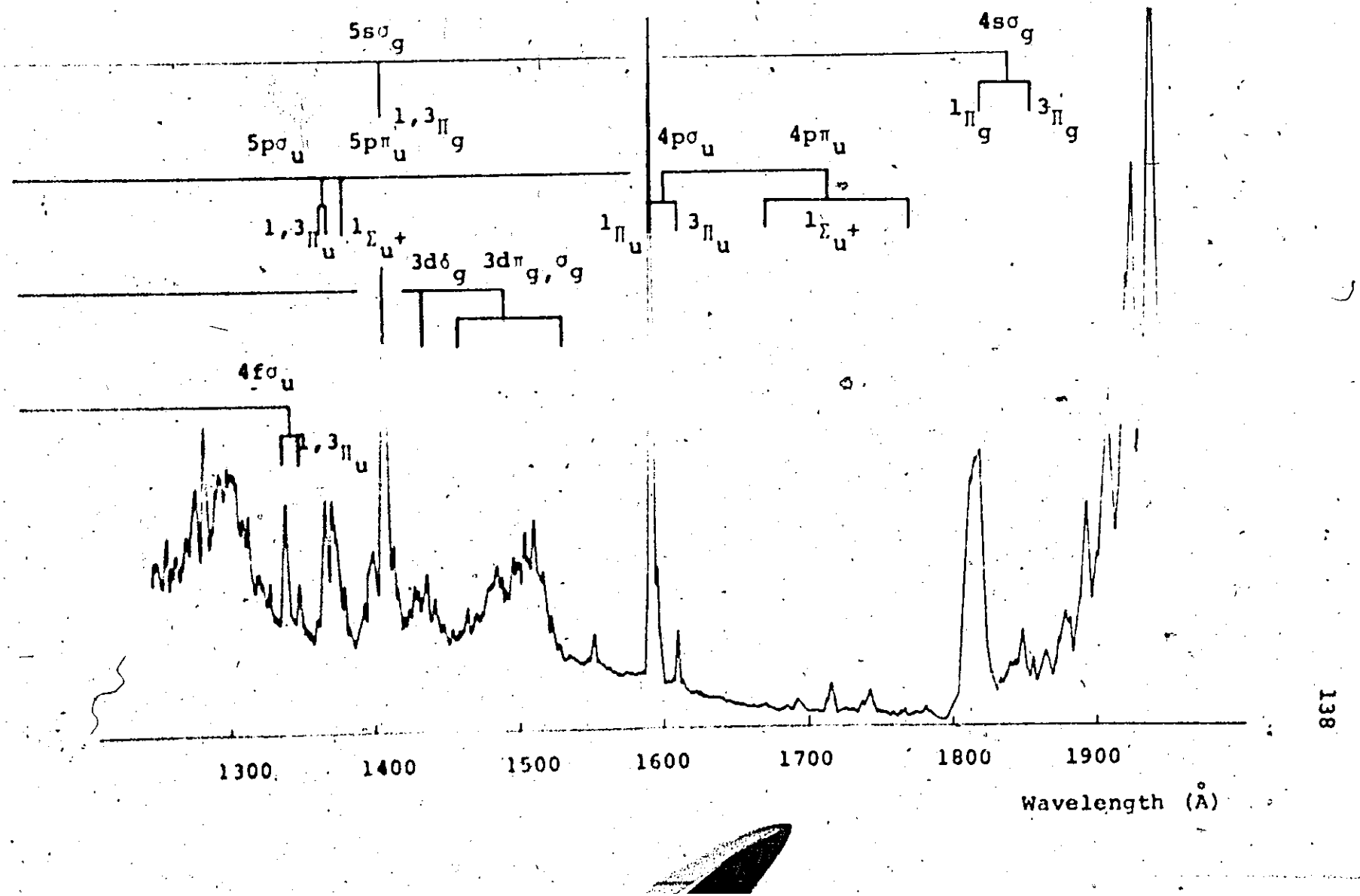

Table 5.I

Calculated Terms for CS_2

n	$ns\sigma_g$ (a.u.)	$np\sigma_u$ (a.u.)	$np\pi_u$ (a.u.)
2	.1039	.0847	.0865
3	.0474	.0416	.0417
4	.0272	.0237	.0245
5	.0176	.0157	.0161
6	.0123	.0112	.0114
7	.0091	.0084	.0085

Table 5.II

Price's Series I and II for CS_2 Compared to Calculated $np\lambda_u$ Series

	Observed(a.u.)		Calculated(a.u.)	
n	Series I	Series II	$np\sigma_u$	$np\pi_u$
2	.0864	.0876	.0847	.0865
3	.0396	.0398	.0416	.0417
4	.0243	.0243	.0237	.0245
5	.0163	.0162	.0157	.0161
6	.0116	.0117	.0112	.0114
7	.0088	.0088	.0084	.0085

Table 5.III

Assignments of the CS_2 Spectrum in the Region 1325-1825 Å

CS_2 Absorption Å	Previous Assignments S.P.McGlynn et al.[59]	J.B.Hasted et al.[72]	Present Work
1818	$\pi_g \rightarrow 4s\sigma_g$	$\pi_g \rightarrow 4s\sigma_g$	$\pi_g \rightarrow 4s\sigma_g, {}^1\Pi_g$
1720	${}^1\Sigma_g^+ \rightarrow {}^1\Pi_g$ (Bent) No config. proposed	$\pi_g \rightarrow 4p\sigma_u$	$\pi_g \rightarrow 4p\pi_u, \{4pa_1\, {}^1B_2\}$
1612	$\pi_g \rightarrow 3d\lambda_g$	-	$\pi_g \rightarrow 4p\sigma_u, {}^3\Pi_u$
1595	$\pi_g \rightarrow 4p\lambda_u$	$\pi_g \rightarrow 4p\pi_u$	$\pi_g \rightarrow 4p\sigma_u, {}^1\Pi_u$
1475-1525	$\sigma_g \rightarrow 2\pi_u, {}^{1,3}\Pi$	-	$\pi_g \rightarrow 3d\sigma_g, \pi_g \{ {}^1\Sigma_g^+$
1440	$\pi_g \rightarrow 5s\sigma_g$	$\pi_g \rightarrow 5s\sigma_g$	$\pi_g \rightarrow 3d\delta_g \}$ and ${}^1\Pi_g$
1410	$\pi_g \rightarrow 4p\lambda_u$	$\pi_g \rightarrow 5p\sigma_u$	$\pi_g \rightarrow 5s\sigma_g, {}^1\Pi_g$
1378 / 1369 First members of Price's series	$\pi_g \rightarrow 4d\lambda_g$	$\pi_g \rightarrow 5p\pi_u$ {Vib Comps}	$\pi_g \rightarrow 5p\sigma_u \{ {}^3\Sigma_u^- / {}^1\Sigma_u^- \}$
1342	$\pi_g \rightarrow 5p\lambda_u$	$\pi_g \rightarrow 6s\sigma_g$	$\pi_g \rightarrow 4f\lambda_u, {}^1\Pi_u$

CHAPTER 6

RYDBERG SERIES IN CSe_2

6.1 Previous Work

In this thesis the vacuum u-v spectra of CO_2 and CS_2 have been analysed using model potential calculations of their Rydberg series. CSe_2 is the next member of this group of 16 valence-electron linear triatomic molecules and model potential calculations were carried out on CSe_2 for the determination of its Rydberg series.

The u-v spectrum of CSe_2 has been investigated by G.W. King and K. Srikameswaran[75]. Up to the present time, no spectra of CSe_2 below 2000 Å have been reported in the literature; the Rydberg series of CSe_2 certainly lie in this region of the spectrum and for this reason CSe_2 was synthesised and vacuum u-v spectra of the gas were obtained.

Synthesis of CSe_2

CSe_2 was synthesised by the method used by K. Srikameswaran[75] and which is a modified version of the procedure first reported by D.J.G. Ives et al.[76] Metallic selenium is heated with methylene chloride, (in milligram quantities), to 600°C when the golden yellow gas CSe_2 forms in >50% yield. The balanced equation for this reaction is:

$$CH_2Cl_2 + 2Se \xrightarrow{600°C} CSe_2 + 2HCl$$

The reaction tube contains, after cooling, CSe_2 and HCl as well as unreacted CH_2Cl_2. The effect of these impurities on the CSe_2 spectrum will be discussed in a later section.

6.2 The vacuum u-v spectrum of CSe_2

A. Experimental

The vacuum u-v spectrum of CSe_2 in the region 1200-2000 Å was obtained using a McPherson Model 225 1-metre scanning monochrometer. A McPherson Model 630 lamp producing a low pressure (~2 mm) discharge in hydrogen at 2000 V and 350 mA was used as the source of vacuum u-v radiation. This discharge lamp provides a good continuum from 2000-1675 Å but below these wavelengths the continuum is overlayed by the hydrogen "many-line" spectrum which extends down to the H α-line at 1215 Å. To eliminate superposition of the source spectrum on the sample spectrum, double-beam operation was used with two matched E.M.I. Type 9635 B photomultipliers and a Burr-Brown Model 1665/16 log ratio amplifier as the detection system. Photomultiplier dark currents were backed-off by applying a variable, reverse D.C., voltage to the photomultiplier outputs, and source "following" in the sample spectrum was checked for by recording the spectrum of the discharge lamp simultaneously with the sample spectrum.

Absorption spectra of CSe_2 were obtained by introducing gas samples into a 10 cm cell, (with LiF windows), that had been previously evacuated to at least 0.002 mm Hg.

B. The effect of Impurities

The vacuum u-v spectrum of CSe_2 was first obtained using

gas samples taken directly from the reaction tube used in the synthesis; the samples therefore consisted of a mixture of CSe_2, CH_2Cl_2 and HCl. With sample pressures ~0.25 mm Hg many intense absorption features were obtained in the vacuum u-v spectrum from 1250-2000 Å. To discover which of these features were due to absorption by CSe_2 and which were caused by the other gases in the sample, the vacuum u-v spectra of HCl and CH_2Cl_2 were obtained separately.

At a pressure of 1 mm Hg, the HCl spectrum showed a very weak continuous absorption from 1800-1400 Å together with stronger discrete features at 1331, 1290 and 1283 Å. These discrete features were apparent in the CSe_2 spectra obtained using gas samples directly from the CSe_2 synthesis, and a procedure for removing HCl from the CSe_2 samples was therefore devised. The CSe_2 sample was passed over Mg ribbon at room temperature and the H_2 gas formed was pumped off the sample at liquid N_2 temperatures. In this way the strong HCl absorptions at 1331, 1290 and 1283 Å were eliminated from the CSe_2 spectrum as shown in Fig. 6.I

At a pressure of 0.2 mm Hg the spectrum of CH_2Cl_2 shows a region of continuous absorption extending from 1700-1450 Å with λ_{Max} ~1510 Å. To shorter wavelengths a strong continuum is observed from 1400-1340 Å overlayed by several discrete bands, the wavelengths of which have been published by A.B.F. Duncan et al.[77] Comparison of the CSe_2 spectrum obtained from

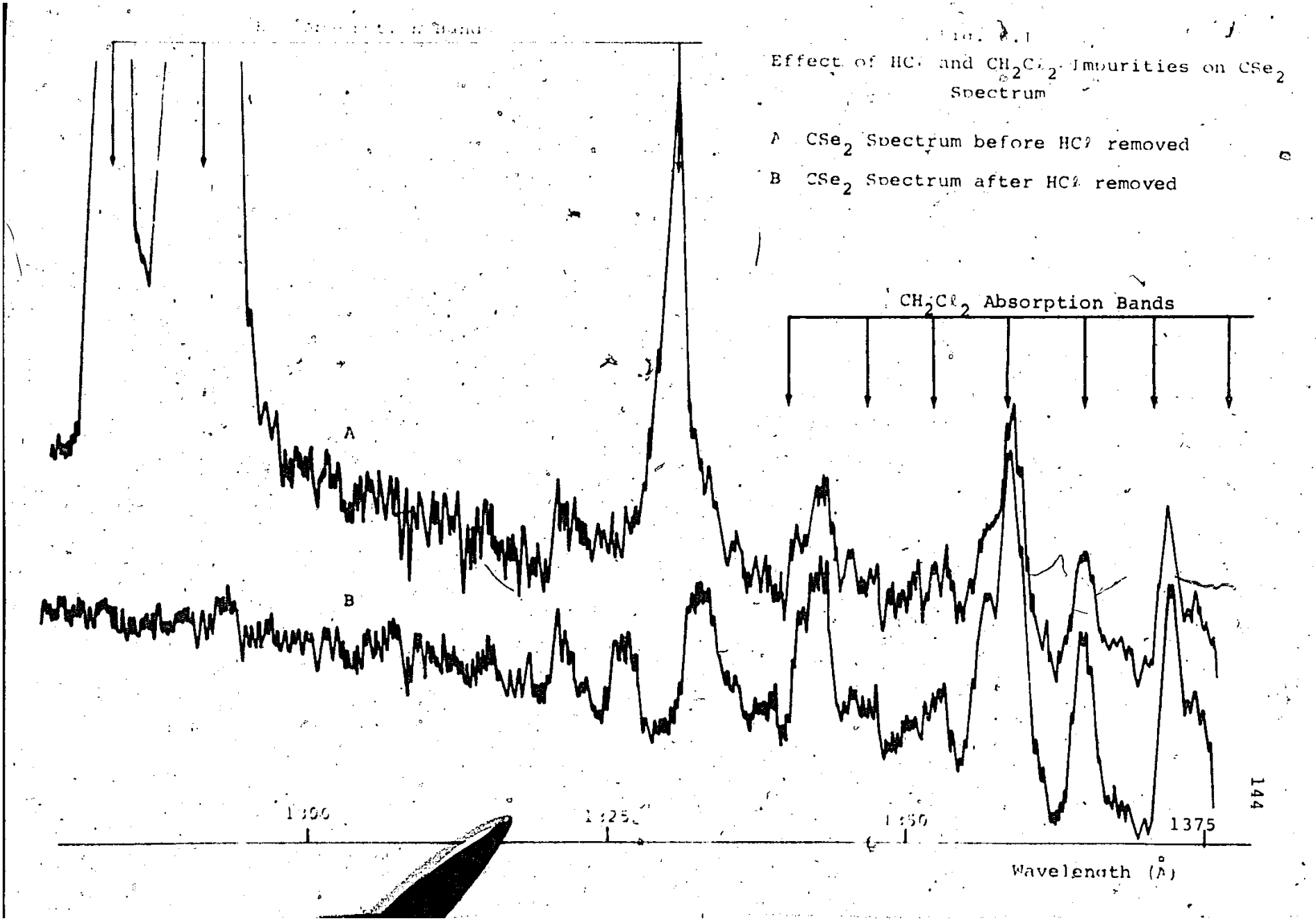

Fig. 3.1

Effect of HCl and CH_2Cl_2 Impurities on CSe_2 Spectrum

A CSe_2 Spectrum before HCl removed

B CSe_2 Spectrum after HCl removed

the CSe_2 sample containing unreacted CH_2Cl_2, showed that the CH_2Cl_2 bands are of much lower intensity than the CSe_2 bands, (See Fig.6.I). Consequently no attempt was made to remove CH_2Cl_2 from CSe_2 samples because the presence of this impurity does not interfere with the analysis of the spectrum.

While the expected impurities, HCl and CH_2Cl_2, did not seriously obscure the CSe_2 spectrum, CS_2 appeared as an unexpected impurity, in the first CSe_2 samples prepared, and obscured parts of the CSe_2 spectrum; this impurity was identified by the presence of discrete bands in the region 1850-2150 Å whose wavelengths fitted the published data on the $\tilde{A}$ system of CS_2[54,73]. The first samples of CSe_2 used for obtaining spectra were prepared from high purity CH_2Cl_2, (Baker "Instra Analysed" Spectrophotometric grade), and Analar Selenium, (B.D.H. Ltd.). However, the CS_2 $\tilde{A}$ system showed up with the same intensity in the vacuum u-v spectrum as the strongest CSe_2 bands. In later samples, ultra high purity (99.999±%) selenium was used, (Chemicals Procurement Labs); while the CS_2 $\tilde{A}$ system was still not completely eliminated from the CSe_2 spectrum, a new system of bands was observed in the same region and was assumed to belong to CSe_2.

6.3 Model Potential Calculations of the Rydberg Series of CSe_2

The model potential calculation developed in this thesis

was applied to CSe_2 to estimate the term values for the $\pi_g \rightarrow ns\sigma_g$, $np\sigma_u$ and $np\pi_u$ Rydberg series. The calculated values are given in Table 6.I in a.u.'s.

Table 6.I

Calculated Terms for CSe_2

n	$ns\sigma_g$ (a.u.)	$np\sigma_u$ (a.u.)	$np\pi_u$ (a.u.)
2	.1060	.0847	.0867
3	.0487	.0404	.0417
4	.0279	.0239	.0245
5	.0180	.0158	.0161
6	.0126	.0112	.0114
7	.0093	.0084	.0085

The most striking feature of the calculated term values for CSe_2 is their close agreement with the calculated values for CS_2, given in table 5.I . This suggests that the analysis of the CSe_2 Rydberg spectrum should follow closely the analysis already proposed for CS_2. The first ionisation potential of selenium is ~0.61 ev lower than the first ionisation potential of sulphur; for this reason the CSe_2 spectrum should resemble the CS_2 spectrum, but shifted ~4900 cm^{-1} to the red. Also, the spin-orbit coupling in selenium is much larger than that in sulphur, and all the Rydberg states of CSe_2 are probably well described by (Ω_c,ω) coupling. Consequently, singlet-triplet intensity ratios should be much closer to unity than those observed in CS_2.

In going from CO_2 to CS_2 the relative intensity of the $\pi_g \rightarrow np\pi_u$ series diminished considerably. This trend should be continued in going from CS_2 to CSe_2 and the series $\pi_g \rightarrow np\pi_u$ may not be observed in the CSe_2 spectrum.

6.4 Analysis of the CSe_2 Vacuum u-v Spectrum

The results of the model potential calculations on CS_2 and CSe_2 indicate that the observed CS_2 term values should be very close to the observed CSe_2 terms. The term value of a Rydberg state, $\psi(n\ell\lambda)$, can be used to locate the transitions $\pi_g \rightarrow n\ell\lambda$ in the spectrum only if the ionisation potential or the limit to which the Rydberg series converge, is known. The first ionisation potential of CSe_2 is unknown but is probably close to (81300 ± 4900) cm^{-1} or ~76,000 cm^{-1}. An accurate value for the first ionisation potential of CSe_2 can be obtained from the identification of Rydberg series in the vacuum u-v spectrum of the molecule; these series will lie at lower excitation energies than 76,000 cm^{-1} or to the red of 1300 Å.

(i) Rydberg series in the 1300-1500 Å region of the CSe_2 spectrum

Two intense Rydberg series were identified in the CSe_2 spectrum in the region 1300-1500 Å, with limits at 74665 ± 15 cm^{-1} and 76785 ± 25 cm^{-1}. These will be designated series I and II respectively, and fit the formulae:

CSe_2 Series I

$$\nu_n = 74665 - \frac{R}{(n - 0.11)^2}$$

$$n = 4,5,\ldots 9$$

CSe_2 Series II

$$\nu_n \simeq 76785 - \frac{R}{(n - 0.12)^2} \quad n=4,5\ldots10$$

The observed bands belonging to these series are given in table 6.II together with their intensities (Relative to I = 10.0 for the CSe_2 transition at 1735.5 Å). Also in the table, the observed frequencies, ν_{obs}, are compared with values, ν_{calc}, determined from the Rydberg formulae.

The Rydberg series I and II in CSe_2 give the lowest ionisation potential of CSe_2 as 9.257 ± 0.002 ev and the spin-orbit coupling constant, $\tilde{A}$, for the ion CSe_2^+ as 2120 ± 30 cm^{-1}.

The small quantum defects found for series I and II, and the fact that the series terminate at n=4; suggests that they constitute $^{1,3}\Pi$ components (Ω=1) of the $\pi_g \rightarrow nf\lambda_u$ Rydberg series of CSe_2 with λ_u either σ_u or δ_u. This assignment brings out the predicted similarity of CSe_2 terms with the equivalent terms in CS_2. Thus the average term value for the lowest members of series I and II in CSe_2 is 7270 ± 20 cm^{-1}. In the CS_2 spectrum the band at 1342 Å was assigned (see p.137) to the first member of the $1\pi_g \rightarrow nf\sigma_u$ series in CS_2 and has a term value of 7240 ± 20 cm^{-1}.

(ii) The Assignment of $ns\sigma_g$, $np\sigma_u$ and $nd\lambda_g$ terms in the CSe_2 Spectrum

Knowing the ionisation potential of CSe_2, the assignment of $\pi_g \rightarrow ns\sigma_g$, $np\sigma_u$ and $nd\lambda_g$ series in CSe_2 can be made by direct

Table 6.II

Principal Rydberg Series of CSe_2 in the Region 1300-1500 Å

CSe_2 Series I

n	λ_{obs} (Å)	I_{rel}	ν_{obs} (cm^{-1})	ν_{calc} (cm^{-1})
4	1483.0	3.0	67430	67415
5	1427.0	6.6	70075	70075
6	1399.5	3.8	71455	71505
7	1382.0	3.0	72360	72355
8	1372.0	2.3	72885	72905
9	1365.0	1.7	73260	73275
10	Obscured	-	-	73540
∞	-	-	-	74665

λ's to ± 0.5 Å

CSe_2 Series II

n	λ_{obs} (Å)	I_{rel}	ν_{obs} (cm^{-1})	ν_{calc} (cm^{-1})
4	1438.0	5.0	69540	69500
5	1386.5	2.4	72125	72180
6	1359.0	3.1	73585	73615
7	1342.5	1.8	74490	74470
8	1333.0	1.4	75020	75020
9	1326.0	0.8	75415	75395
10	1321.5	0.9	75670	75660
∞	-	-	-	76785

comparison with appropriate term values in CS_2.

$\pi_g \rightarrow 5s\sigma_g$

From the observed $4s\sigma_g$ term value in CS_2, the $\pi_g \rightarrow 5s\sigma_g$ excitation energy in CSe_2 can be estimated to be 50100±200 cm^{-1} for the singlet-singlet transition and 48000±200 cm^{-1} for the singlet-triplet transition. This places $\pi_g \rightarrow 5s\sigma_g$ ($^1\Pi_g$) and $\pi_g \rightarrow 5s\sigma_g$ ($^3\Pi_g$) at 1995 and 2085±10 Å respectively. The CSe_2 spectrum in this region shows a weak system extending from 1975 to 2125 Å, with $\lambda_{Max} \simeq$ 2040 Å. This system is certainly due to $\pi_g \rightarrow 5s\sigma_g$. However, the absorption bands are partially obscured by the $\tilde{A}$ system of CS_2 which occurred as an impurity in the CSe_2 samples (see p.145), and no assignment of singlet and triplet components will be made.

$\pi_g \rightarrow 5p\sigma_u$

The observed $4p\sigma_u$ term value in CS_2 is 19150±50 cm^{-1} and the same value for the lowest $np\sigma_u$ term in CSe_2 would place the $\pi_g \rightarrow 5p\sigma_u$ transition at 1802±5 Å (triplet component) and 1738±5 Å (singlet component) in the CSe_2 spectrum. Two very strong transitions are found in the CSe_2 spectrum very close to these values, one at 1735.5 Å and the other, a weaker doublet, at 1802 Å; these are undoubtedly $^1\Pi(1) \rightarrow {}^1\Sigma_g^+$ and $^3\Pi(1) \rightarrow {}^1\Sigma_g^+$ respectively. The intensity ratio, $I(\frac{^1\Pi_g}{^3\Pi}) \simeq 0.5$, is consistent with (Ω_C,ω) coupled states; the tendency away from (Λ,S) and towards (Ω_C,ω) coupling in going from CS_2 to CSe_2 is readily apparent by comparing the first member of the

$\pi_g \rightarrow np\sigma_u$ series in each molecule (See Fig.5.I and Fig.6.II).

The energy interval $E(^1\Pi - {}^3\Pi)$ for $\pi_g \rightarrow 5p\sigma_u$ in CSe_2 equals 2125±10 cm^{-1} and is close to the $\tilde{A}$ value of 2120±30 cm^{-1} found for CSe_2^+; this is also expected for states which are close to ideal (Ω_c,ω) coupling. (See diagram p.87)

$\pi_g \rightarrow 4d\lambda_g$ and higher g ↔ g transitions

Transitions belonging to the $\pi_g \rightarrow 4d\lambda_g$ complex in CSe_2 should occur in the vacuum u-v spectrum between 1525 and 1700 Å. Numerous transitions are observed in this region but they are all weak and diffuse; the strongest occur ∿1545 Å and are probably part of a $\pi_g \rightarrow 4d\delta_g$ transition.

It appears that g ↔ g transitions are weak in the CSe_2 spectrum and higher members of $\pi_g \rightarrow n\ell\lambda_g$ series are certainly obsucred by stronger g ↔ u series.

The higher members of the $\pi_g \rightarrow np\sigma_u$ series of CSe_2

In the discussion of the CS_2 Rydberg spectrum, Price's series I and II were assigned to $1\pi_g \rightarrow np\sigma_u$, $^{1,3}\Pi_u$. In addition the CS_2 transitions at 1595 and 1612 Å were assumed to constitute the first members of Price's series, implying that the quantum defects for these series are 1.44 and 1.46. In view of the similarity of the CS_2 and CSe_2 term values, CSe_2 should exhibit similar $\pi_g \rightarrow np\sigma_u$ series to CS_2 but with a quantum defect ∿2.45. Two series, designated III and IV were found in the CSe_2 spectrum with quantum defects close to this value and are assigned to $\pi_g \rightarrow np\sigma_u$, $^{1,3}\Pi_u$ by analogy with CS_2.

These series fit the formulae:

CSe_2 Series III

$$n = 74665 - \frac{R}{(n - 2.45)^2}$$

$$n = 5,6,\ldots 10$$

CSe_2 Series IV

$$n = 76785 - \frac{R}{(n - 2.46)^2}$$

$$n = 5,6,\ldots 10$$

(See table 6.III)

The occurrence of series III and IV in the CSe_2 spectrum again emphasises the similarity of the CSe_2 and CS_2 Rydberg spectra. Perhaps the most significant difference between the spectra of the two molecules is the increased intensity of $\pi_g \rightarrow nf\lambda_u$ series relative to $\pi_g \rightarrow np\sigma_u$ in CSe_2 compared to CS_2.

The only CSe_2 bands, with significant intensity in the vacuum u-v between 2000 and 1200 Å, that are unassigned in this thesis occur at 1511, 1465, 1448 and 1413 Å. It is probable that these transitions are other $\Omega=1$ components of the $\pi_g \rightarrow nf\lambda_u$ series in addition to those already assigned to series I and II, or alternatively they may constitute the first members of $\pi_u \rightarrow nf\lambda_g$ series in CSe_2.

A diagram showing the assignments of CSe_2 absorptions between 1325 and 1525 Å proposed in this thesis are given in Figs. 6.II and 6.III.

Table 6.III

Additional Rydberg Series of CSe_2 in the Region 1300-1900 Å.

CSe_2 Series III

n	λ_{obs} (Å)	I_{rel}	ν_{obs} (cm^{-1})	ν_{calc} (cm^{-1})
5	1802.0	5.0	55495	57795
6	1519.0	2.7	65835	65960
7	1440.0	5.0	69445	69365
8	1405.0	1.8	71175	71105
9	1386.5(a)	2.4	72125	72740
10	1374.0	1.3	72780	72740
∞	-	-	-	74665

$\lambda \pm 0.5$ Å

CSe_2 Series IV

n	λ_{obs} (Å)	I_{rel}	ν_{obs} (cm^{-1})	ν_{calc} (cm^{-1})
5	1735.5	10.0	57620	59785
6	1471.5	3.5	67960	68035
7	1399.5(a)	3.8	71455	71465
8	1365.0(a)	1.7	73260	73210
9	1346.0	0.8	74295	74220
10	1335.0	0.6	74880	74885
-	-	-	-	76785

(a) Superimposed with another band

Fig. 6.II

CSe_2 Spectrum from 1700-2000 Å Showing $\pi_g \rightarrow n\ell\lambda$ Assignments

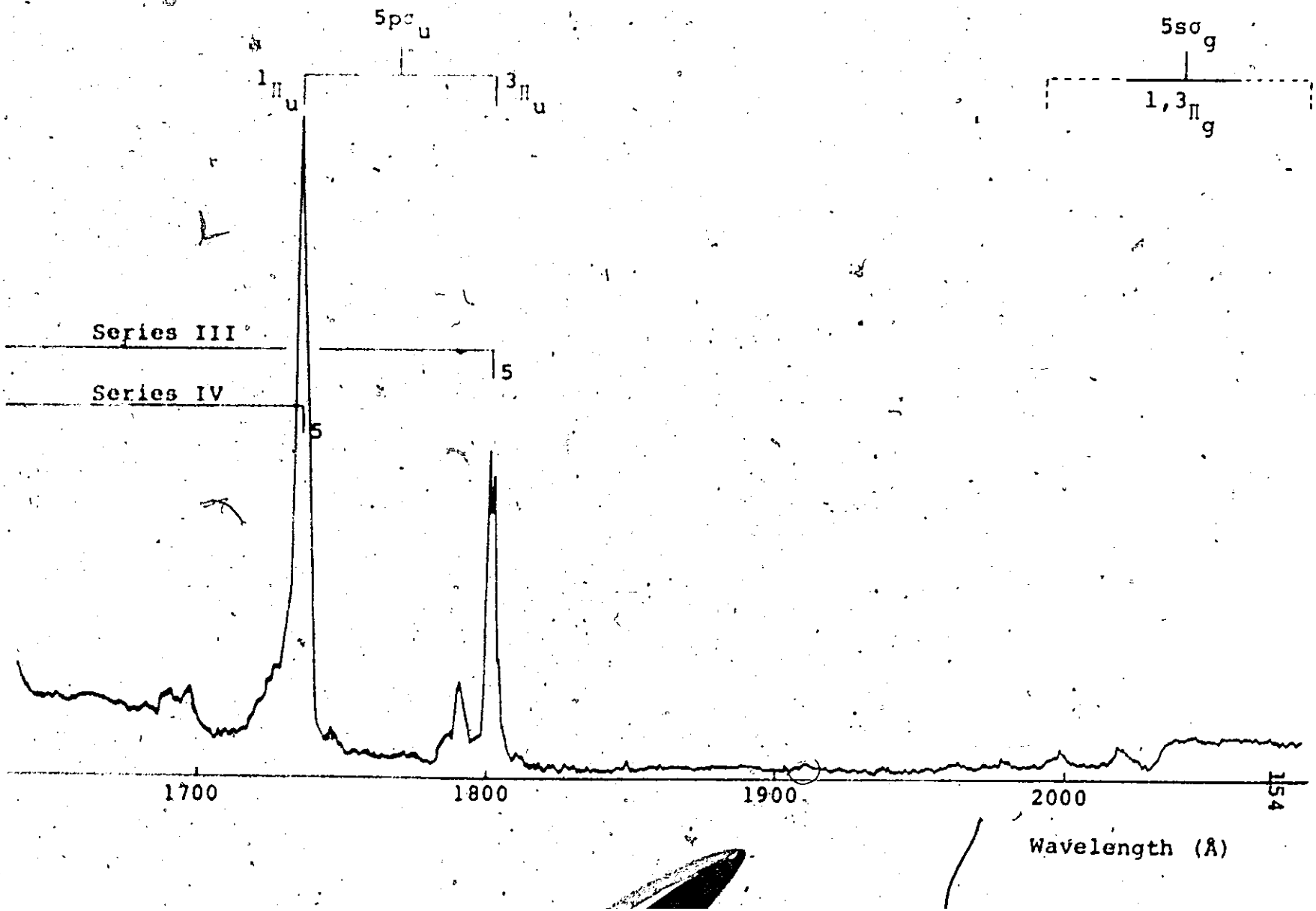

Fig. 6.III

CSe_2 Spectrum from 1300-1600 Å Showing $^1\Sigma_g^+ \rightarrow n\ell\lambda$ Assignments

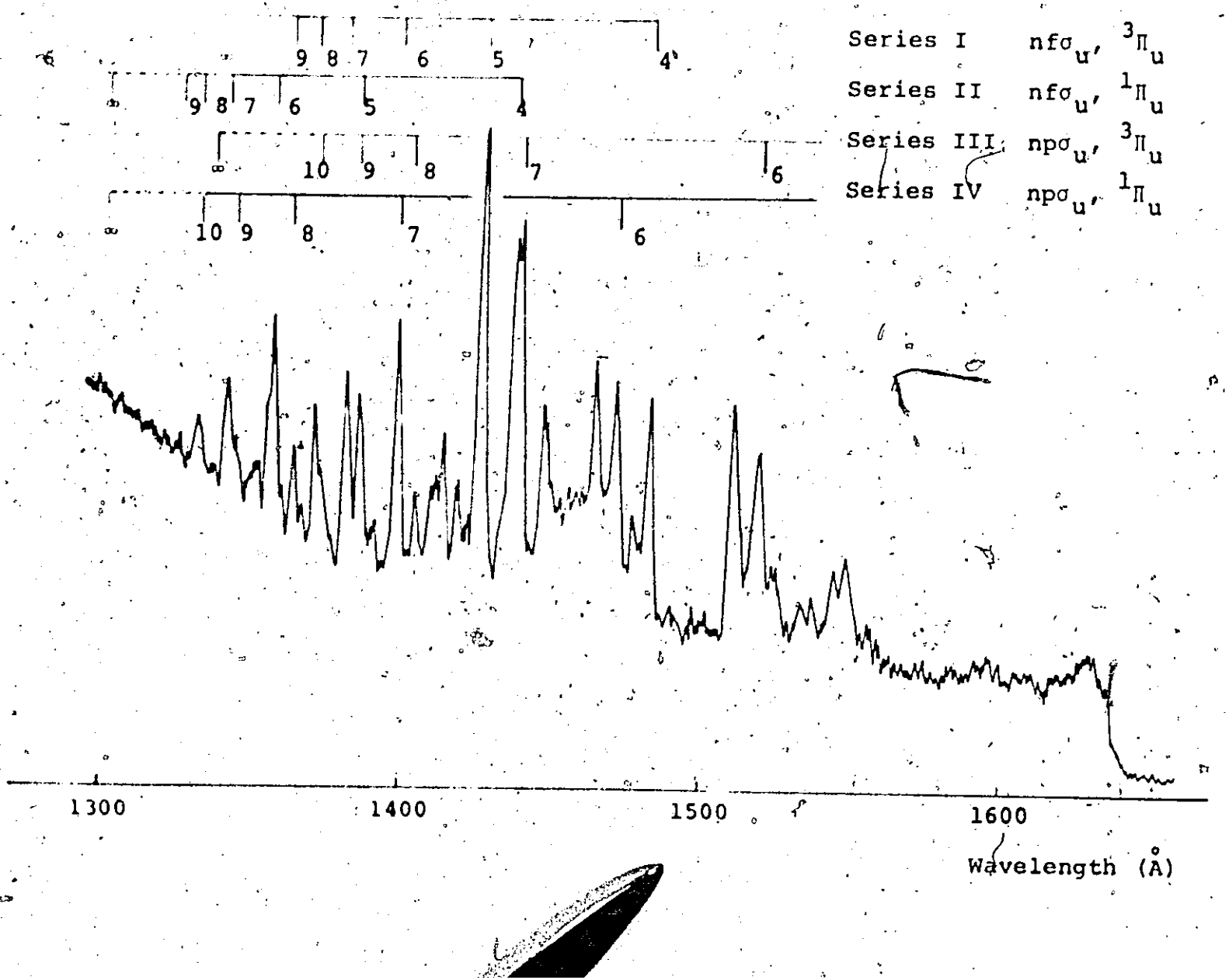

CONCLUSIONS

"Don't suppose that you can tell it precisely the first dozen times you try, but at 'em again...Not that the story need be long, but it will take a long time to make it short."

H.D. Thoreau

In this thesis a theoretical method was developed for the calculation of Rydberg series in triatomic molecules. The method is an extension of that proposed by S.A. Rice et al. and involves the determination of parameters which establish atomic model potentials for use in molecular calculations. A new parametrisation procedure was used in the present work which optimises not only the energy eigenvalue but also the asymptotic phase-shift of the model Rydberg A.O.

We suggest that further work on atomic model potentials should be aimed at finding connecting formulae between the quantum defect and model potential parameters.

The first one-centre calculations of Rydberg series in CO_2, CS_2 and CSe_2 were carried out in Chapter 2 of this thesis, and an estimate of the ℓ-purity of Rydberg states in these molecules was made by comparison with H_2^+ wavefunctions. The conclusion that the ℓ-purity is very high even in the lowest Rydberg states was confirmed by two-centre calculations of ns Rydberg series in CO_2; these calculations demonstrated the

united-atom (single-centre) character of CO_2 Rydberg MO's.

The CO_2 and CS_2 $\pi_g \rightarrow ns\sigma_g$, $np\sigma_u$ and $np\pi_u$ Rydberg series were determined using the model calculations and compared with the Rydberg series assigned by previous investigators; their assignments were shown to be unacceptable in several cases and new assignments were proposed where necessary.

The previously unreported vacuum u-v spectrum of CSe_2 was obtained and analysed in terms of Rydberg series determined from the model calculation. The CS_2 and CSe_2 calculations predicted that the Rydberg terms in these molecules should be very similar and this was confirmed in the course of the analysis proposed for CSe_2.

The main difference between observed and calculated Rydberg terms in CO_2, CS_2 and CSe_2 was accounted for by the neglect of bonding effects in the core of the molecular model potential employed in the calculation. It was also suggested that smaller differences between calculated and observed Rydberg terms arose from changes in geometry in certain Rydberg excited state configurations; spectroscopic evidence was presented supporting proposed assignments of bent ← linear transitions.

BIBLIOGRAPHY

1. T. Lyman, "The Spectroscopy of the Extreme Ultra-violet" Longmans, London, 1914.
2. N. Bohr, Phil. Mag. 26, 1 (1913).
3. N. Bohr, Proc. London Phys. Soc. 35, 296 (1923).
4. H.E. White, "Introduction to Atomic Spectra". McGraw-Hill, New York, 1934.
5. A.B.F. Duncan, "Rydberg Series in Atoms and Molecules" Academic Press, New York, 1971.
6. M. Born and R.J. Oppenheimer, Ann. Physik 84, 457 (1927).
7. J.C. Slater, Phys. Rev. 31, 333 (1928).
8. D.R. Hartree, "The Calculation of Atomic Structures". Wiley, New York, 1957.
9. W. Heisenberg, Z. Physik 39, 499 (1927).
10. R.S. Mulliken, J. Am. Chem. Soc. 86, 3183 (1964).
11. C. Herring, Phys. Rev. 57, 1169 (1940).
12. J.C. Phillips and L. Kleinman, Phys. Rev. 116, 287 (1959).
13. M.H. Cohen and V. Heine, Phys. Rev. 112, 1821 (1961).
14. I.V. Abarenkov and V. Heine, Phil. Mag. 12, 529 (1965).
15. A.S. Eddington, Nature 120, 117 (1927).
16. Y. Sugiura, Phil. Mag. Ser. 7, Vol 4, 498 (1927).
17. L.J. Slater, "Confluent Hypergeometric Functions". Cambridge, 1960.
18. H. Buchholz, "The Confluent Hypergeometric Function". Springer, New York, 1969.

19. D.R. Hartree, Proc. Camb. Phil. Soc. 24, 89, 111 and 426 (1928); ibid, 25, 310 (1929).

20. R.T. Birge, Astrophys. J. 32, 112 (1910).

21. G.H. Wannier, Phys. Rev., 64, 358 (1943).

22. H.A. Bethe and E.E. Salpeter, "Quantum Mechanics of One- and Two-Electron Atoms" Academic Press, New York, 1957.

23. M.J. Seaton, Monthly Notices Roy. Ast. Soc. 118, 504 (1958).

24. M. Blume, N. Briggs and H. Brooks, "Tables of Coulomb Wavefunctions" Technical Report 260, Cruft Lab., Harvard, 1959. (Available from National Technical Information Service U.S. Dept. of Commerce, Springfield, Va.)

25. A.U. Hazi and S.A. Rice, J. Chem. Phys. 48, 495 (1968).

26. T. Betts and V. McKoy, J. Chem. Phys. 54, 113 (1971).

27. C.E. Moore, "Atomic Energy Levels" N.B.S. Circular 467, Washington D.C., (First Published 1949, Revised 1958).

28. D.R. Hartree and M.M. Black, Proc. Roy. Soc. (London), A139, 311 (1933).

29. H. Hosoya, J. Chem. Phys. 48, 1380 (1968).

30. C.E. Wulfman, J. Chem. Phys. 31, 381 (1959).

31. W.A. Bingel, J. Chem. Phys. 30, 1254 (1959).

32. H. Hosoya, Int. J. Quant. Chem. 6, 801 (1972).

33. J.C. Slater, "Quantum Theory of Atomic Structure", Volume I, McGraw-Hill, New York, 1960.

34. H. Kopferman, "Nuclear Moments", Academic Press, New York, 1958.

35. A. Edmonds, "Angular Momentum in Quantum Mechanics", Princeton, 1957.

36. T.F. Lin and A.B.F. Duncan, J. Chem. Phys. 48, 866 (1968).

37. G. Herzberg and C. Jungen, J. Mol. Spect., 41 (3), 425 (1972).

38. L. Szasz and G. McGinn, J. Chem. Phys. 48, 2997 (1968).

39. G. Simons and A. Mazziotti, J. Chem. Phys. 52, 2449 (1970).

40. I. Prigogine and S.A. Rice (Eds) "Advances in Chemical Physics", Interscience 16, 283, 1969.

41. R.F.W. Bader and P.M. Beddall, Chem. Phys. Lett. 8 (1), 29 (1971).

42. R.S. Mulliken, J. Am. Chem. Soc., 88, 1849 (1966).

43. D.R. Bates, K. Ledsham and A.L. Stewart, Phil. Trans. Roy. Soc. (London), A246, 215 (1954).

44. K. Helfrich and H. Hartmann, Theoret. Chim. Acta., 16, 263 (1970).

45. R.S. Berry and S.E. Nielsen, J. Chem. Phys., 49, 116 (1968).

46. G.G. Hall, "Advances in Quantum Chemistry" 1, 241. Ed. P.O. Löwdin, Academic, 1964.

47. T.C. Chen, J. Chem. Phys., 29, 347 (1958).

48. E. Finn, Ph.D. Thesis, McMaster University, 1973.

49. P.O. Löwdin, "Advances in Quantum Chemistry", 5, 185, Academic, 1970.

50. J.H. Wilkinson, "The Algebraic Eigenvalue Problem", Oxford, 1965.

51. J.F. Mulligan, J. Chem. Phys., 19, 347 (1951).

52. A.D. McLean and M. Yoshimine, "Tables of Linear Molecule Wavefunctions", I.B.M. Special Publication, 1967.

53. S.D. Peyerimhoff, R.J. Buenker and J.L. Whitten, J. Chem. Phys. 46, 1707 (1967).

54. G. Herzberg, "Electronic Spectra and Electronic Structure of Polyatomic Molecules", D. Van Nostrand, Princeton, 1966.

55. G. Herzberg, "Spectra of Diatomic Molecules", 2nd Edition, D. Van Nostrand, Princeton, 1950.

56. A. Recknagel, Zeits. f. Physik, 87, 397 (1934).

57. N.W. Winter, C.F. Bender and W.A. Goddard III (Cal. Tech.) Private communication (To be published).

58. A.D. Walsh, J. Chem. Soc., 2266 (1953).

59. J.W. Rabalais, J.M. McDonald, V. Scherr and S.P. McGlynn, Chem. Rev., 71, 73 (1971).

60. W.C. Price and D.M. Simpson, Proc. Roy. Soc. (London) A169, 501 (1938).

61. Y. Tanaka, A.S. Jursa and F.J. LeBlanc, J. Chem. Phys. 32, 1199 (1960).

62. R.S. Nakata, K. Watanabe and F.M. Matsunaga, Science of Light, 14, 54 (1965).

63. V.D. Meyer and E.N. Lassettre, J. Chem. Phys., 42, 3436 (1965).

64. E.N. Lassettre and J.C. Shiloff, J. Chem. Phys., 43, 560 (1965).

65. E.N. Lassettre, A. Skerbele, M.A. Dillon and K.J. Ross, J. Chem. Phys., 48, 5066 (1968).

66. J.F. Mulligan, J. Chem. Phys., 19, 1428 (1950).

67. M. Krauss, S.R. Mielszarek, D. Neumann and C.E. Kuyatt, J. Geophys. Res., 76, 3733 (1971).

68. P.S. Julienne, D. Neumann and M. Krauss, J. Atmos. Sci., 28, 833 (1971).

69. E. Lindholm, Arkiv För Fysik, 40, 97 and 125 (1969).

70. W.C. Price and D.M. Simpson, Proc. Roy. Soc. (London) A165, 272 (1938).

71. Y. Tanaka, A.S. Jursa and F.J. LeBlanc, J. Chem. Phys., 32, 1205 (1960).

72. V.Y. Foo, C.E. Brion and J.B. Hasted, Proc. Roy. Soc. (London) A322, 535 (1971).

73. A.E. Douglas and I. Zanon, Can. J. Phys., 42, 627 (1964).

74. M. Ogawa and H.C. Chang, Can. J. Phys., 48, 2455 (1970).

75. K. Srikameswaren, Ph.D. Thesis, McMaster University, 1968.

76. D.J.G. Ives, R.W. Pittman and W. Wardlaw, J. Chem. Soc., 1080 (1947).

77. C.R. Zobel and A.B.F. Duncan, J. Am. Chem. Soc., 77, 2611 (1955).